



저작자표시-비영리-변경금지 2.0 대한민국

이용자는 아래의 조건을 따르는 경우에 한하여 자유롭게

- 이 저작물을 복제, 배포, 전송, 전시, 공연 및 방송할 수 있습니다.

다음과 같은 조건을 따라야 합니다:



저작자표시. 귀하는 원저작자를 표시하여야 합니다.



비영리. 귀하는 이 저작물을 영리 목적으로 이용할 수 없습니다.



변경금지. 귀하는 이 저작물을 개작, 변형 또는 가공할 수 없습니다.

- 귀하는, 이 저작물의 재이용이나 배포의 경우, 이 저작물에 적용된 이용허락조건을 명확하게 나타내어야 합니다.
- 저작권자로부터 별도의 허가를 받으면 이러한 조건들은 적용되지 않습니다.

저작권법에 따른 이용자의 권리는 위의 내용에 의하여 영향을 받지 않습니다.

이것은 [이용허락규약\(Legal Code\)](#)을 이해하기 쉽게 요약한 것입니다.

[Disclaimer](#)

The Effect of Graphite-Powder-Mixed Kerosene on Tool Wear in Micro EDM

A Ph.D. Dissertation
Yooseok Kim

August 2019

Seoul National University
School of Mechanical and Aerospace Engineering
Precision Engineering and Manufacturing Lab.



**In memories of
Prof. Chong-Nam Chu**

공학박사학위논문

**미세 방전 가공의 공구 마모에 대한
흑연 파우더 혼합 등유의 영향**

**The Effect of Graphite-Powder-Mixed Kerosene on
Tool Wear in Micro EDM**

2019 년 8 월

서울대학교 대학원
기계항공공학부
김 유 석

**THE EFFECT OF GRAPHITE-POWDER-
MIXED KEROSENE ON TOOL WEAR IN
MICRO EDM**

DISSERTAION

SUBMITTED TO THE SCHOOL OF MECHANICAL
AND AEROSPACE ENGINEERING AND THE COMMITTEE ON
GRADUATE STUDIES OF SEOUL NATIONAL UNIVERSITY
IN PARTIAL FULFILLMENT OF THE REQUIREMENTS
FOR THE DEGREE OF DOCTOR OF PHILOSOPHY

YOOSEOK KIM

August 2019

Abstract

Yooseok Kim

School of Mechanical and Aerospace Engineering

The Graduate School

Seoul National University

This study investigates the tool wear reduction mechanism of graphite-powder-mixed kerosene (GPMK) in micro electrical discharge machining (EDM). Because an RC discharge circuit generates small and short discharge pulses, it is widely used in micro EDM rather than a transistor circuit. In this case, a tool electrode is negatively charged for high material removal rate (MRR) and low tool wear length (TWL) given that an anode has higher energy proportion than cathode by massive electron collisions to the positively charged workpiece. However, during the discharge phase, the direction of current flow is reversed by the stray inductance of an RC discharge circuit before the discharge plasma channel is extinguished. This reverse current intensifies the TWL and deteriorates the machining efficiency. In this study, TWL was decreased with GPMK by creating circumstance which facilitates the early extinction of discharge plasma channel before the generation of reverse current by two manners. Owing to the enlarged discharge gap by GPMK, the intensity of discharge energy becomes low and the plasma channel is easily flushed by dielectric fluid. Furthermore, even though a tool electrode comes close to a workpiece, the discharges occur with small values of energy before a capacitor is fully

charged and these early discharges is also extinguished quickly before the generation of reverse current. The machining performance and quality of micro ED-milling and ED-drilling with GPMK were evaluated in comparison with those of pure kerosene (PK). With optimal machining conditions, MRR was increased by 140%, and TWL and surface roughness were respectively decreased by 55% and 57% with GPMK in micro ED-drilling. On the other hand, in micro ED-milling, MRR was increased by 61% and TWL and surface roughness were decreased by 61% and 23%, respectively by GPMK.

Keywords: micro EDM; graphite-powder-mixed kerosene (GPMK); Tool wear

Student number: 2015-30997

Contents

Abstract	i
Contents	iii
List of Figure	vi
List of Table	x
1. Introduction	1
2. Tool Wear in Electrical Discharge Machining	10
2.1 Principle of EDM	11
2.2 Types of EDM	16
2.2.1 Die-sinking EDM	16
2.2.2 ED-drilling and ED-milling	18
2.2.3 Wire and Strip-EDM	20
2.2.4 Micro EDM	22
2.3 Principle of tool wear	24
2.4 Previous research of tool wear problem	32
2.4.1 Long pulse-on time in kerosene	32
2.4.2 Tool material change	34
2.4.3 Deionized water	35
2.4.4 Linear compensation method	37
2.4.5 Uniform wear method	39
2.4.6 Wire and Strip-EDM	41
3. Powder mixed EDM	42

6.2.3 Final results	103
6.3 Micro powder mixed ED-milling	107
6.3.1 Depth of cut	109
6.3.2 Open voltage	116
6.3.3 Capacitance	119
6.3.4 Final results	122
7. Application-a micro mold	127
7.1 ED-finishing with stray capacitance	128
7.1 Micro WC-Co mold	130
7.2 Micro zirconia mold	133
8. Conclusions	137
References	140
국문 초록	148

List of Figures

Figure 1. Schematic diagram of an EDM system	13
Figure 2. The machining mechanism of EDM	15
Figure 3. Die-sinking EDM system.....	17
Figure 4. ED-drilling and ED-milling systems	19
Figure 5. Wire and strip-EDM systems.....	21
Figure 6. Micro EDM system	23
Figure 7. Atomic-scale view of discharge plasma channel	27
Figure 8. Polarities of a tool electrode and a workpiece and current direction	28
Figure 9. Different types of electrode wear	29
Figure 10. The disadvantages of length wear in micro EDM	30
Figure 11. The disadvantages of edge wear in micro EDM	31
Figure 12. Long pulse EDM	33
Figure 13. EDM system with deionized water	36
Figure 14. Linear compensation method	38
Figure 15. Uniform wear method	40
Figure 16. The mechanism of PMEDM	44
Figure 17. Low surface roughness of PMEDM	46
Figure 18. Discharge signals	48
Figure 19. The charge and delay time of pure and powder-mixed dielectric fluids.....	49
Figure 20. Previous explanation of low tool wear in PMEDM	51

Figure 21. Tool size effect on wear length	53
Figure 22. The system of micro PMEDM	57
Figure 23. WEDM system for micro tool fabrication and micro tool	58
Figure 24. Tool feed control	62
Figure 25. The modeling of RC-discharge circuit	69
Figure 26. The simulation results of RC-discharge circuit	70
Figure 27. The experimental results of single discharge	71
Figure 28. The discharge time of virtual discharge switch.....	72
Figure 29. The experimental results of multiple discharges	73
Figure 30. The generation mechanism of discharge plasma channel.....	74
Figure 31. Two experiments to investigate the effect of gap	76
Figure 32. The modified experimental set up for discharge crater analysis	78
Figure 33. The discharge craters at the discharge gaps	81
Figure 34. The comparisons of discharge craters at the different discharge gap ...	82
Figure 35. The discharge crater at 5 μm in PK	84
Figure 36. The discharge craters at 5 μm in GPMK	85
Figure 37. The comparisons of discharge craters at 5 μm	86
Figure 38. Mechanism of tool wear reduction in PMEDM	88
Figure 39. The results at different gap distances	90
Figure 40. The effect of powder size and concentration on discharge gap	94
Figure 41. The schematic diagram and coordinates of micro ED-drilling	95
Figure 42. The machining results of open voltage	99
Figure 43. The machining results of capacitance	102

Figure 44. The optimum machining results of micro ED-drilling in PK	104
Figure 45. The optimum machining results of micro ED-drilling in GPMK	105
Figure 46. The performance evaluation of GPMK compared with PK in micro ED-drilling	106
Figure 47. The schematic diagram and coordinates of micro ED-milling	107
Figure 48. The machining results of PK and GPMK with several DoCs	111
Figure 49. The cross section views in lateral Y-Z plane and the micro tool electrode after machining by PK with several DoCs	112
Figure 50. The cross section views in lateral Y-Z plane and the micro tool electrode after machining by GPMK with several DoCs	113
Figure 51. Curvature radius of the bottom surface of the micro channel.....	114
Figure 52. The slope of bottom surface of the micro channel along the stroke direction (X-Z plane) with several DoCs	115
Figure 53. The machining results of open voltage	118
Figure 54. The machining results of capacitance	121
Figure 55. The optimum machining results in micro ED-milling	124
Figure 56. The performance evaluation of GPMK compared with PK in micro ED-milling	126
Figure 57. The finishing step of ED-milling.....	129
Figure 58. Micro WC-Co mold and replicated PDMS.....	132
Figure 59. Machining process of AE EDM	134
Figure 60. Micro zirconia mold and replicated PDMS.....	136

List of Tables

Table 1. Dielectric fluid characteristics	54
Table 2. Measuring equipment	59
Table 3. Gap status and feed command	61
Table 4. Nomenclature in the modeling of RC-discharge circuit	66
Table 5. Experimental conditions for discharge crater analysis	79
Table 6. Machining conditions	89
Table 7. Machining conditions for micro ED-drilling	96
Table 8. The optimum machining conditions in micro ED-drilling	103
Table 9. Machining conditions for micro ED-milling.....	108
Table 10. The optimum machining conditions in micro ED-milling.....	123
Table 11. Machining conditions for the micro WC-Co mold.....	131
Table 12. Machining conditions for the zirconia micro mold.....	135

1

Introduction

Electrical discharge machining (EDM) is one of the non-traditional machining which uses thermal and non-contacting machining method. It uses electro-thermal energy generated by discharge spark between a tool electrode and a workpiece. The generated heat melts or evaporates discharged area of a tool electrode and a workpiece, and dielectric fluid is also evaporated. With continuous supply of current, expansion pressure of evaporated dielectric fluid further removes molten material of a tool electrode and a workpiece. As one of non-contact machining methods, EDM can machine any conductive materials regardless of its

hardness [1-3]. Moreover, it can be applied in the industry which needs micro machining of hard-to-cut materials since there is near zero stress on a tool electrode.

Given that EDM is mutual process between a tool electrode and a workpiece, tool wear is inevitable and a chronic problem of micro EDM. The discharge spark always melts or evaporates not only a workpiece, but also a tool electrode. This inherent problem lowers the efficiency and accuracy of micro EDM. In micro ED-drilling, a micro tool electrode should be refabricated after the certain amount of machining. In micro ED-milling, the tool wear problem causes dimensional error as well as lowers the machining efficiency. Thus, the tool wear problem has been an obstacle preventing the broader use of micro EDM in actual industry applications.

Many engineers have attempted to solve this tool wear problem over the past few decades. Marafona et al. explained the tool wear protection mechanism by means of the deposition of a carbonaceous layer onto the tool electrode [4]. To build up this sacrificial layer, the tool electrode should be charged positively and a pulse duration of tens of microseconds is needed. However, because micro EDM usually uses a negatively charged tool electrode and pulse durations of tens or hundreds of nanoseconds to minimize the discharge energy and stabilize the machining condition, a long pulse duration may not be suitable for micro EDM. Moreover, due to the increased discharge energy stems from long pulse duration, the machined surface becomes rough. Tsai et al. showed that materials with a high melting point and low thermal conductivity could alleviate tool wear [5]. The material which has

high melting point such as tungsten or polycrystalline diamond (PCD) could mitigate the tool wear problem. Copper could lower the tool wear problem because the electro-thermal energy generated from discharge spark is not concentrated and the heat dissipates easily due to the high thermal conductivity. However, as tool size becomes smaller, only cemented tungsten carbide should be selected as the tool material given that it does not bend during the high-speed rotation of a spindle. Furthermore, PCD could not be used in real applications in the industry due to its high cost. Song et al. used deionized water as a dielectric fluid to machine tungsten carbide [6, 29]. Owing to its high thermal capacity, the cooling effect of deionized water relieve the thermal stress on a tool electrode. Deionized water, however, causes electrolytic corrosion on the periphery of machined structures of cemented tungsten carbide because cobalt binder is easily dissolved in water with electric field. The electrolytic corrosion can lower not only the machining accuracy, but also the hardness of machined surface. Furthermore, an ion filter is continuously necessary to maintain the dielectric strength of deionized water. Bleys et al. used a real-time tool wear compensation method in ED-milling [7, 34-37]. In ED-milling process, the bottom surface of machined channel should be slant along the stroke direction because of the wear length of a tool electrode. To complement this dimensional error, a tool electrode moves along the diagonal path. However, it is impossible to compensate for the side wear of a tool electrode and hard to determine an accurate amount of compensation during the machining. Moreover, although this

method could enhance the accuracy of micro EDM, low efficiency still remains as the method did not reduce tool wear. Wire EDM and stripe EDM are the most effective ways to solve the tool wear problem [1, 2, 8-10]. With continuous supply of new wire or strip as a tool electrode, these methods totally eliminate the tool wear problem. However, due to the size of wire or strip electrode, these methods cannot be used in micro ED-drilling or ED-drilling whose machined features are usually under one millimeter.

It is known that powder-mixed electrical discharge machining (PMEDM) can mitigate the tool wear problem in micro EDM. There were various studies of PMEDM, but the mechanism of tool wear reduction has not been clarified. Jeswani added graphite powder into kerosene to increase the material removal rate (MRR) and reduce the wear ratio [11]. The study showed that the addition of graphite powder lowers the insulating strength of a dielectric fluid, but the link to tool wear was not explained. Yeo proposed a hypothesis involving a crater-formation mechanism when a powder-mixed dielectric fluid was used [12]; the size of the crater is reduced, and a larger amount of re-solidified materials forms because the increased viscosity and enhanced thermal conductivity of the mixed fluid decreases the plasma heat flux in the workpiece and raises the rate of heat dissipation away from the molten cavity. However, this study focused only on crater formation and not on the tool wear reduction relationships. Singh et al. explained that particles between a tool electrode and a workpiece become charged by electric fields and help

to bridge the discharge gap via a process termed the ‘bridging effect’ [13]. This effect decreases the insulating strength of the dielectric fluid, causing more frequent discharges to occur and in turn increasing the MRR. Moreover, the surface roughness decreases because the plasma channels become enlarged and more open. This study, however, as well did not explain the mechanism causing the tool wear reduction. Singh et al. stated that the discharge gap enlarged by powder led to reductions of the discharge impact force and energy density between a tool and a workpiece [14]. This may explain the mechanism of tool wear reduction, but potential conflicts exist with regard to higher MRR results in PMEDM.

The present study proposes a new explanation of the mechanism of tool wear reduction in micro PMEDM. An RC discharge circuit was used in our experiments because it can achieve a shorter pulse duration than a transistor circuit, which shows better machining performance outcomes [15]. The tool electrode is negatively charged in micro EDM because the energy density is lower at the cathode [16] and a sacrificial carbonaceous layer is hardly deposited on an anode given the short pulse duration of micro EDM. However, the polarity of the tool electrode fluctuated before the plasma channel is extinguished due to stray inductance, which aggravates the tool wear because reverse current flows or electrons collide with a tool electrode and increase the energy density [17]. It was found that adding graphite powder into kerosene eliminated the fluctuation of the discharge current [18]. Owing to the enlarged discharge gap with graphite powder, the energy density of discharge

plasma channel becomes weak and easily dissipated before the current oscillated. Furthermore, even though the tool electrode comes close to the workpiece than enlarged discharge gap by feed control of the tool electrode, the discharges occur with small values of energy before a capacitor is fully charged and these early discharges is also extinguished quickly before the generation of reverse current. In other words, the addition of graphite powder eventually prevented the current from oscillating, thus reducing the tool wear.

Moreover, this study evaluates the machining performance of graphite-powder-mixed kerosene (GPMK) compared to pure kerosene (PK) in micro ED-drilling and ED-milling. Graphite powder was selected as an additive because it has low density, good conductivity, and no flammability. Due to the enlarged discharge gap of GPMK, the size of tool electrode should be smaller than that of PK in order to machine the same-size features. Furthermore, the machining parameters such as open voltage, capacitance, and depth of cut (DoC) should be optimized according to each machining fluids.

This dissertation consists of eight chapters.

Chapter 1 introduces the purpose of this study; clarifying the mechanism of tool wear reduction in micro PMEDM and performance evaluations in machining same-size micro features with GPMK.

Chapter 2 reviews the basic principle of EDM and tool wear mechanism. In the atomic-scale view, the tool wear problem stems from the collision of electrons

with a tool electrode. To prevent this collision, a tool electrode is usually negatively charged, but the current oscillation due to the second response of RLC discharge circuit makes electrons collide with a tool electrode. Many studies which attempt to solve this inevitable tool wear problem are introduced such as long-pulse EDM, tool-material-change method, deionized water, compensation method, and wire or strip-EDM.

Chapter 3 introduces the PMEDM and its four characteristics; low surface roughness, high MRR, low tool wear, and small tool size. The main mechanism of PMEDM is bridging effect, which means that polarized conductive particles in electric field serve as bridges in the discharge gap. This mechanism not only lowers the insulation strength of dielectric fluid and enlarges the discharge gap, but also facilitates the occurrence of discharge.

Chapter 4 introduces the experimental set up for PMEDM and the process for micro tool fabrication. Furthermore, measuring equipment and the principle of tool feed control is briefly explained.

Chapter 5 suggests a new explanation of the mechanism of tool wear reduction in micro PMEDM with GPMK. An RC discharge circuit is modeled, and the simulation results are compared to the experimental discharge signals. As a result of second order response of the RLC circuit, the reverse current flows because the polarity of a tool electrode oscillates before discharge plasma channel extinguishes, which intensifies tool wear. However, with GPMK, the discharge

plasma channel is quickly dissipated before reverse current flows, which alleviates the tool wear problem. The two reasons of this early extinction of discharge plasma channel are explained with the comparisons between discharge craters of PK and GPMK.

Chapter 6 evaluates the machining performance of GPMK in micro ED-drilling and ED-milling. While the machining parameters in ED-drilling are open voltage and capacitance, the evaluation indexes are MRR, tool wear length (TWL), taper angle of machined hole, machining gap, and surface roughness. On the other hand, in ED-milling, while the machining parameters are DoC, open voltage, and capacitance, the evaluation indexes are MRR, TWL, bottom curvature, bottom slope, machining gap, surface roughness. With optimal machining conditions, the machining performance of GPMK is evaluated in micro ED-drilling and ED-milling.

Chapter 7 introduces the application of PMEDM technique; a micro mold. It is necessary to use material which has superior mechanical strength and wear erosion resistance for micro mold fabrication. As one of non-contacting machining methods, PMEDM successfully machines micro features on cemented tungsten carbide (WC-Co). Moreover, with the assisting electrode method, PMEDM also can machine micro features on zirconia which is one of non-conducting engineering ceramics but has superior chemical resistance as well as wear resistance.

CHAPTER 1. INTRODUCTION

Chapter 8 concludes this study along with mechanism of tool wear reduction of PMEDM, and performance evaluations of GPMK in micro ED-drilling and ED-milling.

This dissertation cites forty-six references comprised of journal papers, books, and articles from technical magazines. These references were chosen to create a research project that is based not only on theoretical study, but that is also practical and demonstrates an actual machining process.

2

Tool Wear in Electrical Discharge Machining

This chapter introduces the basic principles of EDM and tool wear problem. Tool wear is an inherent problem because EDM basically uses the spark energy generated from the discharge between a tool electrode and a workpiece. This mutual process always wears a tool electrode as well as machine a workpiece. Many studies have attempted solve this problem, but tool wear is still a chronic problem in micro EDM.

2.1 Principles of EDM

An EDM system consists of four major components: a tool electrode, a workpiece, a discharge circuit, and a dielectric fluid, as shown in Fig. 1. A discharge circuit includes a power source such as AC or DC and the components which can make discharge pulse signal like a MOSFET or resistance & capacitance (RC). A discharge circuit supplies electrical energy to a tool electrode and a workpiece through the form of pulse because continuous supply of energy could aggravate the machining performance such as MRR, TWL, and surface roughness. A tool electrode and a workpiece are submerged into dielectric fluid. The role of dielectric fluid is an insulator before the discharge occurs and a conductor during the discharge. Moreover, after discharge, a dielectric fluid flushes debris away from the machining gap and prepare the next discharges by recovering insulation strength between a tool electrode and a workpiece. It also serves as a coolant of the tool electrode to alleviate the wear [19].

The machining process of EDM consists of six steps as shown in Fig. 2 [20-22].

Step 1) Since there is a difference of electrical potential energy between the tool electrode and the workpiece, the electric field is generated and becomes intense as a tool electrode moves toward a workpiece. The voltage between them maintains at pre-set value, called open voltage, and the current is at

CHAPTER 2 Tool Wear in ELECTRICAL DISCHARGE MACHINING

zero level.

Step 2) When a tool electrode reaches the certain distance from the workpiece, called discharge gap, discharge occurs. The discharge means electrical potential energy ionize the molecules of a dielectric fluid and electrons and positive ions serve as carriers in the discharge plasma channel for the flow of current. Therefore, the voltage drops and current starts to flow.

Step 3) By intensive heat flux of discharge plasma channel, some portions of a tool electrode and a workpiece melt and evaporate. Moreover, a dielectric fluid also vaporizes due to the heat of discharge plasma channel. The voltage maintains at certain level as the current flows.

Step 4) With the continuous supply of energy, the discharge plasma channel and vaporized dielectric fluid expand. The expansion pressure further eliminates the molten material from a tool electrode and a workpiece. The voltage maintains at certain level as the current flows.

Step 5) As the current stops after pre-set pulse duration, the discharge plasma channel is extinguished. The machining process ends and both the voltage and current drops to zero level.

Step 6) Debris between a tool electrode and a workpiece are flushed away

CHAPTER 2 Tool Wear in ELECTRICAL DISCHARGE MACHINING

from the discharge gap as near dielectric fluid fills the gap up. The insulation strength of discharge gap is recovered and the voltage and current prepare the next discharge to be initiated.

By repeating step 1 to 6 several thousand times in a second, EDM can machine the desirable shape on a workpiece.

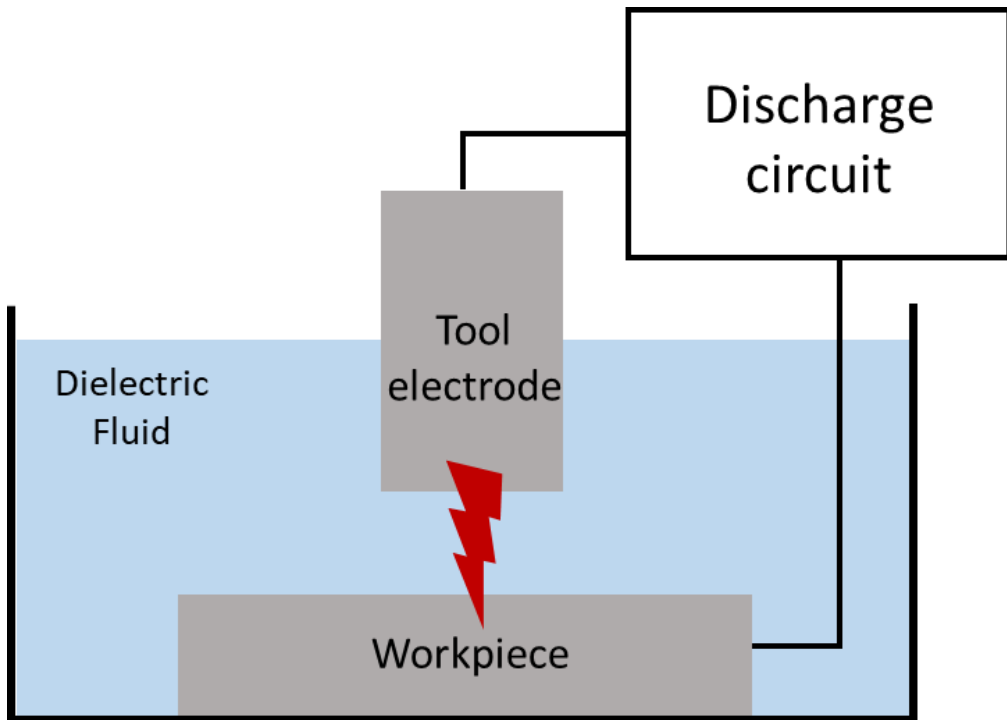
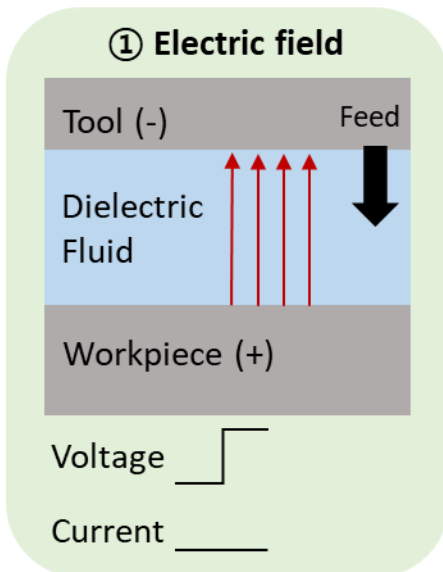
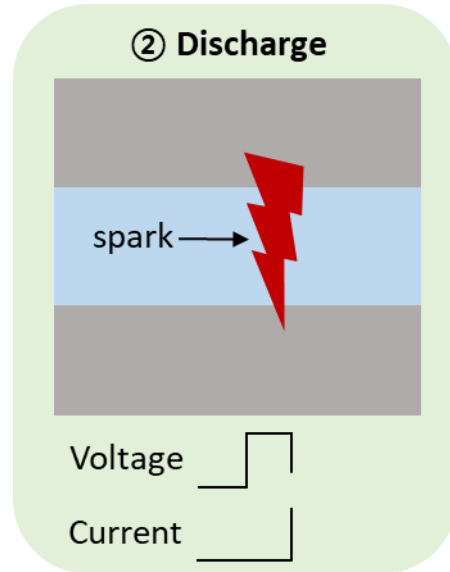


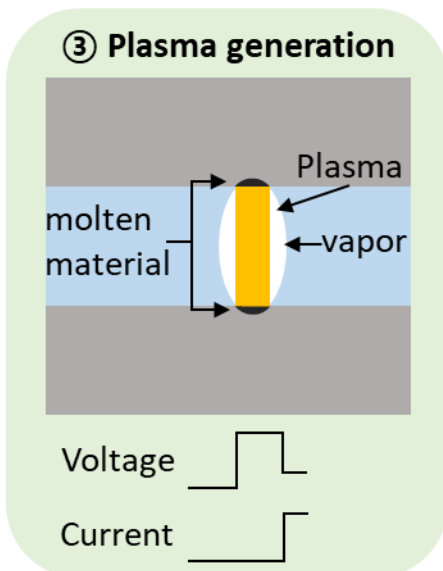
Figure 1. An EDM system.



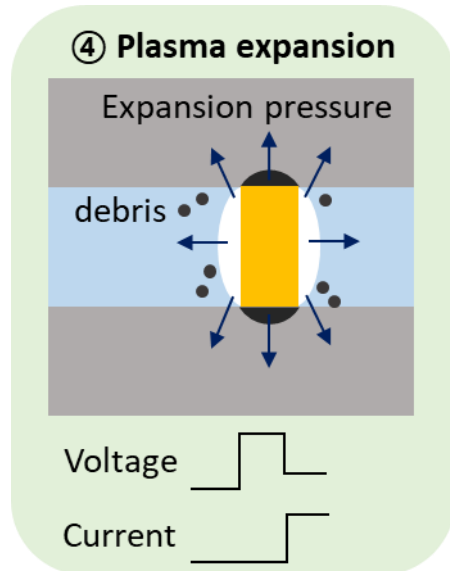
(a)



(b)



(c)



(d)

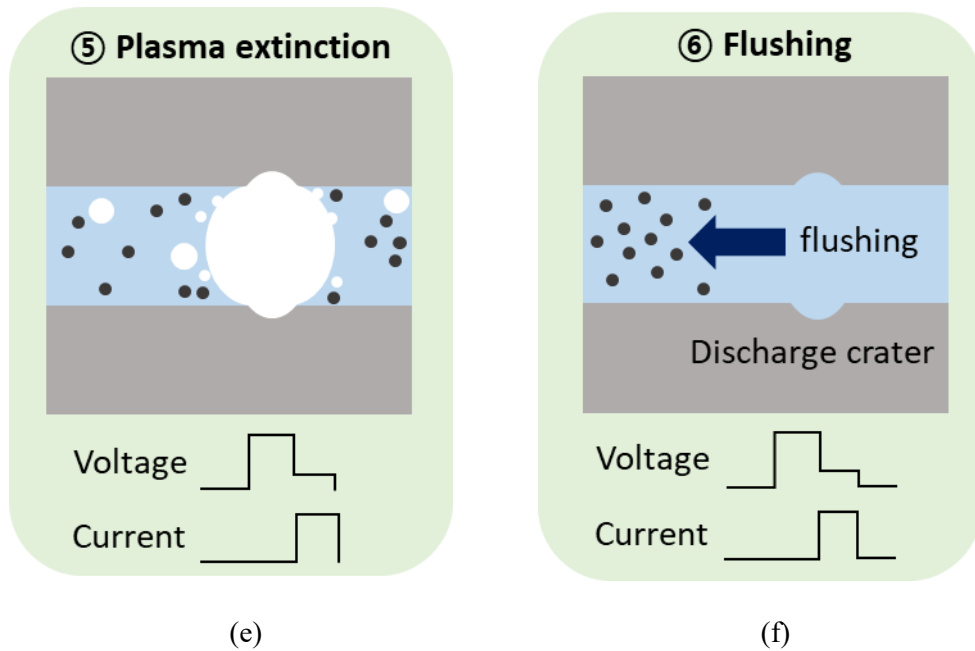


Figure 2. The machining mechanism of EDM: (a) Generation of electric field. (b) Occurrence of discharge. (c) Plasma generation. (d) Plasma expansion. (e) Plasma extinction. (f) Flushing.

2.2 Types of EDM

2.2.1 Die-sinking EDM

Die-sinking EDM, also known as general EDM, ram EDM, and vertical EDM, was developed to machine blind shapes on a workpiece such as a mold and a die. The strength of die-sinking EDM is to fabricate complex shapes on a workpiece repeatedly using just one tool electrode since the shape of tool electrode is directly casted on the workpiece. Graphite block is generally used to fabricate the tool electrode by cutting process since it is easy-to-cut material and high wear resistance in die-sinking EDM process. The die-sinking EDM system is illustrated in Fig. 3. The pre-fabricated tool electrode is held on the z-stage of the system and moves vertically. The tool electrode is positively charged and the workpiece is negatively charged, which are submerged into the dielectric fluid. Hydrocarbon-based oils such as kerosene are used in die-sinking EDM because carbon ions decomposed from the oil attaches on the tool electrode and protects the tool electrode from wear. During machining, the tool electrode not only moves downward, but also vibrates or makes jumping motions in order to improve flushing of debris [23, 24].

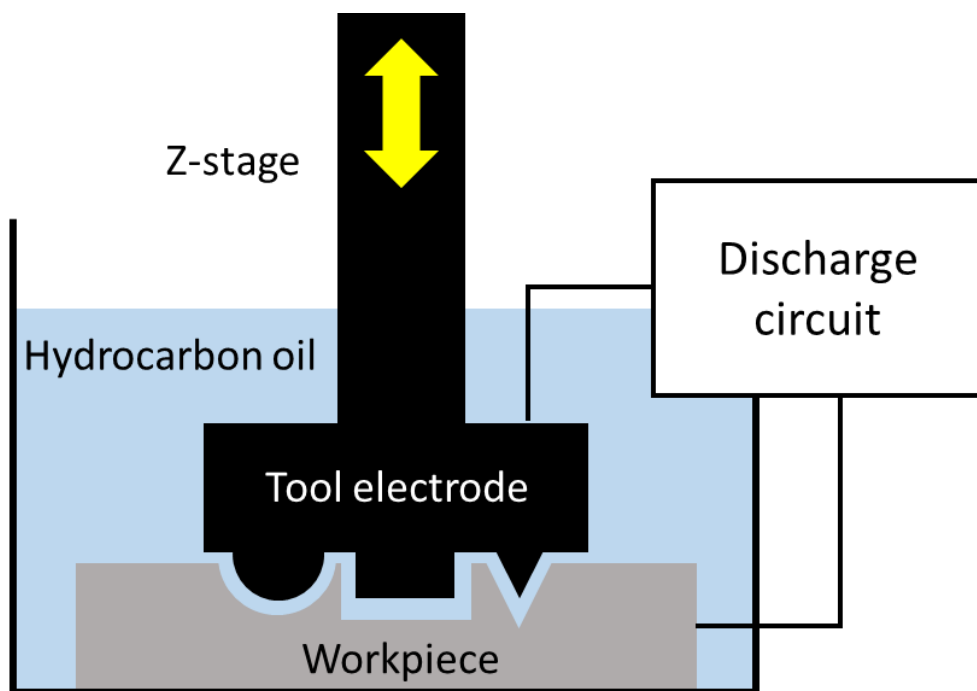


Figure 3. Die-sinking EDM system.

2.2.2 ED-drilling and ED-milling

ED-drilling and ED-milling processes are similar with conventional drilling and milling except machining mechanism. Fig. 4 shows a schematic diagram of ED-drilling and ED-milling processes. Both systems use a cylinder-shape tool electrode which rotates during the machining process. The major difference of EDM from conventional cutting machining is non-contact process. Since EDM uses a dielectric fluid as an insulator, continuous supply of the fluid is critical. However, it is hard to supply a dielectric fluid to the machined surface through narrow discharge gap as machined features become deepen. For sufficient supply of a dielectric fluid, a tube electrode is widely used as the tool in ED-drilling and ED-milling systems. A dielectric fluid is supplied through the inner holes of a tube electrode; thus, continuous supply and discharge are stable. Both hydrocarbon-based oil and deionized water are used as dielectric fluids in an application of the industry.

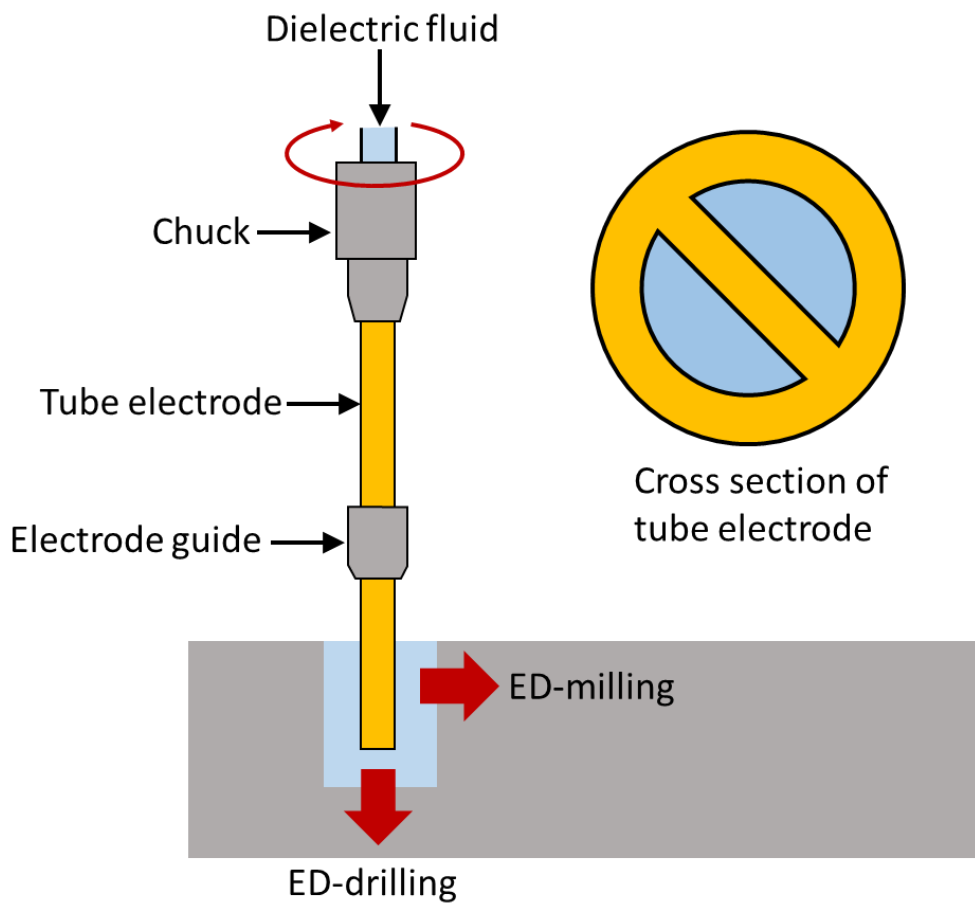


Figure 4. ED-drilling and ED-milling systems.

2.2.3 Wire and Strip-EDM

Wire and strip-EDM were developed to eliminate tool wear problem [1, 2, 8-10]. The most critical defect of EDM process is tool wear. As explained in chapter 2.1, tool wear is inevitable because the machining mechanism of EDM is a mutual process between an anode and a cathode. The tool wear problem lowers machining accuracy and efficiency. The basic concept of both wire and strip EDM is the use of continuously supplied wire and strip as a tool electrode. As shown in Fig. 5, worn wire and strip are replaced with new ones; thus, machining accuracy and efficiency are drastically improved.

Strip-EDM was developed to complement the weaknesses of wire-EDM. If excessive discharge energy is induced in wire-EDM, thin wire is easily cut off since it is pulled tightly for high machining accuracy [25]. Given that strip is a kind of broad wire, it is free from the breakage problem. Furthermore, strip-EDM can be applied in milling and turning process [9, 8]. Wire ED-milling system was also developed with a reciprocating motion of wire guide which prevents thin wire from getting tangled [10]. However, this system needs additional a reciprocating motion while strip-EDM does not need it.

Deionized water is widely used in wire and strip-EDM process with an AC power source. Deionized water has high MRR but causes electrolytic corrosion on

some kinds of metal workpieces. Although an AC power source deteriorates the degree of tool wear significantly, it can suppress electrolytic corrosion of metal since the average applied voltage is zero [26]. Because wire and strip-EDM eliminates tool wear problem, AC power source is suitable for both systems.

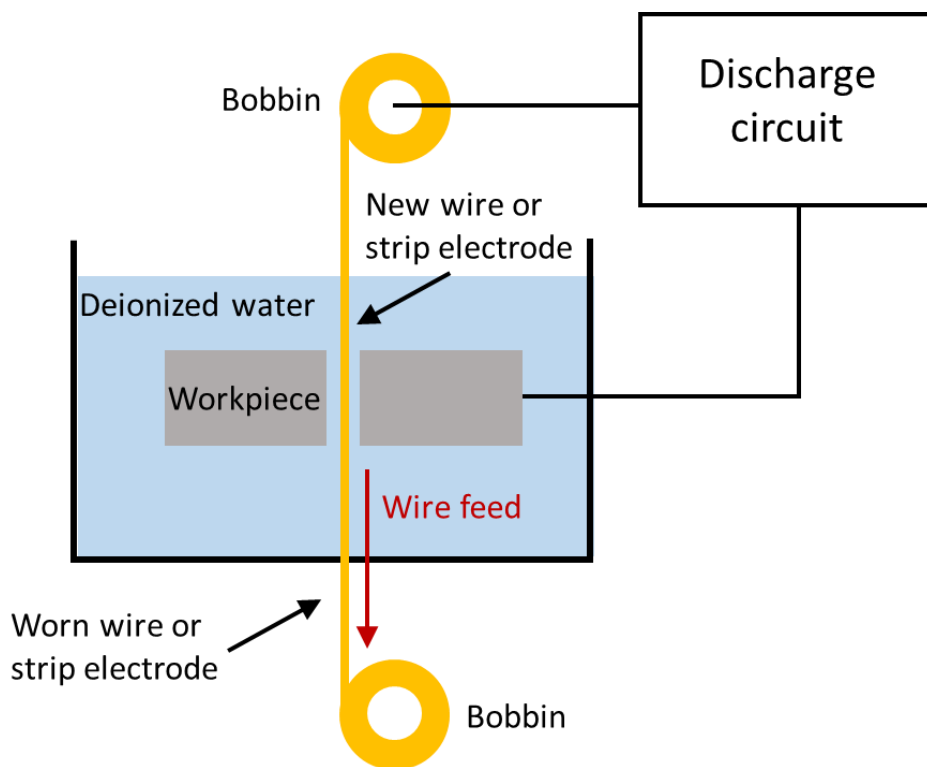


Figure 5. Wire and strip-EDM systems.

2.2.4 Micro EDM

Machining micro features on hard-to-cut materials is one of advantages of EDM. In conventional cutting process, the mechanical strength of a tool become crucial as the size of it is reduced and the hardness of workpiece is increased. Based on non-contact and thermal process, EDM can machine micro features without the breakage of a tool electrode.

Micro EDM uses an RC-discharge circuit because of its short pulse duration. The key factor of micro EDM is to generate single discharge energy as small as possible. There are two types of discharge circuit: RC and TR-discharge circuits. Because an RC-discharge circuit creates discharge pulse trains by periodical charging and discharging of a capacitor, the discharge energy is controlled by adjusting the size of a capacitor. On the other hand, given that a TR-discharge circuit produces discharge pulse trains through the switching of a FET, the pulse-on time determines the discharge energy [20]. However, due to the limitation of switching speed of a FET, an RC-discharge circuit can generate smaller discharge energy than a TR-discharge circuit. Fig. 6 shows schematic diagram of micro EDM system with RC discharge circuit.

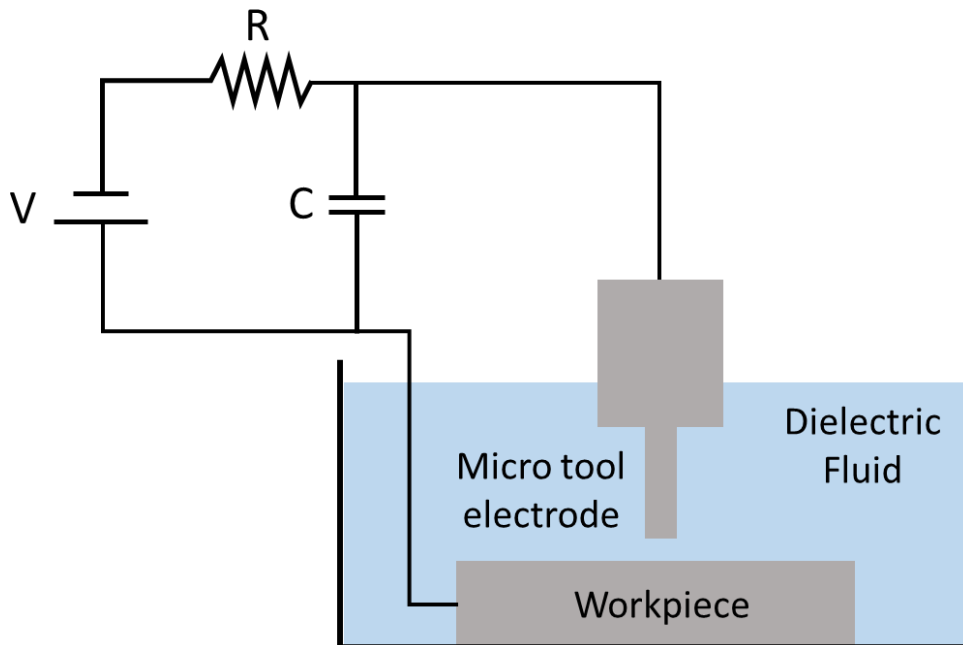


Figure 6. Micro EDM system.

2.3 Principle of Tool wear

An atomic-scale view of the discharge plasma channel is illustrated in Fig. 7. If a tool electrode is negatively charged and a workpiece is positively charged, the cathode emits electrons when the discharge is initiated. Due to the electric field between a tool electrode and a workpiece, the electrons accelerate toward an anode. Given that there are many molecules inside a dielectric fluid, electrons collide with molecules and convey the kinetic energy. This energy makes the other electrons of molecules escape from the atomic nuclear and these electrons also starts to accelerate toward an anode. Moreover, these electrons also collide with molecules of a dielectric fluid and release another electron. Due to this chain reaction, tons of electrons eventually collide with an anode and make temperature increase intensively, which is called electron avalanche [27, 28]. On the other hand, molecules that lose the electrons due to the collisions become positive ions and start to accelerate a cathode. However, its mass is very heavy in comparison with electrons; thus, it needs relatively longer time to reach a cathode than the time necessary for electrons to reach an anode. Therefore, the energy distribution of an anode is higher than a cathode, and electrons are considered as the primary source of energy for EDM material removal [20]. The collisions of electrons and positive ions with each side cause the surface materials of both an anode and a cathode to melt or vaporize. The phenomenon occurring on the surface of a workpiece is

CHAPTER 2 Tool Wear in ELECTRICAL DISCHARGE MACHINING

referred to as machining and the phenomenon occurring at a tool electrode is referred to as tool wear.

Micro EDM uses pulse duration of tens or hundreds of nanoseconds for stable machining status. This short pulse duration allows the lower number of heavy positive ions to reach a cathode. Because an anode has higher energy distribution, a tool electrode is negatively charged, and a workpiece is positively charged for high MRR and low tool wear. Therefore, current flows from the workpiece to a tool electrode, which is hereafter called forward current. If the polarities of a tool electrode and a workpiece are reversed, current flows from a tool electrode to a workpiece, which is hereafter called reverse current. Fig. 8 shows the relationship between polarities and machining performance in micro EDM.

There are two types of tool wear during EDM process: length wear and edge wear (Fig. 9). The length wear is determined by the difference between the length of a tool electrode before and after machining. Since the bottom surface of a tool electrode mainly experiences discharge spark during EDM process, the length wear is more severe than the edge wear. The length wear lowers the machining efficiency of micro ED-drilling process and sloped bottom surface of micro channel along the stroke direction in ED-milling process (Fig. 10). The edge wear is determined by the curvature of the edge of a tool electrode after machining. Given that the density of electric field is more intense at the edge than the flat surface of a tool electrode,

CHAPTER 2 Tool Wear in ELECTRICAL DISCHARGE MACHINING

the density of discharge current increases and the edge becomes blunt. The edge wear could cause shape error in machined micro feature; a tapered hole in micro ED-drilling process and the curved bottom surface of a channel in micro ED-milling process (Fig. 11).

To estimate the amount of tool wear quantitatively, relative wear ratio (RWR) is commonly used in EDM process. RWR is calculated by the ratio of the worn volume of a tool electrode to the machined volume of a workpiece.

$$\text{RWR [\%]} = \frac{\text{Worn volume of a tool electrode}}{\text{Machined volume of a workpiece}} \times 100[\%] \quad (1)$$

On the other hand, in micro EDM, TWL is also used as the machining performance index rather than RWR because the fabrication of a micro tool whose diameter under 100 μm is a custom process and length wear is directly related to the machining efficiency. Therefore, TWL was used to evaluate the amount of tool wear in this study.

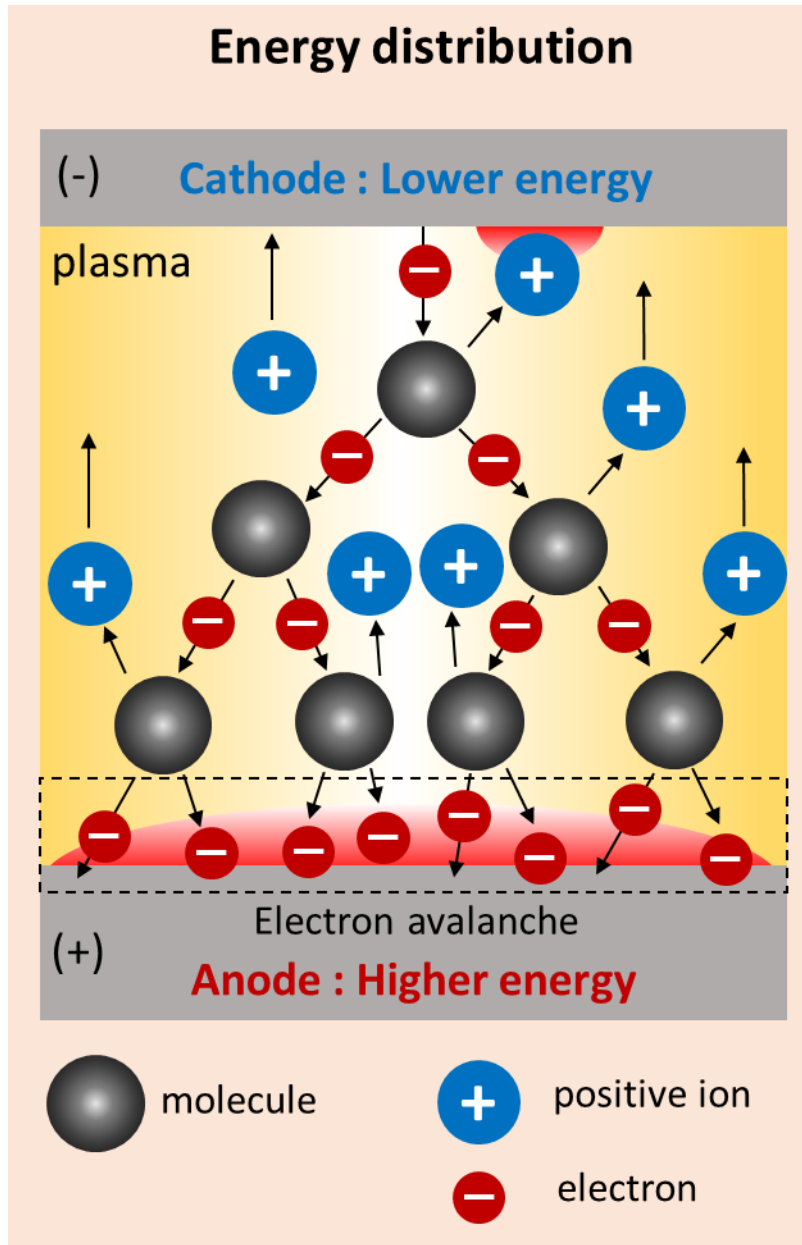


Figure 7. An atomic-scale view of discharge plasma channel.

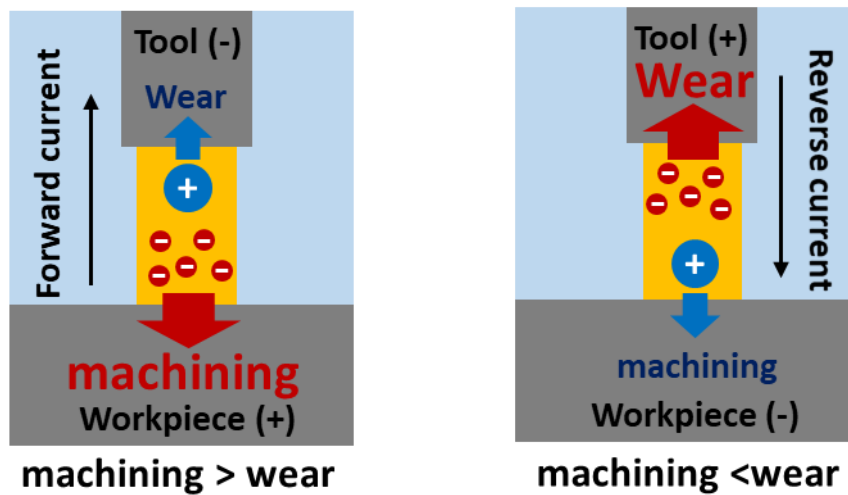


Figure 8. Polarities of a tool electrode and a workpiece and current direction.

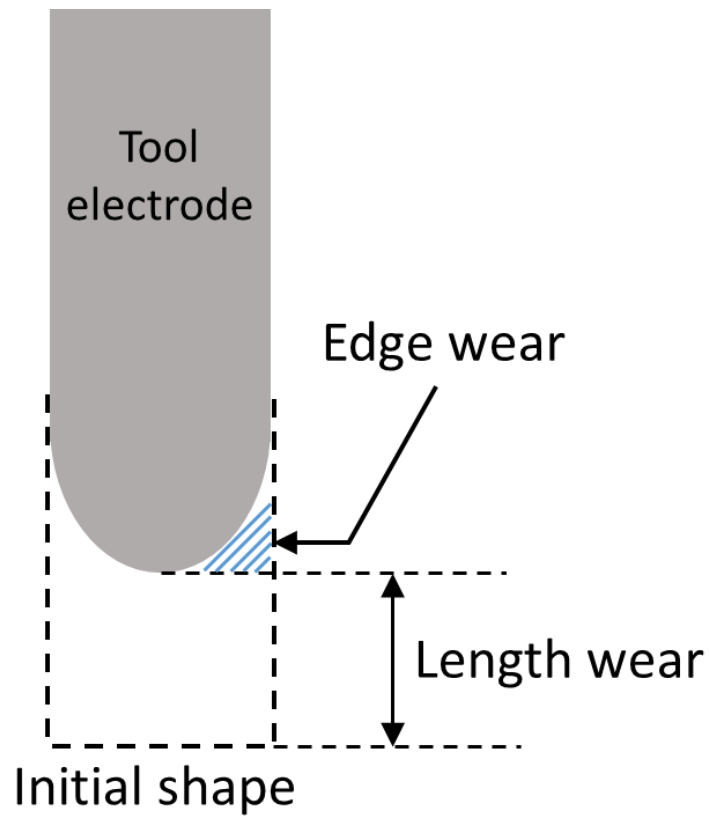


Figure 9. Different types of electrode wear.

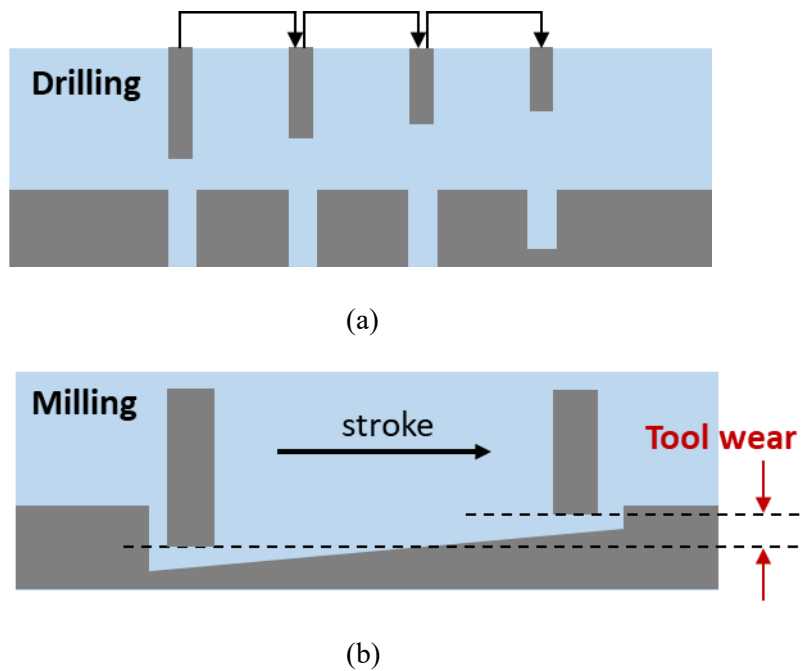
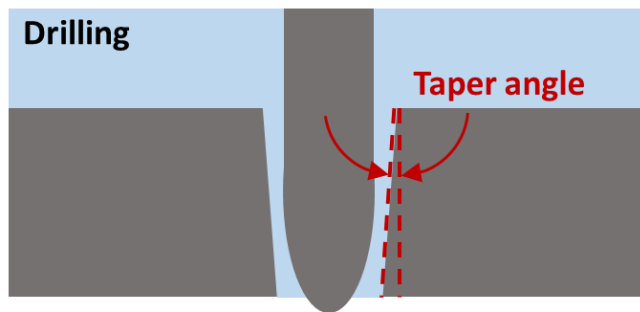
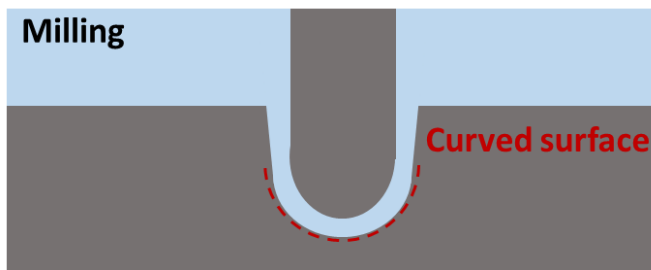


Figure 10. The disadvantages of length wear in micro EDM: (a) Low efficiency in micro ED-drilling. (b) Low accuracy in micro ED-milling.



(a)



(b)

Figure 11. The disadvantages of edge wear in micro EDM: (a) Tapered hole in micro ED-drilling. (b) Curved bottom surface in micro ED-milling.

2.4 Previous research of tool wear problem

2.4.1 Long pulse EDM

In die-sinking EDM, a tool electrode is positively charged and a workpiece is negatively charged, and hydrocarbon-based oil such as kerosene is used as a dielectric fluid as shown in Fig. 12. When pulse duration is over tens or hundreds of micro seconds, carbon ions decomposed from a dielectric fluid attach on an anode or a tool electrode as the temperature of discharge plasma channel decreases. This carbon layer plays as sacrificial layer which protects a tool electrode from wear [20, 21]. Even though this long pulse strategy can reduce tool wear, MRR decreases because the energy density of an anode is higher than a cathode. Moreover, long pulse strategy is not proper in micro EDM since it could cause low machining stability. Long pulse does not allow enough time for debris to evacuate from the discharge gap. The debris in the discharge gap could cause concentrated discharge, or arc discharge, which deteriorates the machining stability and surface roughness and needs a proper flushing system. It is hard to install an effective flushing system in micro EDM due to its small features; thus, the long pulse is not suitable for micro EDM.

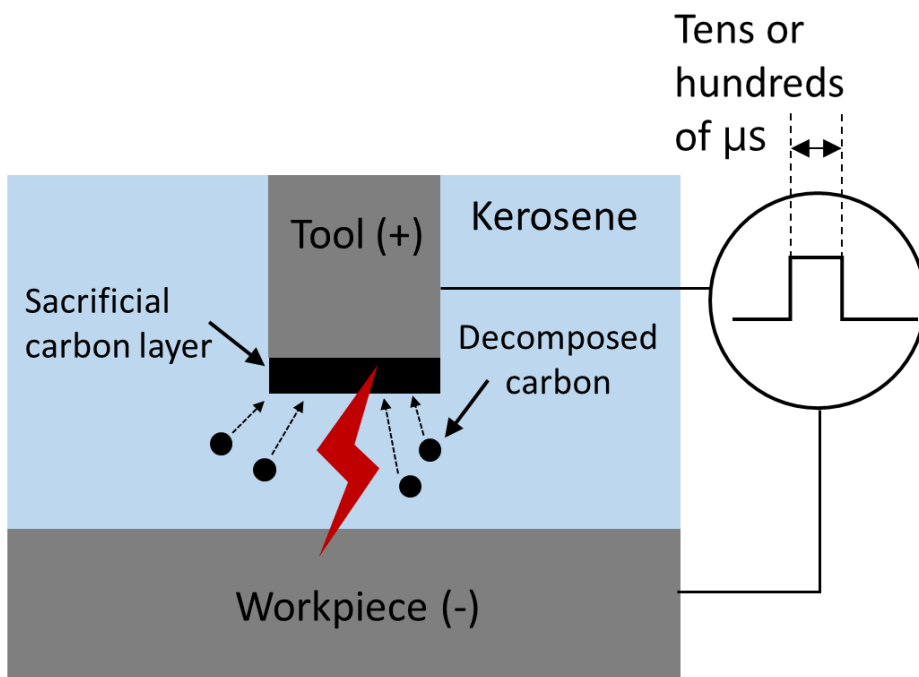


Figure 12. Long pulse EDM.

2.4.2 Tool material change

The use of material which has high melting point or high thermal conductivity can decrease tool wear [5]. Since EDM process is mutual process between a tool electrode and a workpiece, it cannot prevent the temperature of a tool electrode from rising. However, the material whose melting point is higher than the workpiece such as PCD and tungsten could alleviate tool wear. Moreover, the use of copper could also mitigate tool wear because it has high thermal conductivity. It can avoid the accumulation of discharge energy; thus, temperature of discharge spot increases with slower speed than the material which has lower thermal conductivity. However, the use of PCD is very expensive and lowers the machining efficiency. Furthermore, when micro tool diameter is under 100 μm , only cemented tungsten carbide could be used as tool material because it has high mechanical strength and other materials except PCD could be bent during micro EDM. Therefore, it is hard to use other materials except cemented tungsten carbide as a tool material in micro EDM.

2.4.3 Deionized water

The use of deionized water as a dielectric fluid can lower tool wear owing to its high heat capacity [6, 29]. Basically, water is hardly used as a dielectric fluid in EDM because many ions in water cannot keep electrical insulation status in electric field. Hence, water is deionized using ion filter before filling up the discharge gap. Owing to its high heat capacity, the cooling effect decrease tool wear. However, as depicted in Fig. 13, deionized water should be replaced with new one because many ions are generated during EDM process and the used water loses insulation strength. This method needs continuous supply of deionized water which pass through the ion filter. Moreover, cemented tungsten carbide suffers from electrolytic corrosion since cobalt binder in the material easily dissolved into deionized water when electric field is applied. It seriously devastates the quality of machining surface. The hardness become weaker and unwanted portion of material is excessively removed. There were previous studies which improve the electrolytic corrosion of cemented tungsten carbide in deionized water by using AC power source, spray deionized water, bipolar pulse [6, 19, 26, 29-33]. These methods successfully prevent the electrolytic corrosion, but additional device should be equipped.

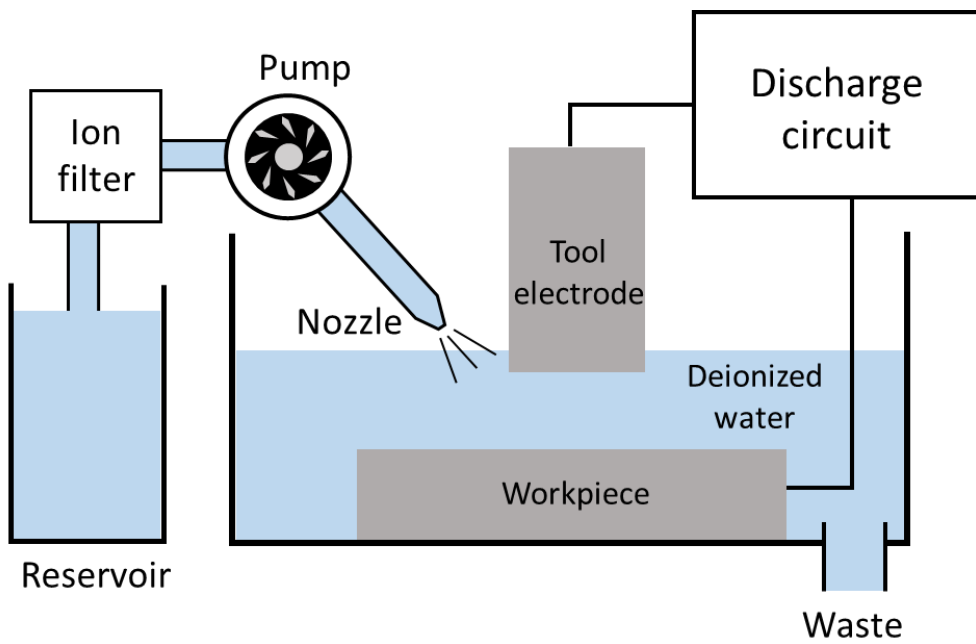


Figure 13. EDM system with deionized water.

2.4.4 Linear compensation method

Linear compensation method (LCM) refers that a tool electrode moves downward as well as horizontally in ED-milling process [7, 34-37]. When a tool electrode moves along the horizontal path during the machining process, the bottom surface of machine channel is slant due to the length wear. To compensate this length wear, tool electrode path is planned to move not only along the horizontal line, but also the direction of wear as illustrated in Fig. 14. However, it is difficult to predict the compensation length and this method could intensify the edge wear of a tool electrode. Furthermore, even though it can compensate the dimensional error of machined features, the machining efficiency is still low because it is not fundamental strategy which can solve the tool wear problem.

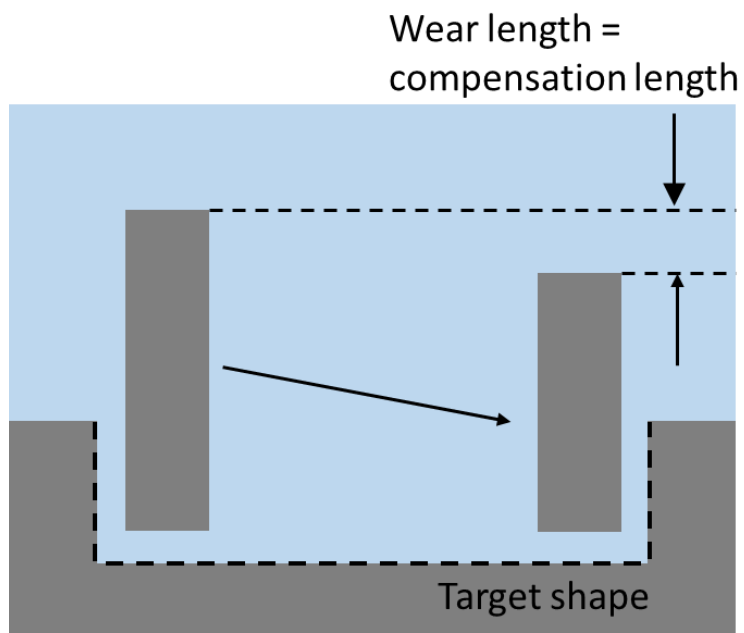


Figure 14. Linear compensation method.

2.4.5 Uniform wear method

The basic concept of uniform wear method (UWM) is layer-by-layer machining process in micro ED-milling (Fig. 15) [38]. Due to the edge wear of a tool electrode, it is difficult to machine micro features of complex three-dimensional shape with micro ED-milling process. However, owing to the uniform wear at the end of a tool electrode, the edge wear is reduced and the original shape of a tool electrode is maintained even though a simple cylinder-shape tool electrode is used. It converts the three-dimensional electrode wear to a linear one; thus, complicated three-dimensional cavities can be successfully machined with LCM. In machining simple straight micro channel, the basic equation for the compensation is derived as follows. After n layers of machining, the total wear of a tool electrode is

$$(n \cdot \Delta Z - n \cdot L_w) S_e = n \cdot L_w \cdot S_w \cdot v. \quad (2)$$

By reordering in terms of L_w

$$L_w = \Delta Z / (1 + v \cdot \frac{S_w}{S_e}) \quad (3)$$

is obtained where L_w is average machined depth for one layer, S_e is cross-sectional area of the electrode (X-Y plane), S_w is cross-sectional area of the micro channel (X-Y plane), and v is volumetric relative wear. However, the machining time increases remarkably when thickness of each layer become thin. Thus, the relationship of

shape error and machining speed should be evaluated.

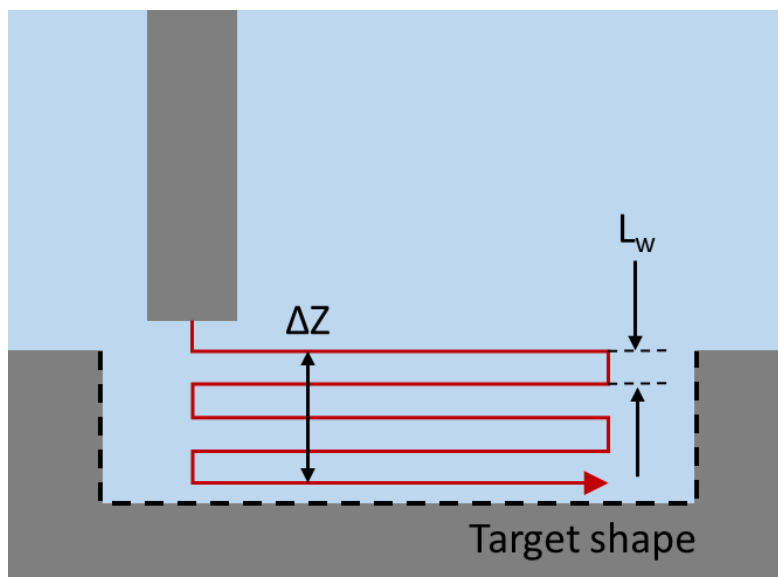


Figure 15. Uniform wear method.

2.4.6 Wire and Strip-EDM

Wire and Strip-EDM totally eliminate tool wear problem by continuous supply of wire and strip as a tool electrode [1, 2, 8-10]. Worn wire and strip after discharge is removed and replaced with new one to solve any problems regarding tool wear. Wire EDM is widely used in real industry with AC power source in order to machine material vulnerable to electrolytic corrosion in deionized water such as cemented tungsten carbide. AC power source perfectly prevent electrolytic corrosion in deionized water but causes severe tool wear [26]. Because wire EDM eliminates tool wear problem, it is well suitable for AC power source. However, thin wire easily break after arc discharge occurs or excessive tension is engaged in wire EDM [25]. To complement this defect, strip-EDM was developed and showed more stable machining stability [8, 9]. It successfully proved its superior machining performance in cutting, milling, and turning process. However, both machining method are not suitable for micro ED-milling and ED-drilling process because of the size of guide for wire and strip electrodes.

3

Powder Mixed EDM

This chapter introduces the basic principle of powder mixed EDM (PMEDM) and its four characteristics. Conductive or semi-conductive powders are added into a dielectric fluid in PMEDM. By electric field between a tool electrode and a workpiece, powder is polarized and weaken the insulation strength of a dielectric fluid. It eventually enlarges the discharge gap and facilitates the occurrence of discharge. PMEDM increases MRR by high discharge frequency and improves surface roughness by lower expansion pressure of vaporized dielectric fluid due to the enlarged discharge gap. PMEDM also mitigate the tool wear, but the mechanism is not clarified. Moreover, due to the enlarged discharge gap, a tool electrode should

become smaller than normal EDM to machine same-size micro features. The mechanism of tool wear reduction and quantitative evaluation of machining performance in machining of same-size micro features are the research objectives of this study.

3.1 Principle of powder mixed EDM

The basic mechanism behind PMEDM is bridging effect [13]. As shown in Fig. 16, conductive or semi-conductive particles become polarized due to the electric field between a tool electrode and a workpiece. The particles adjacent to a tool electrode generate micro discharges and are connected electrically [39]. By repetition of micro discharges, the gap between a tool electrode and a workpiece becomes narrow, which means that electrical breakdown can occur even though the gap is larger than the discharge gap of a pure dielectric fluid. The polarized particles serve as stepping stones of path of electrons in the discharge gap and cause series discharge which means discharge occurs through the polarized particles, not directly between an anode and a cathode [40]. Thus, it reduces the insulation strength of a mixed fluid and enlarges the discharge gap in comparison with a pure dielectric fluid.

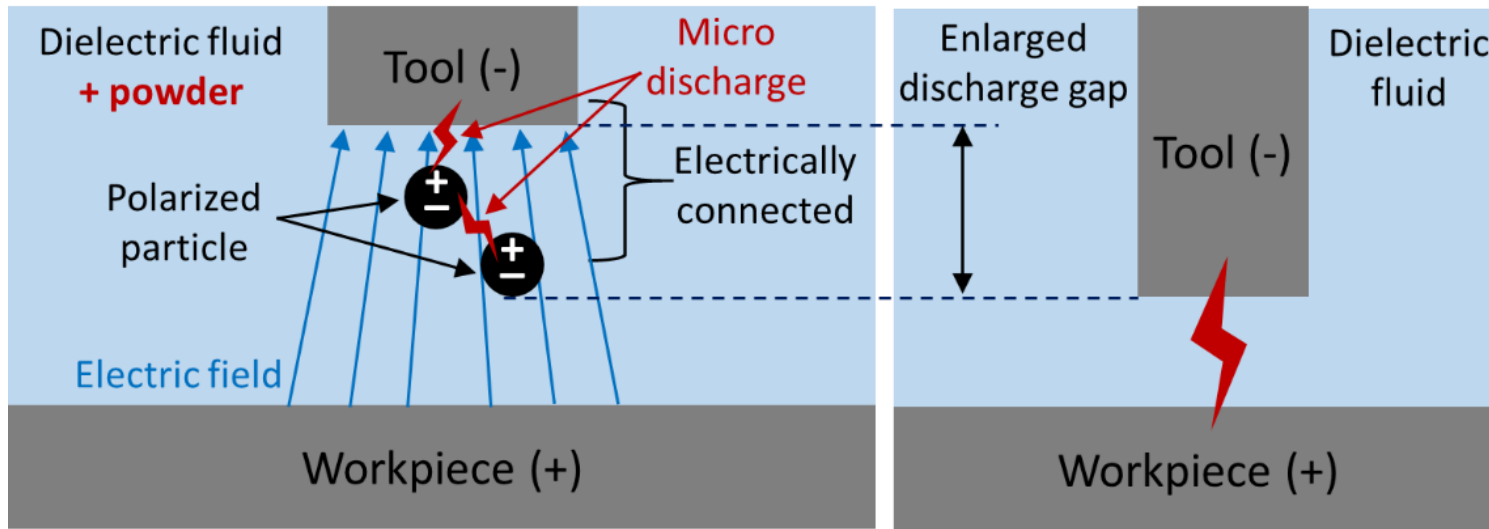


Figure 16. The mechanism of PMEDM: bridging effect.

3.2 Characteristics of powder mixed EDM

3.2.1 Low surface roughness

The expansion pressure of a dielectric fluid removes molten material of the workpiece physically as explained in chapter 1, which determines the surface roughness. This mechanism necessarily leaves machining vestige called a discharge crater. The depth and diameter of crater determine the surface roughness of a machined surface. In general, the larger expansion pressure of dielectric fluid is, the rougher a machined surface is generated.

In PMEDM, the surface roughness of machined surface is improved [41]. Due to the enlarged discharge gap, the expansion pressure of dielectric fluid decreases, and it makes a swallow discharge crater. The mechanism of low surface roughness of PMEDM is illustrated in Fig. 17.

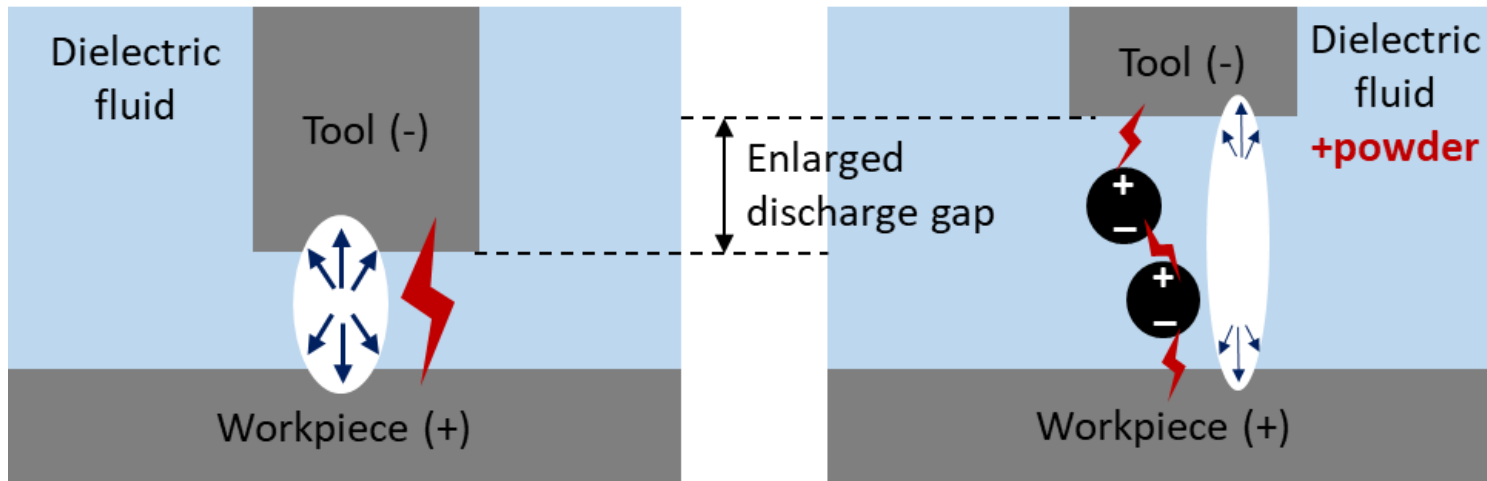
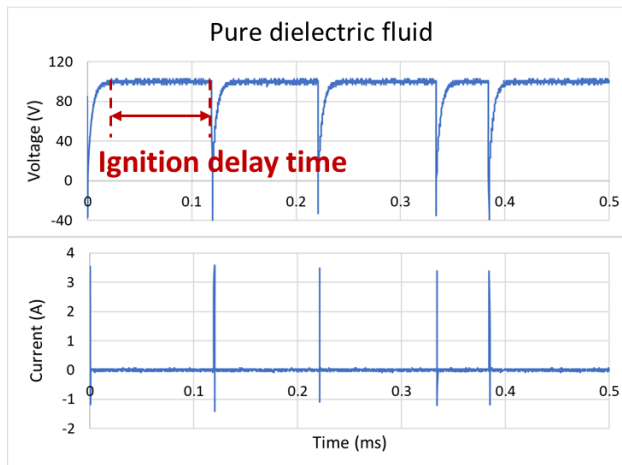


Figure 17. Low surface roughness of PMEDM.

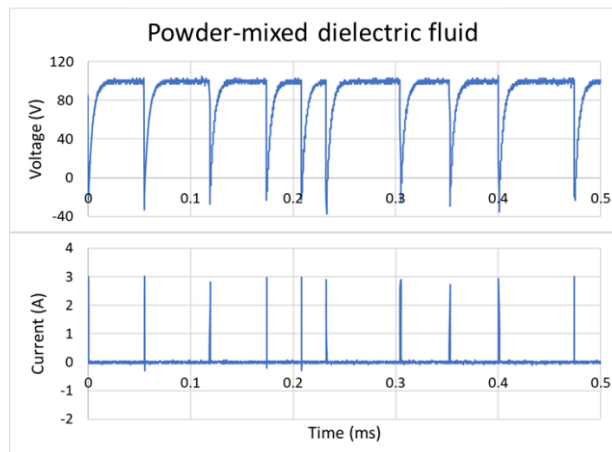
3.2.2 High MRR

During PMEDM, high MRR is possible due to the high frequency of the discharge signal. When open voltage is applied between an anode and a cathode, a uniform and even density electrical field is generated. Given that the homogeneous insulation property limits the electrical breakdown [39, 40], discharges occur after an irregular delay time even if the gap voltage is at the breakdown point. However, by adding conductive particles between the two polarities, the electric field is disturbed due to the resulting polarized conductive particles. Figs. 18(a) and (b) correspondingly show the multiple discharge signals when the pure dielectric fluid and the powder-mixed dielectric fluid are used. The tool diameter was 300 μm , the open voltage was 100 V, and the capacitance was 5 nF for both fluids. Graphite powder was used for the experiment. Even though machining conditions of both experiments are identical, it is clear that the ignition delay time is reduced, and more frequent discharges occur in the powder-mixed dielectric fluid. Fig. 19 shows the charge and delay time in both dielectric fluids. Furthermore, according to the first-stage-expansion model of Natsu et al., machining occurs at the initial stage of discharge and the temperature of the discharge plasma channel decreases as the channel expands [42]. Then, with a continuous supply of current, machining occurs again when the temperature of the plasma channel reaches the melting point of the workpiece. Given that the machining process of micro-EDM is more stable with

short discharge durations, the frequent occurrence of a short discharge contributes to a high MRR in micro-EDM.



(a)



(b)

Figure 18. Discharge signals: (a) The pure dielectric fluid. (b) The powder-mixed dielectric fluid.

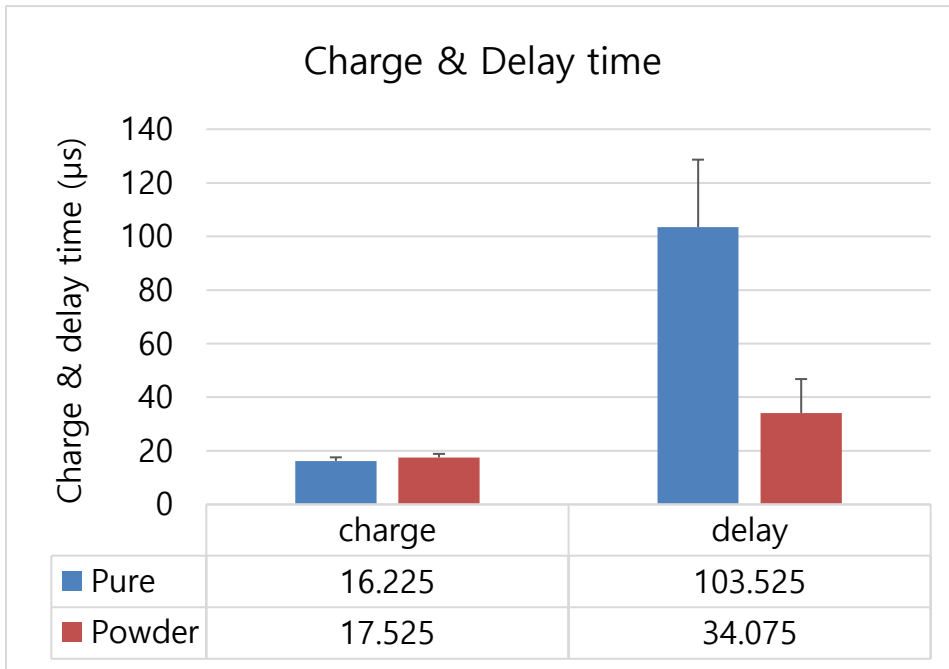
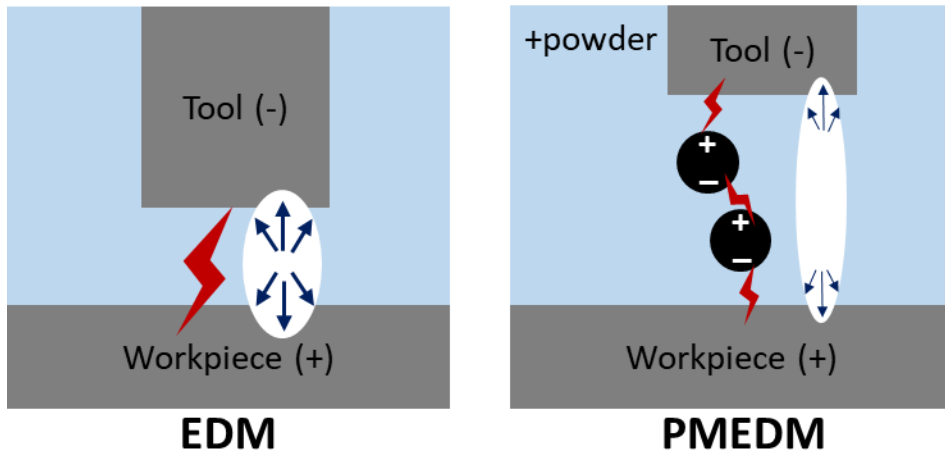


Figure 19. The charge and delay time of pure and power-mixed dielectric fluids.

3.2.3 Low tool wear

PMEDM shows lower tool wear than normal EDM, but the mechanism behind this characteristic is not clarified. One of the previous explanations of low tool wear is reduction of expansion pressure due to enlarged discharge gap [14] as shown in Fig. 20(a). As like the mechanism of low surface roughness, less amount of material of a tool electrode is removed by the reduced expansion pressure of dielectric fluid. However, this explanation has a limitation; low expansion pressure could cause low MRR because the machining mechanism of EDM process is a

mutual process between a tool electrode and a workpiece. The other previous explanation of low tool wear in PMEDM is improved flushing of debris due to enlarged discharge gap as shown in Fig. 20(b) [43]. Debris can cause abnormal discharges such as arc, which intensifies the tool wear. With powder, the enlarged discharge gap improves flushing of debris, and it could decrease the probability of abnormal discharges. The evacuation of debris from the discharge gap is related with tool wear, but abnormal discharges rarely occur with proper tool feeding condition which determines the gap size. Furthermore, the decreased number of abnormal discharges necessarily reduces MRR because abnormal discharge generally increases MRR due to its high energy. However, MRR is increased with low tool wear in PMEDM. Therefore, the other explanation also has a potential conflict with high MRR.



(a)

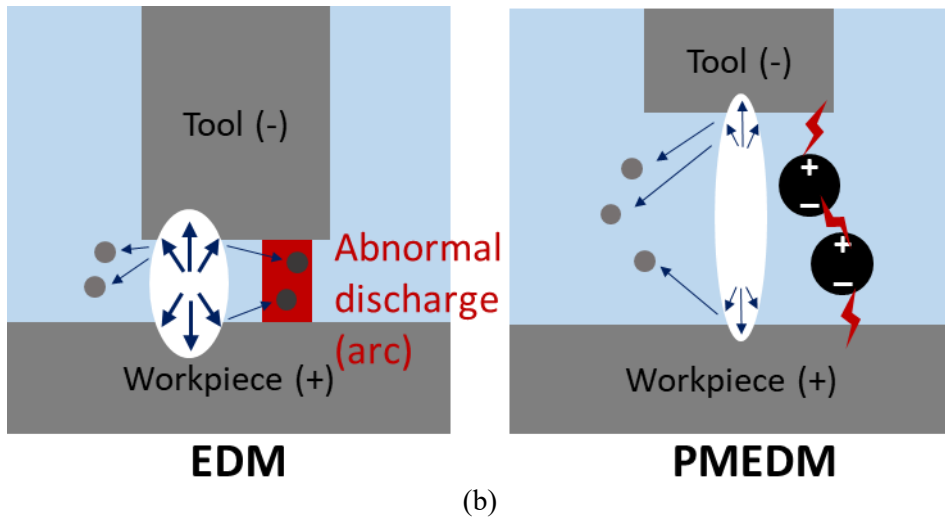


Figure 20. Previous explanation of low tool wear in PMEDM: (a) Reduction of expansion pressure. (b) Improved flushing of debris.

3.2.4 Smaller tool size than normal EDM

The size of machined features is determined by the size of a tool electrode, the discharge gap, and secondary discharges by debris. During ED-drilling process, the machined hole becomes widen as well as deepen. Since the diameter of hole increases until discharge is terminated in lateral direction, the diameter is determined by the size of a tool electrode and discharge gap. However, debris can cause secondary discharges during the evacuation through the discharge gap because it can be regarded as a conductive particle which enlarges discharge gap. The secondary discharge gap further increases the hole diameter. The gap between a

tool electrode and a machined feature is called machining gap. The machining gap is usually larger than discharge gap given that it also considers the effect of secondary discharges by debris.

In PMEDM, the size of a tool electrode should become smaller than that of normal EDM and reduced size of a tool electrode could cause severe tool wear length. Due to the enlarged discharge gap, the reduced size of a tool electrode is needed to machine same-size micro features in PMEDM. However, due to the size effect as shown in Fig. 21, the tool wear length could be increased even though same volume is removed by same discharge energy. One of characteristics of PMEDM is low tool wear; thus, quantitative evaluation of tool wear is needed with optimum condition considering the reduced size of a tool electrode.

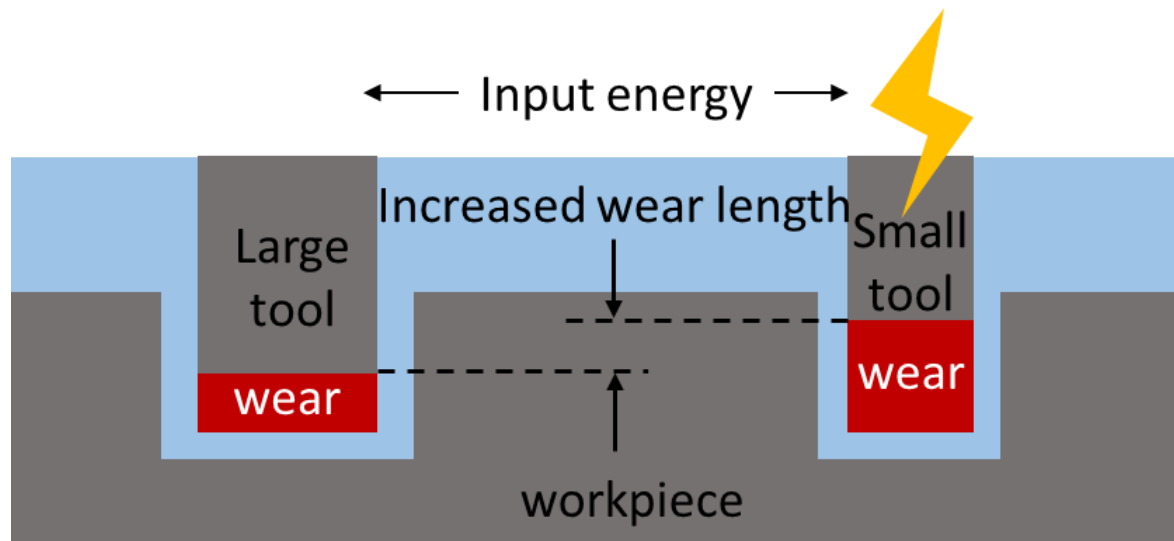


Figure 21. Tool size effect on wear length.

3.3 Research Objectives

The research objectives of present study are as follows.

- 1) Clarifying the mechanism of tool wear reduction in micro PMEDM
- 2) Performance evaluation of PMEDM in machining same-size micro features

The characteristics of a pure dielectric fluid and a powder-mixed dielectric fluid are tabulated in Table 1.

Table 1. Dielectric fluid characteristics.

	Pure dielectric fluid	Powder-mixed dielectric fluid
Discharge gap	Small	Large
Surface roughness	High	Low
MRR	Low	High
Tool wear	High	Low
Tool size	Large	Small

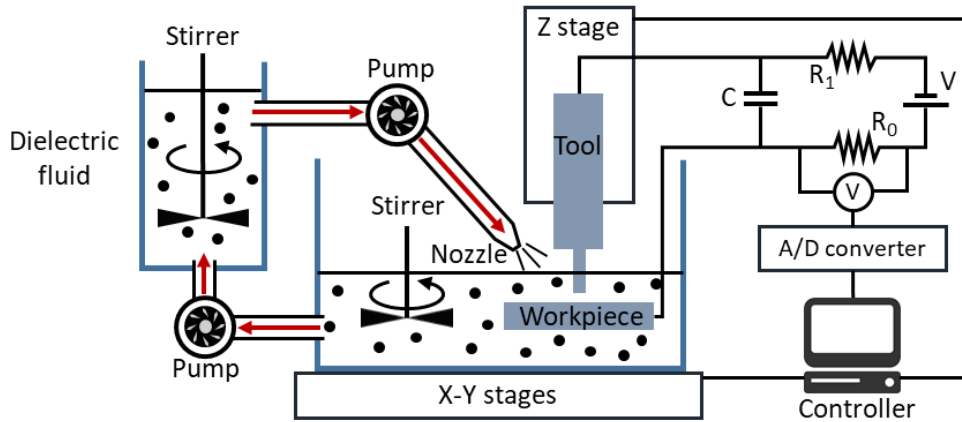
4

Experimental Set Up

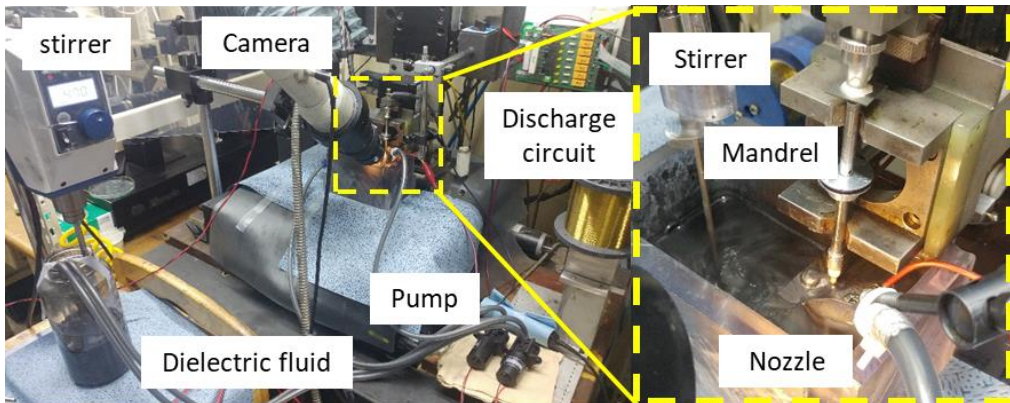
This chapter briefly introduces the PMEDM system, the process for micro tool fabrication, measuring equipment, and tool feed control mechanism. Based on the RC discharge circuit, the circulation system for a powder-mixed dielectric fluid was installed in micro EDM system. A micro tool was fabricated by WEDG [44]. Measuring equipment were a scanning electron micro scope, an oscilloscope, a 3D surface profiler by confocal method, and a 2D surface profiler by contact method. To adjust the gap between a tool electrode and a workpiece, servo control algorithm was employed.

4.1 System for powder mixed EDM

The system for micro PMEDM is illustrated in Fig. 22. The custom-made micro-EDM system is composed of an RC discharge circuit, a precision three-axis stage (806CT for X-Y, 404XR for Z, Parker, USA), and a controller (Clipper, Delta Tau, USA). In this study, kerosene was used as a dielectric fluid and graphite powder was selected because it has low density, good electrical conductivity, high melting point, and no flammability. Hereafter, pure kerosene is called PK and graphite-powder-mixed kerosene is called GPMK. Because the density of graphite is greater than that of kerosene, an overhead stirrer was installed in the bottle of GPMK and the machining tank to mix the graphite powder with kerosene. Centrifugal pumps were used to circulate the mixed fluid. To fabricate a micro tool electrode, a WEDG system developed by Masuzawa et al. was employed as shown in Fig. 23 [44]. The measuring equipment are tabulated in Table 2.

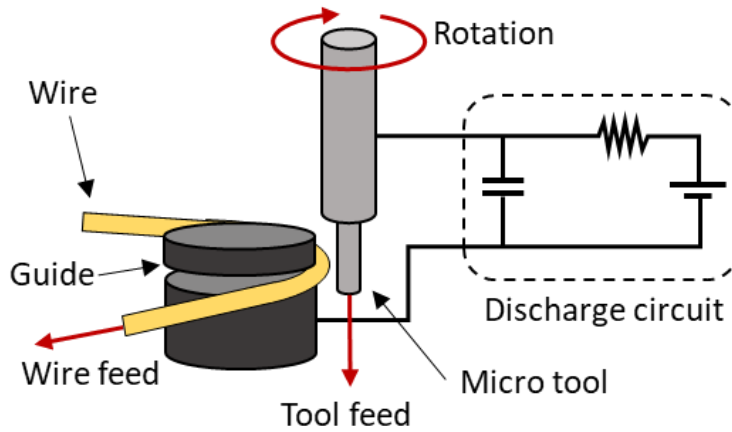


(a)

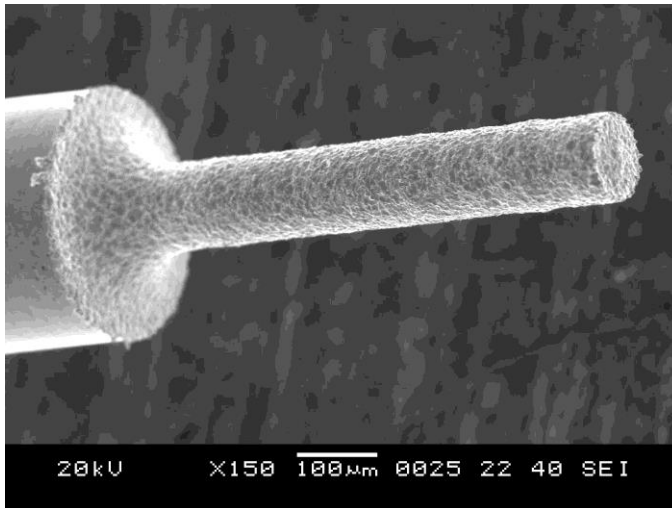


(b)

Figure 22. The system of micro PMEDM: (a) A schematic diagram. (b) A real picture.



(a)







(b)

Figure 23. (a) WEDG system for micro tool fabrication. (b) The micro tool.

CHAPTER 4. Experimental set up

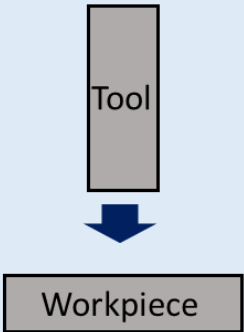
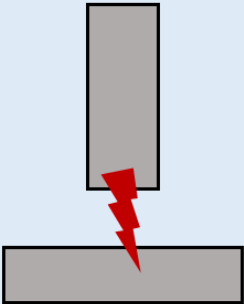
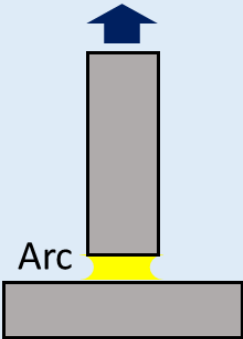
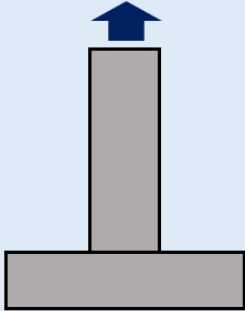
Table 2. Measuring equipment.

		
Name	Scanning Electron Microscope (JEOL-6360, JEOL, Japan)	Oscilloscope (MDO 3024, Tektronix, USA)
Specification	Micro dimension measuring	Bandwidth : 200 MHz Sampling rate : 2.5 GS/s Voltage, Current measuring
		
Name	3D profiler (µsurf, Nanofocus, Germany)	Surface profiler (Form Talysurf Series 2, Taylor-Hobson, UK)
Specification	Confocal type Resolution : 5 nm 3D profile measuring	Contact type Tip radius : 2 µm Resolution : 10 nm Surface roughness measuring

4.2 Tool feed control

In micro EDM, it is crucial to maintain the proper gap between a tool electrode and a workpiece. The proper gap condition facilitates the evacuation of debris and induce discharge to occur continuously. Tool feed command is classified according to four gap status as shown in Table 3: excess, proper, shortage, and contact. In excess status, which means the gap is larger than the discharge gap, the control system commands a tool electrode to move forward. In proper status, a tool electrode holds for pre-set duration. In shortage and contact status, the control system commands a tool electrode to retract for pre-set distance. To determine the gap status, the controller uses the voltage applied in R_0 in Fig. 24(a). The value of R_0 is much smaller than R_1 to avoid excessive voltage applied in the controller. The average value of the number of samples which acquired during pre-set duration is used, and two criteria-the upper and lower threshold values-can be customized to decide which command is necessary instantly according to the gap status (Fig. 24(b)). The value of lower threshold is directly related the gap distance. Increased value of lower threshold makes a tool electrode maintain close gap from the workpiece because it enlarges the range of forward command. In other words, the gap distance is inversely proportional to the value of lower threshold.

Table 3. Gap status and feed command.

	Excess	Proper	Shortage	Contact
Gap status				
Feed command	Forward	Hold	Backward	

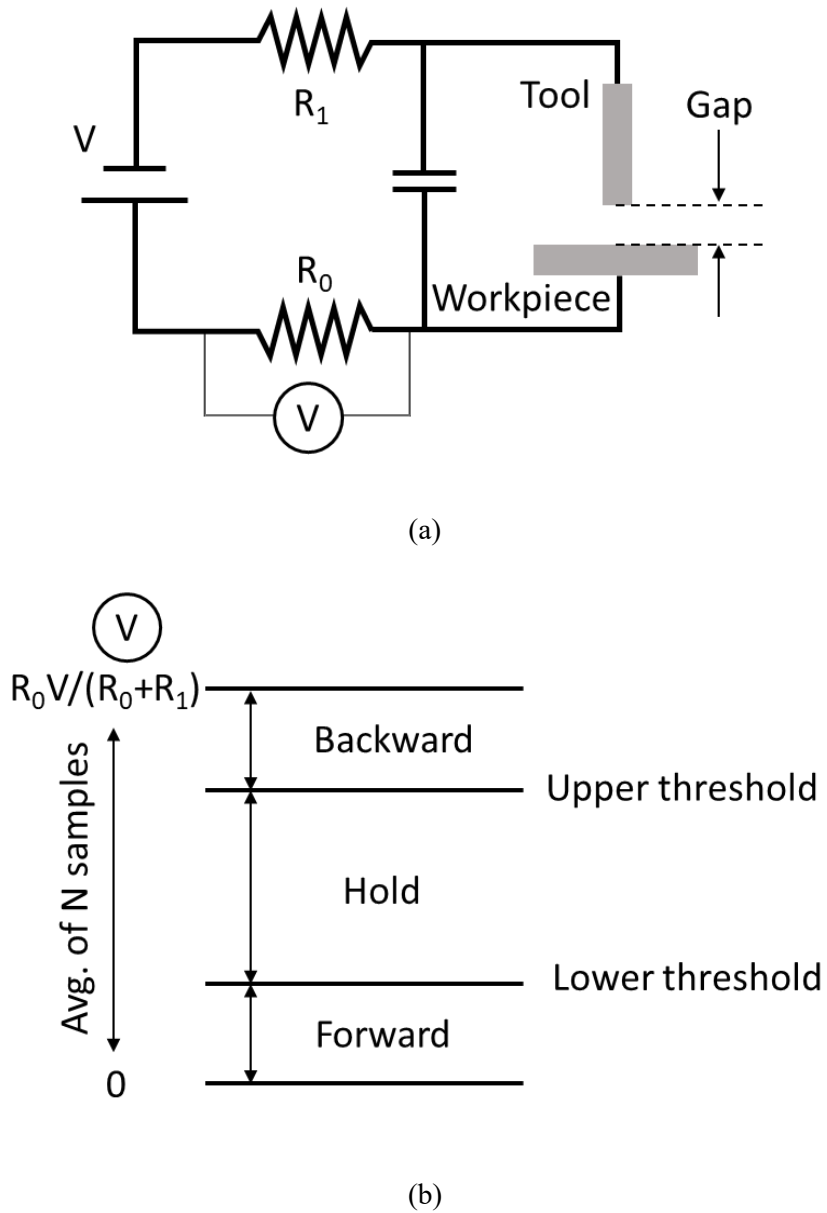


Figure 24. (a) RC discharge circuit for tool feed control. (b) Tool feed control strategy.

5

Mechanism of Tool Wear Reduction in Powder Mixed EDM

This chapter clarifies the mechanism of tool wear reduction in PMEDM. The limits of previous explanations of low tool wear are a potential conflict with high MRR since MRR and tool wear generally have proportional relationship with discharge energy. However, by preventing reverse current which intensifies tool wear, high MRR and low tool wear can be explained simultaneously. The RC-discharge circuit was modeled with stray inductance which induces the current oscillation by a second order response. The reverse current was generated and

CHAPTER 5. Mechanism of tool wear reduction in PMEDM

caused higher energy distribution at a tool electrode. In PMEDM, discharge plasma channel extinguished before reverse current flowed, and hence a tool electrode maintained lower energy distribution than the workpiece continuously.

To examine the reason of early extinction of discharge plasma channel in PMEDM, discharge craters were compared with normal EDM. The shape of discharge crater is a key to analyze discharge phenomenon. The discharge craters of PMEDM was smaller and shallower than those of normal EDM, which means the discharge plasma channel of PMEDM has less amount of discharge energy than that of normal EDM. Therefore, in PMEDM, the discharge plasma channel has shorter duration than normal EDM and extinguishes before reverse current flows.

5.1 Modeling of RC-discharge circuit

The comparison between the simulation and experimental results explains the relationship between the generation of reverse current and the mechanism of tool wear reduction in PMEDM. The RC discharge circuit was modeled in Fig. 25. The entire circuit consists of charging and discharging loops, and a virtual discharge switch connects them. The charging loop is composed of a power source (V), a resistor (R_1) and a capacitor (C), while stray inductance (L) and a resistor (R_2) constitute the discharging loop. The stray inductance and R_2 are inevitable and inherent components which stem from basic electrical components such as wires and the discharge plasma channel. The open and closed statuses of the virtual discharge switch represent the charging and discharging statuses of the entire circuit, respectively. Before discharge occurs, only the charging loop is valid, and the C is charged by the power source. The governing equation of the RC charging circuit is shown below.

$$dV_C(t)/dt + V_C(t)/R_1C = V/R_1C \quad (4)$$

As soon as the insulation of the dielectric fluid breaks and the discharge is initiated, the virtual discharge switch closes and the entire circuit becomes the RLC circuit. The governing equations of the RLC discharging circuit are as follows.

$$d^2I_L(t)/dt^2 + (1/(R_1C) + R_2/L) \cdot dI_L(t)/dt +$$

CHAPTER 5. Mechanism of tool wear reduction in PMEDM

$$(R_1 + R_2) I_L(t)/(R_1 LC) = V/(R_1 LC) \quad (5)$$

Table 4. Nomenclature in the modeling of RC-discharge circuit.

C	Capacitance 1 (=5 nF)
I_L	Current of stray inductance
L	Stray inductance
R_1	Resistance 1 (=1 k Ω)
R_2	Resistance 2
T	Time
V	Open voltage (=100 V)
V_C	Voltage of capacitor

Figs. 26(a) and (b) are the simulation results of the RC and the RLC circuit, respectively. The specific values are tabulated in Table 4 and R_0 was neglected due to its small value. The simulation result of the RC circuit shows only charging voltage with a gentle slope, whereas the RLC circuit displays the discharging and charging voltage with a rather steep slope, which depicts the status after the discharge starts. Because the simulation result of the RLC circuit does not consider the time when the discharge channel extinguishes, the V_C and I_L oscillate until the

CHAPTER 5. Mechanism of tool wear reduction in PMEDM

discharge energy dissipates. During the oscillations, reverse current flows. However, during actual EDM process, the oscillating of V_C stops and is charged with a gentle RC charging slope and I_L becomes zero directly after the discharge plasma channel becomes extinct.

Figs. 27(a) and (b) are the experimental signals of a single discharge of PK and GPMK, respectively. As shown in Fig. 27(a), when the discharge started, the voltage dropped below zero with RLC discharging. After the RLC discharging step, the charging slope was steep, as in the RLC charging step, but it suddenly became a very gentle slope, as in the RC charging simulation result. This indicates that the discharge plasma channel was extinguished and the circuit became the RC circuit via the open switch at the slope-changing point of the charging slope. Thus, current signals continued until this changing point and reverse current flowed, which intensified the tool wear by increasing the energy distribution at the tool electrode. On the other hand, as depicted in Fig. 27(b), RLC charging was not observed when GPMK was used as the dielectric fluid. The physical meaning of this result is that the discharge plasma channel dissipated immediately after the RLC discharging step. This early extinction did not allow reverse current to flow; thus, the tool electrode can maintain its lower energy distribution than the workpiece and tool wear was alleviated. Fig. 28 indicates the discharge time of the virtual discharge switch when $V=100$ V, $C=5$ nF, and $R_1=1$ k Ω in both PK and GPMK.

CHAPTER 5. Mechanism of tool wear reduction in PMEDM

Figs. 29(a) and (b) show the experimental signals of multiple discharges in PK and GPMK, respectively. While PK shows regular discharges with reverse current, GPMK shows early discharges without reverse current, which indicates that discharge occurred even though V_C did not reach the pre-set open voltage or 100 V. Given that the duration of discharge plasma channel is proportional to the amount of discharge current, the duration of early discharges which have low discharge current is shorter than that of normal discharge. Because these early discharges did not generate reverse current likewise the single discharge signal in Fig. 27(b), they could contribute to the reduction tool wear by maintaining lower energy distribution at the tool electrode.

The mechanism of early extinction of the discharge plasma channel with GPMK is as follows. In RC discharge circuit, discharge plasma channel is extinguished when the whole charged energy in a capacitor is consumed. Because of short duration in micro EDM, while 10-15% of the charged energy is consumed through conduction and material removal, the rest of energy is consumed through the generation and expansion of the discharge plasma channel [46]. Given that the size of the discharge plasma channel is proportional to the amount of its energy in micro EDM, the discharge duration is proportional to the amount of charged energy in a capacitor. As illustrated in Fig. 30, while a large and single discharge occurs in PK, small and series discharges occur in GPMK. The charged energy is dispersed

into small discharge plasma channels, and thus these small channels extinguish quickly owing to their small amount of energy.

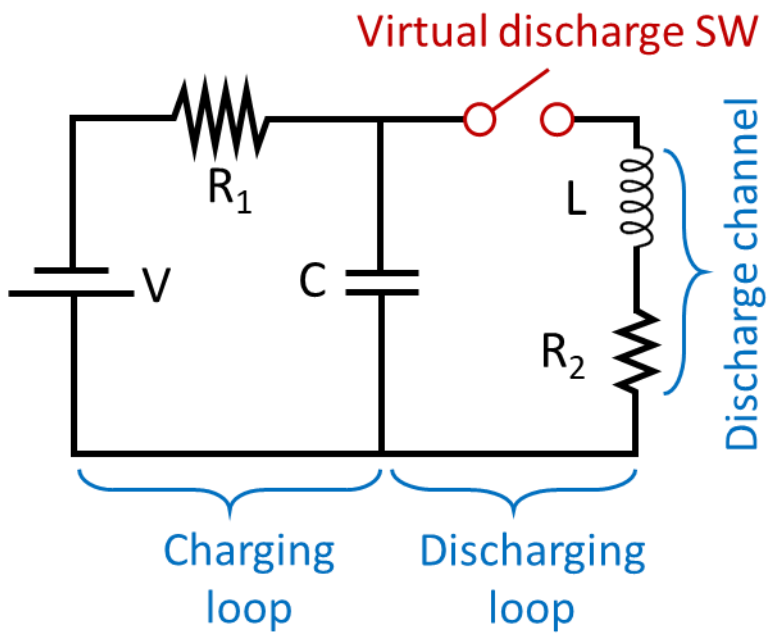
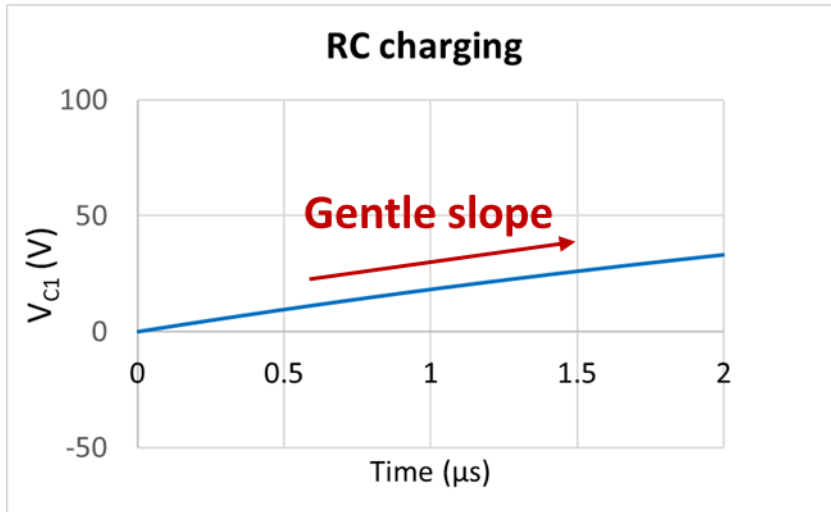
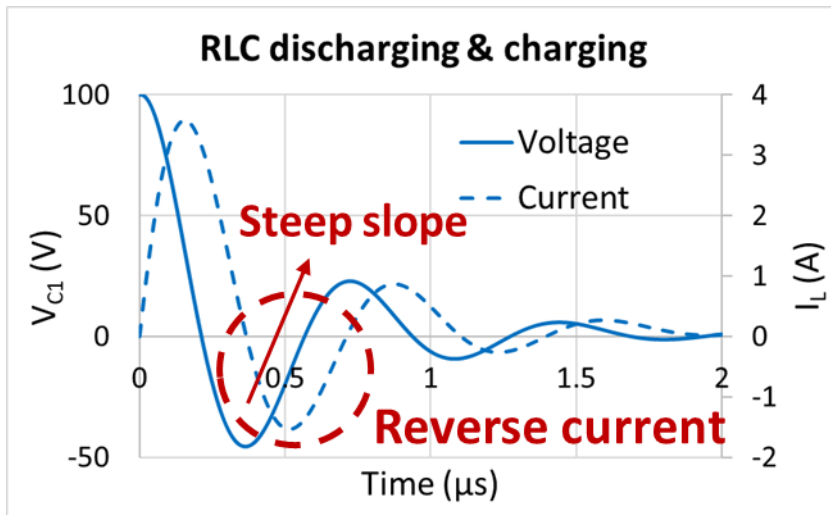


Figure 25. The modeling of RC-discharge circuit.

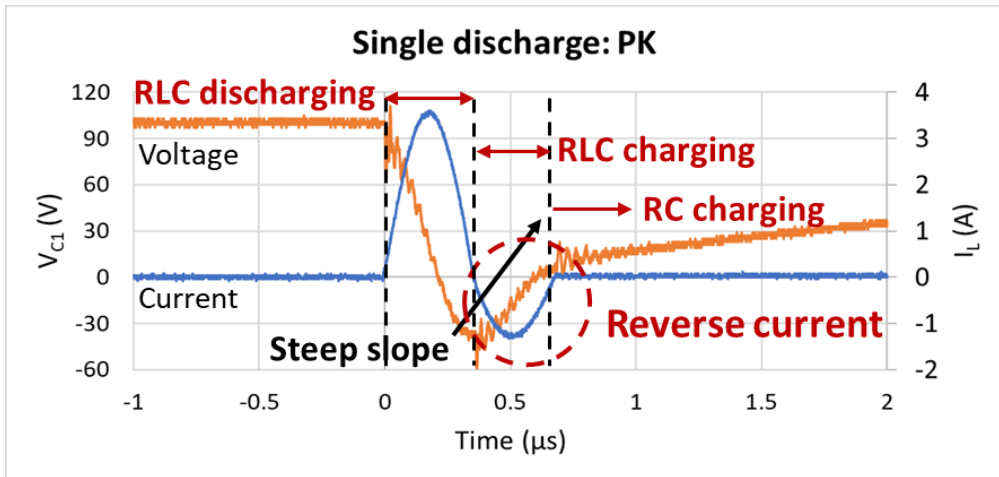


(a)

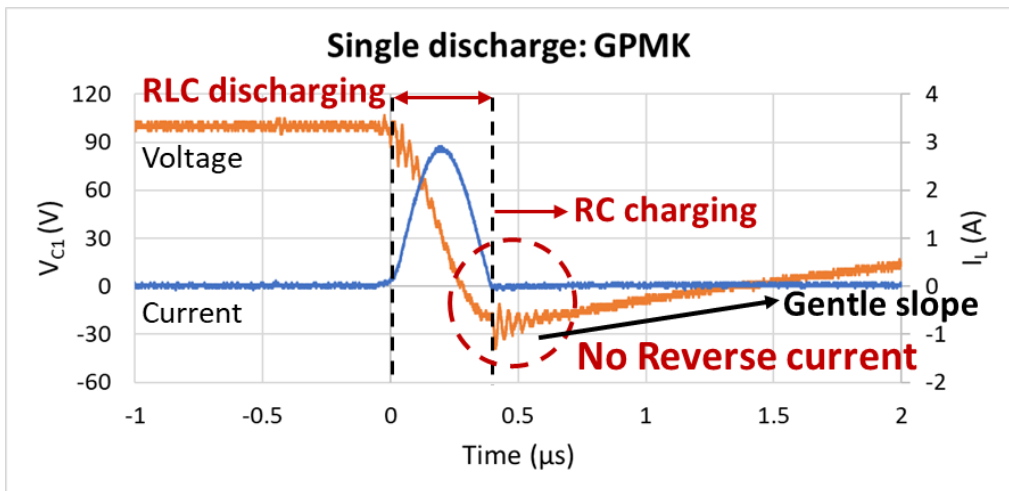


(b)

Figure 26. The simulation results of RC-discharge circuit: (a) RC charging. (b) RLC discharging and charging.



(a)



(b)

Figure 27. The experimental results of single discharge: (a) PK. (b) GPMK.

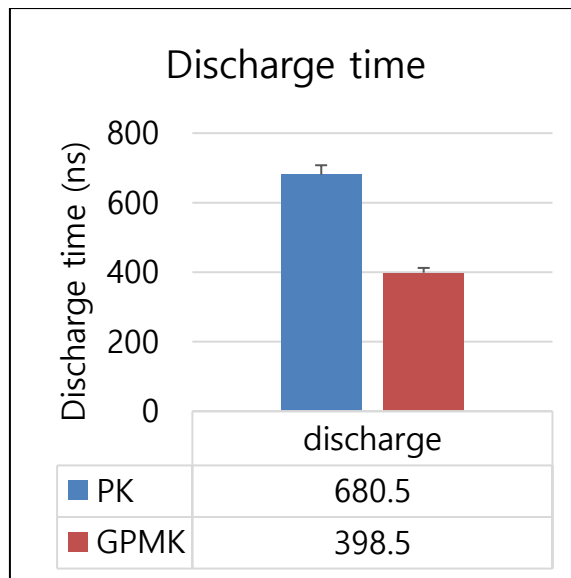
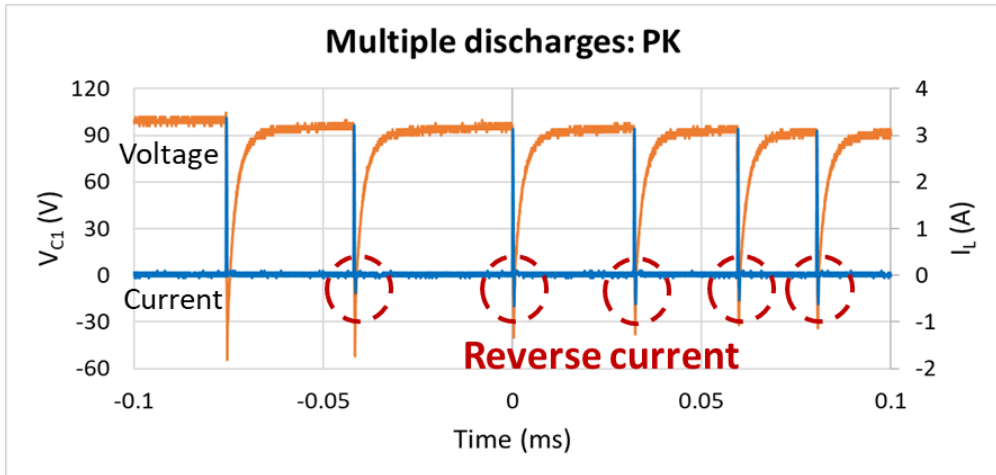
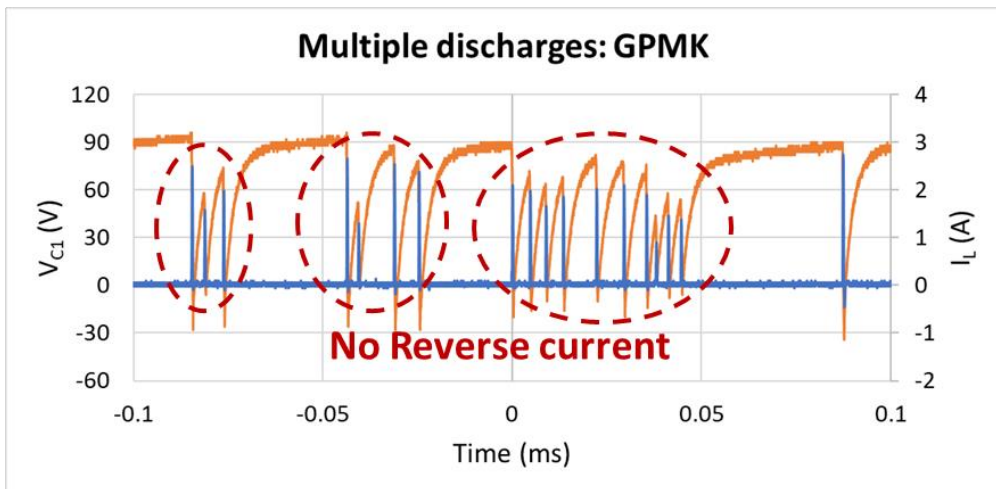


Figure 28. The discharge time of virtual discharge switch.



(a)



(b)

Figure 29. The experimental results of multiple discharges: (a) PK. (b) GPMK.

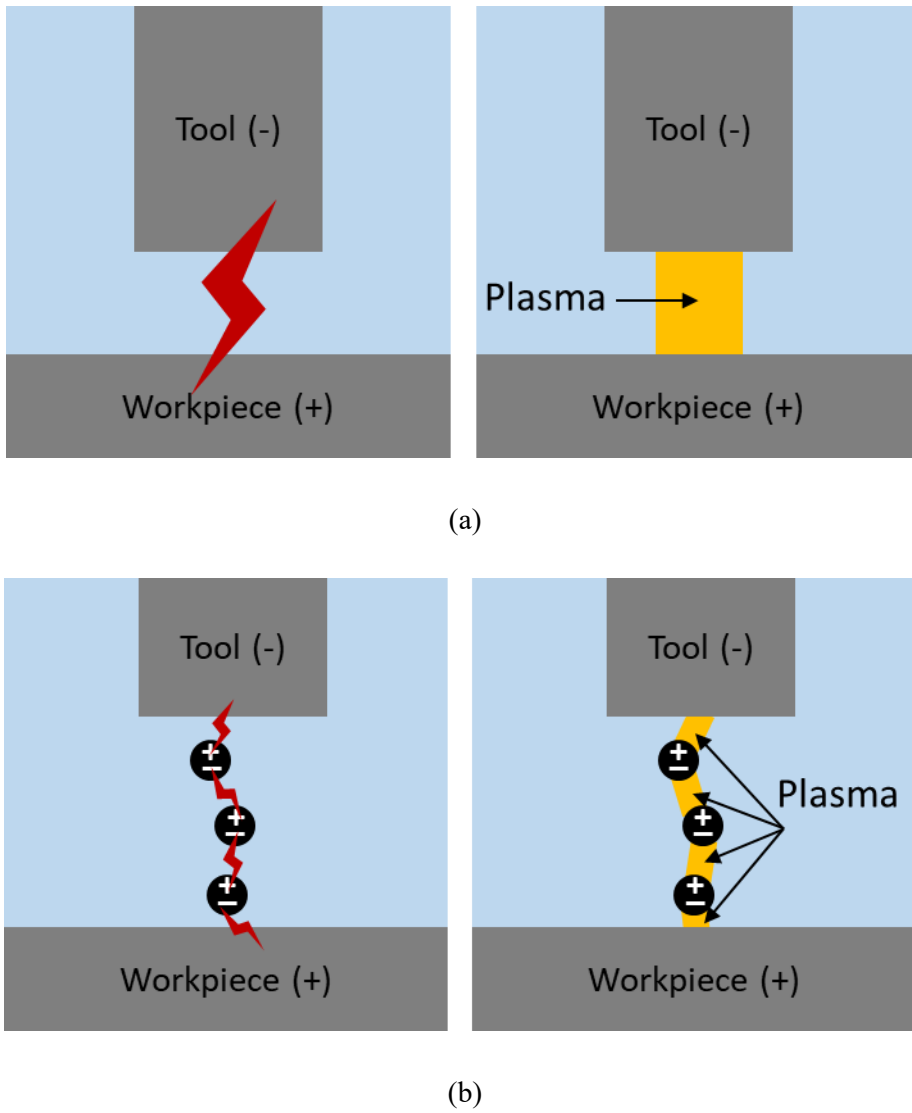
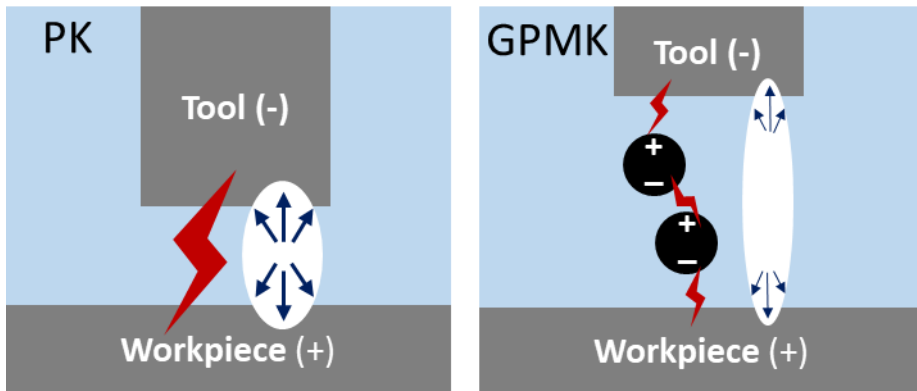


Figure 30. The generation mechanism of discharge plasma channel: (a) PK. (b) GPMK.

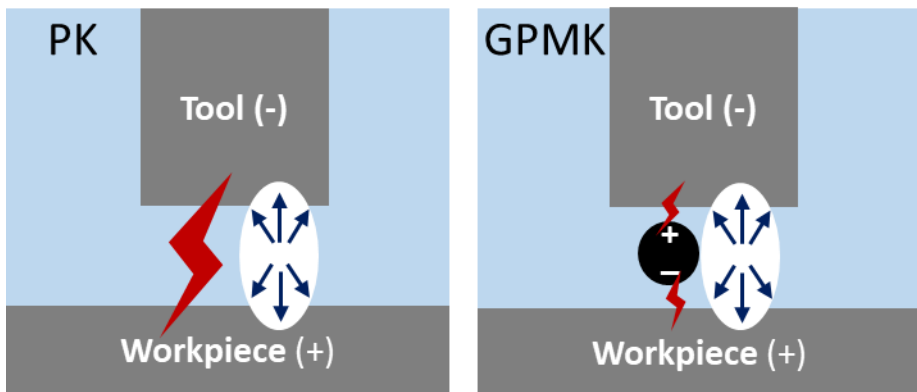
5.2 Discharge crater analysis

The duration of discharge plasma channel is directly related to the density or amount of discharge energy and analyzed via the discharge craters. In both single and multiple discharges, the reverse current did not flow in GPMK because of the early extinction of discharge plasma channel. The reason of these phenomena could be found in the discharge crater.

Two experiments were conducted to investigate the effect of gap between the tool electrode and the workpiece as shown in Fig. 31. The first experiment was designed to make discharge craters at the different discharge gap. In this experiment, the energy density of discharge plasma channel was decreased by the enlarged discharge gap in GPMK. The second experiment was designed to generate discharge craters at the same gap. In this experiment, the amount of discharge energy was decreased by early discharges. By these two reasons, the discharge plasma channel dissipated before reverse current flowed.



(a)



(b)

Figure 31. Two experiments to investigate the effect of gap: (a) At the different discharge gap. (b) At the same gap.

5.2.1 Experimental set up for crater analysis

To compare the discharge craters of GPMK and PK, the original experimental set up in Fig. 22 was slightly modified with an N-MOSFET and a pulse generator to generate discharge signals with desired duration, as shown in Fig. 32. A snubber circuit was added to dampen the overshoot of N-MOSFET signal when the N-MOSFET status was changed by the pulse generator. The gap between the tool electrode and the workpiece was adjustable by the zeroing circuit and the precision z-stage. The zeroing circuit was used to determine the position of the tool electrode where it contacts with the workpiece. To eliminate the effect of stray capacitance, the voltage of zeroing circuit was decreased to 20 V because the stray capacitance can machine the workpiece slightly and it could affect the zeroing position. To analyze the discharge craters clearly, the values of open voltage and capacitance were increased to generate large craters. The detail experimental conditions are tabulated in Table 5. The diameter and depth of discharge craters were analyzed by the optical microscope and the 3D profiler, respectively, and discharge frequency was calculated through counting the number of discharge craters. The experiment was repeated 10 times.

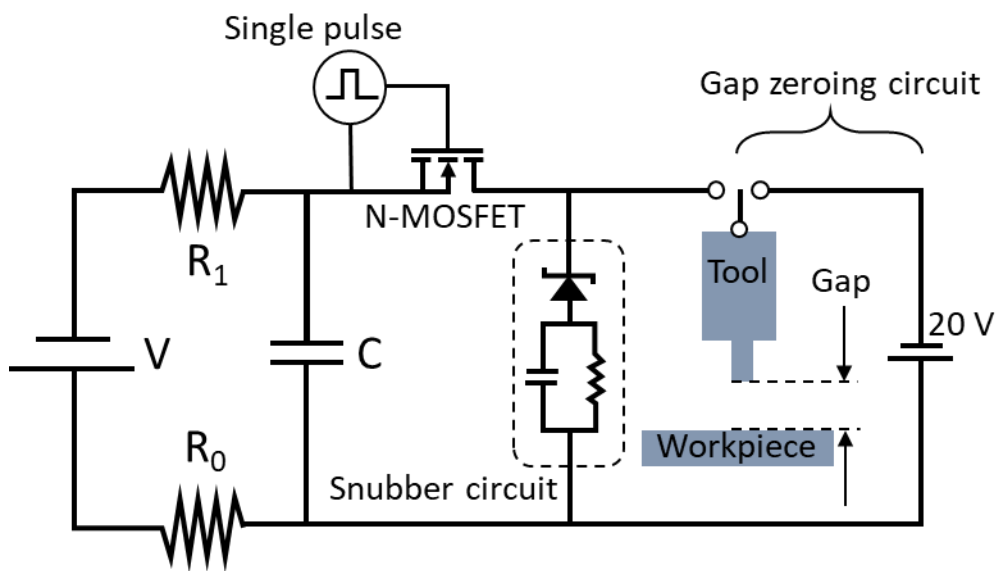


Figure 32. The modified experimental set up for discharge crater analysis.

CHAPTER 5. Mechanism of tool wear reduction in PMEDM

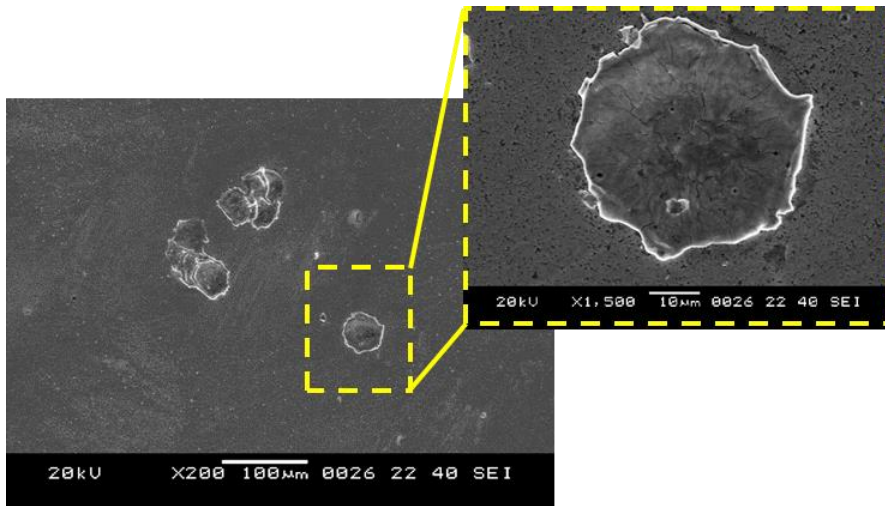
Table 5. Experimental conditions for discharge crater analysis.

	PK		GPMK	
Workpiece	WC-Co, Anode			
Tool electrode	WC-Co, ϕ 300 μm , Cathode			
Open voltage V	150 V			
Capacitance C	47 nF			
Resistance R_0	20 Ω			
Resistance R_1	1 k Ω			
Gap	5 μm	10 μm	5 μm	35 μm
Pulse width	200 μs	100 ms	200 μs	100 ms
Avg. particle diameter	N/A		40 nm	
Concentration	N/A		2 g/l	

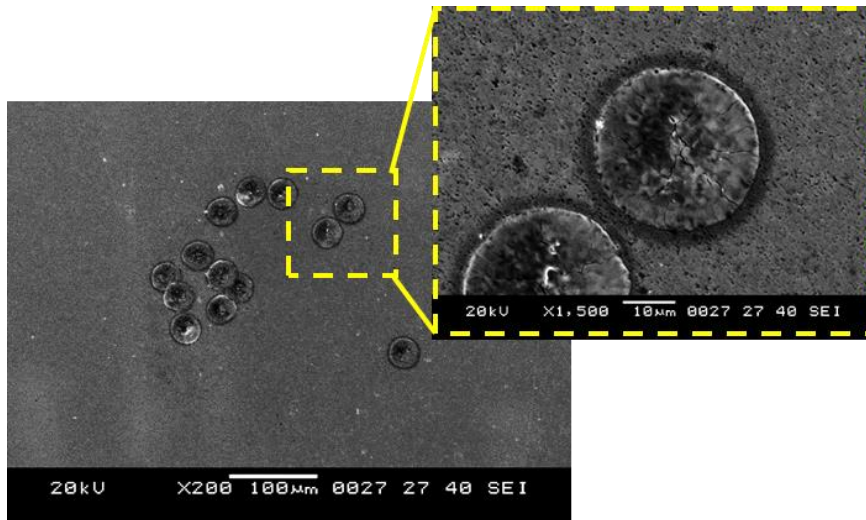
CHAPTER 5. Mechanism of tool wear reduction in PMEDM

5.2.2 Experiment 1 : Discharge crater at the different discharge gap

Fig. 33 shows the result of the first experiment. In both PK and GPMK, the gap was determined where discharge start to occur at open voltage of 150 V. The discharge gaps were 10 μm and 35 μm with PK and GPMK, respectively. Fig. 34 shows the comparisons of discharge craters in PK and GPMK in terms of diameter, depth, and frequency. The craters of GPMK were smaller and shallower than those of PK because the lower energy density of discharge plasma channel by enlarged gap. However, the discharge frequency was higher in GPMK than PK due to the shorten ignition delay time.



(a)



(b)

Figure 33. The discharge craters at the discharge gaps: (a) 10 µm in PK. (b) 35 µm in GPMK.

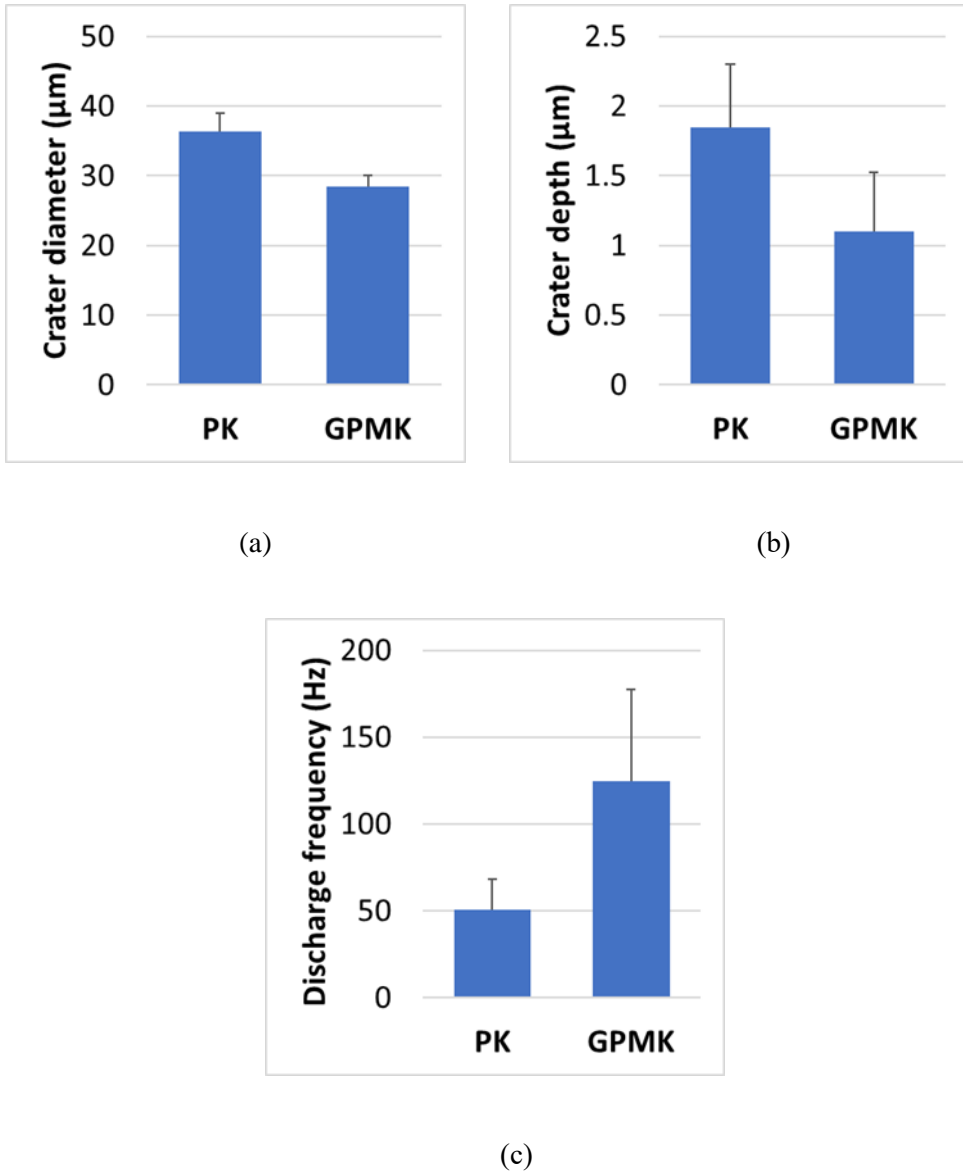
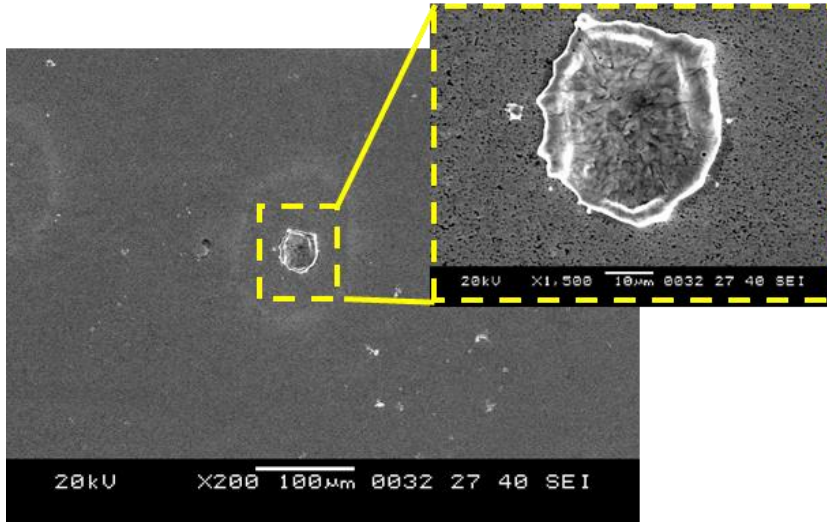


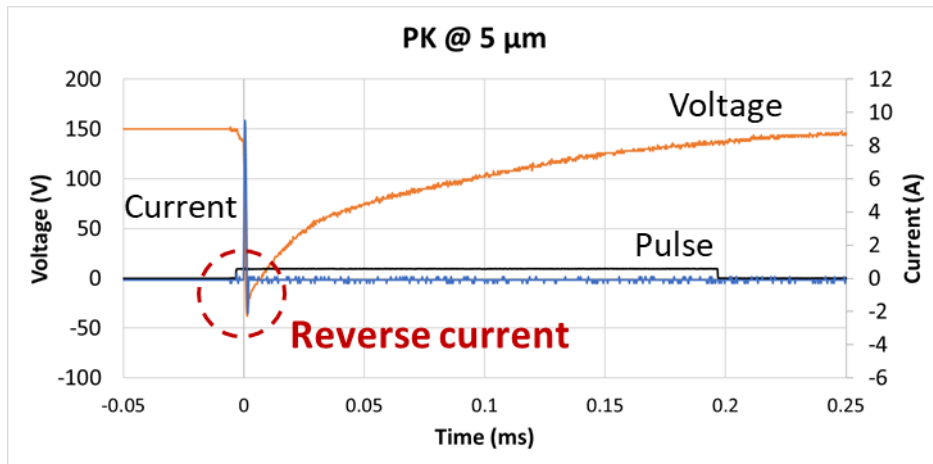
Figure 34. The comparisons of discharge craters at the different discharge gap: (a) Diameter. (b) Depth. (c) Frequency.

5.2.3 Experiment 2 : Discharge crater at the same gap

Figs. 35 and 36 are the discharge craters of PK and GPMK, respectively, each of which consists of pictures of discharge craters and signals. The gap between the tool electrode and the workpiece was 5 μm in both fluids. In PK, the single crater was generated with reverse current as soon as the N-MOSFET was closed by the pulse generator. After the single discharge, the charging voltage was recovered without additional discharges during the single pulse. On the other hand, in GPMK, multiple discharges occurred during the single pulse. These discharges were classified by two kinds. The first one was caused by the discharge which occurred as soon as the N-MOSFET was closed likewise the case of PK. This first discharge occurred due to the alternation of N-MOSFET status. The second one was the early discharge which occurred without reverse current before the charging voltage was recovered to the pre-set open voltage. Since graphite powder lowers the insulation strength of kerosene, the discharge occurred even though the charging voltage did not reach 150 V. As shown in Fig. 37, each early discharge had smaller and shallower discharge crater than those of single discharge in PK due to its lower amount of current. However, early discharge showed much higher discharge frequency than the single discharge in PK due to the shorten charging time.

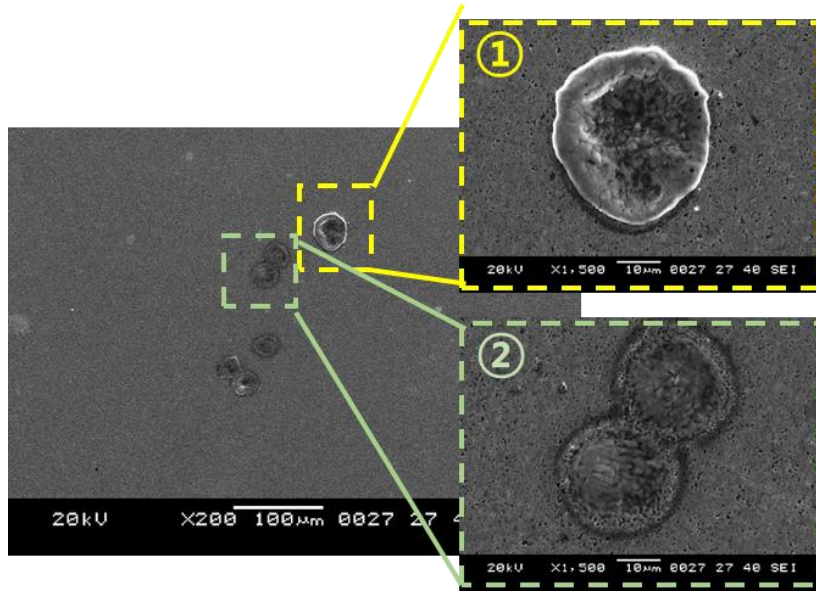


(a)

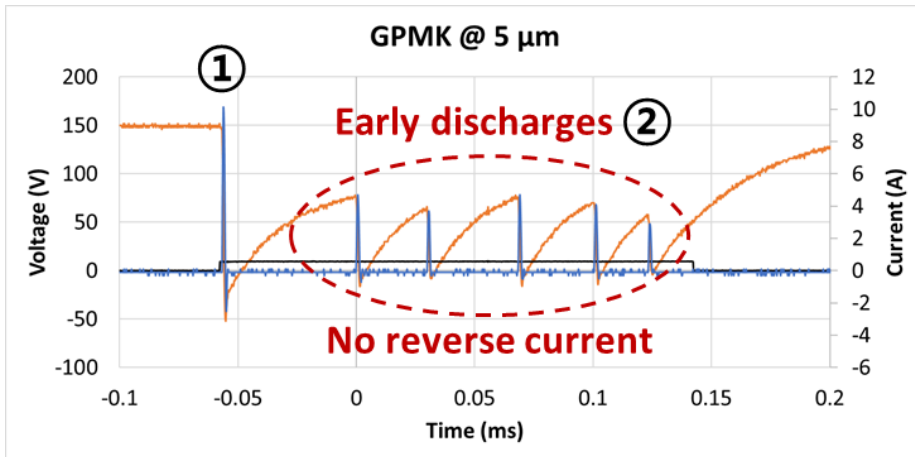


(b)

Figure 35. The discharge crater at 5 μm in PK: (a) SEM image (b) Discharge signal.



(a)



(b)

Figure 36. The discharge craters at 5 μm in GPMK: (a) SEM image. (b) Discharge signals.

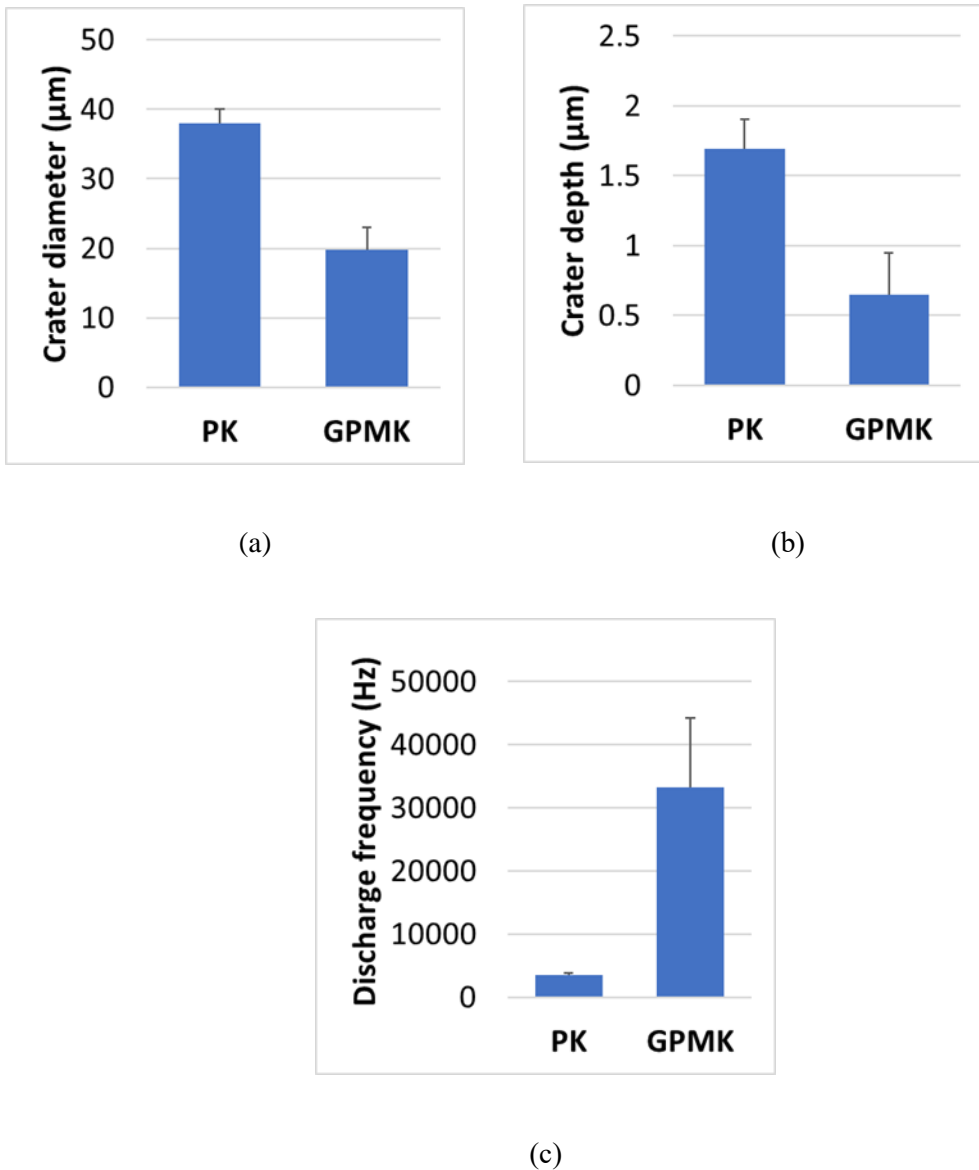


Figure 37. The comparisons of discharge craters at 5 μm : (a) Diameter. (b) Depth. (c) Frequency.

5.3 Mechanism of tool wear reduction in PMEDM

By analyzing experiments 1 and 2, the mechanism of tool wear reduction in PMEDM was investigated as illustrated in Fig. 38. At the different discharge gap, reverse current does not flow because the discharge gap is enlarged by graphite powder, and the energy density of discharge plasma channel is decreased. At the same gap, reverse current does not flow since the amount of discharge current is decreased by early discharges. Both cases maintain lower energy distribution at the tool electrode, which can alleviate the tool wear. Furthermore, discharge frequency of GPMK is higher than PK in both cases because of reduced ignition delay time and charging time. By these reasons, low tool wear can be explained with high MRR simultaneously in PMEDM.

To check that the above tool wear reduction mechanism of PMEDM is valid in real machining process, micro ED-drilling was performed. The detailed machining conditions are tabulated in Table 6, and the results are plotted in Fig. 39. As explained in tool feed control mechanism of chapter 4.2, the gap between the tool electrode and the workpiece is adjustable by changing the value of lower threshold. As indicated in Fig. 39, GPMK shows higher MRR and lower TWL than PK in large gap condition. On the other hand, in small gap condition, GPMK shows much higher MRR with still lower TWL than PK because of the increased difference of discharge frequency between PK and GPMK.

CHAPTER 5. Mechanism of tool wear reduction in PMEDM

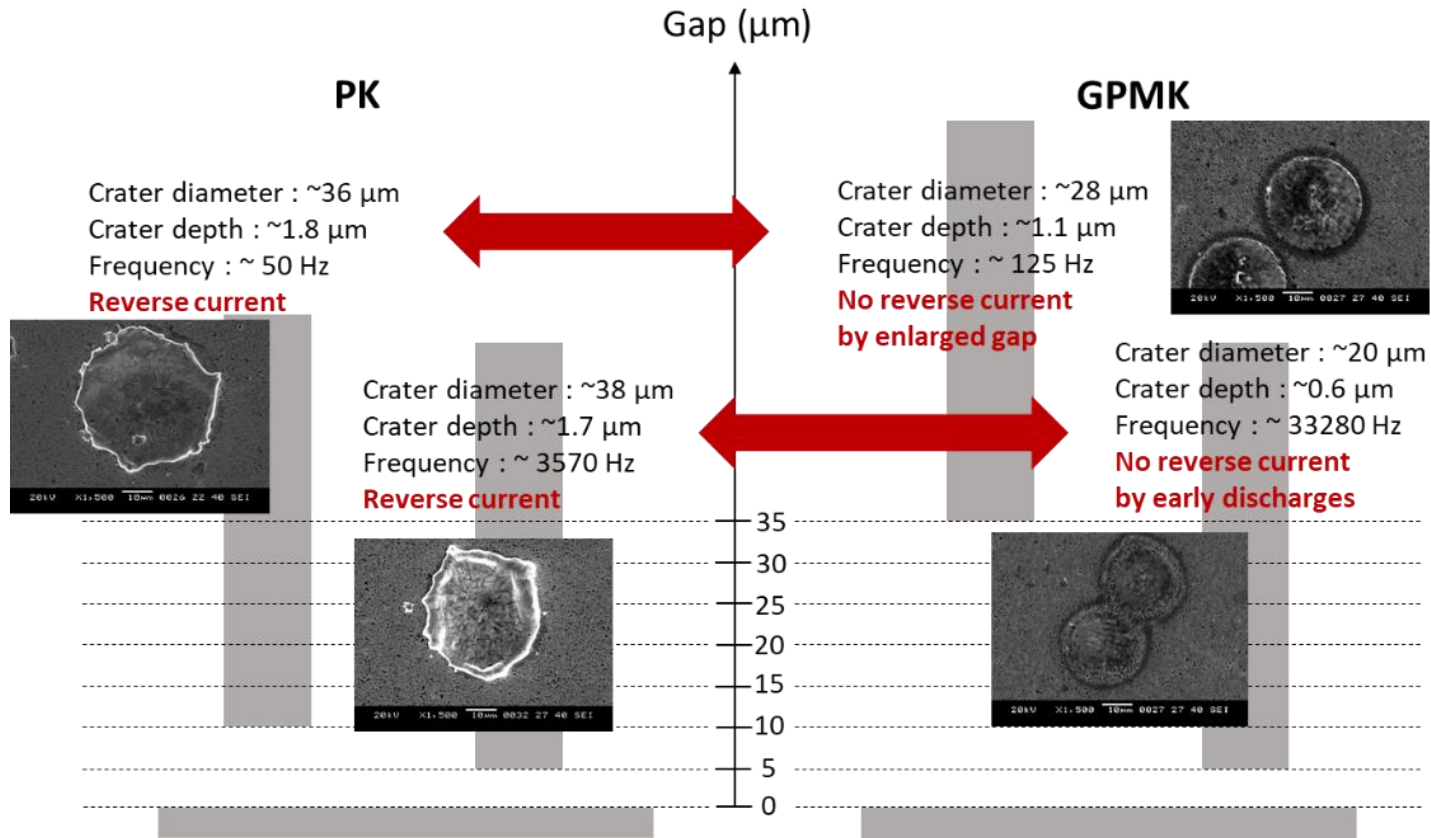


Figure 38. Mechanism of tool wear reduction in PMEDM.

CHAPTER 5. Mechanism of tool wear reduction in PMEDM

Table 6. Machining conditions.

	PK	GPMK
Type	Drilling, Thru hole	
Workpiece	WC-Co, Anode, 500 μm	
Tool electrode	WC-Co, ϕ 100 μm , Cathode	
Open voltage V	100 V	
Capacitance C	5 nF	
Resistance R_0	20 Ω	
Resistance R_1	1 k Ω	
Max. feedrate	100 $\mu\text{m/s}$	
Avg. particle diameter	N/A	40 nm
Concentration	N/A	2 g/l

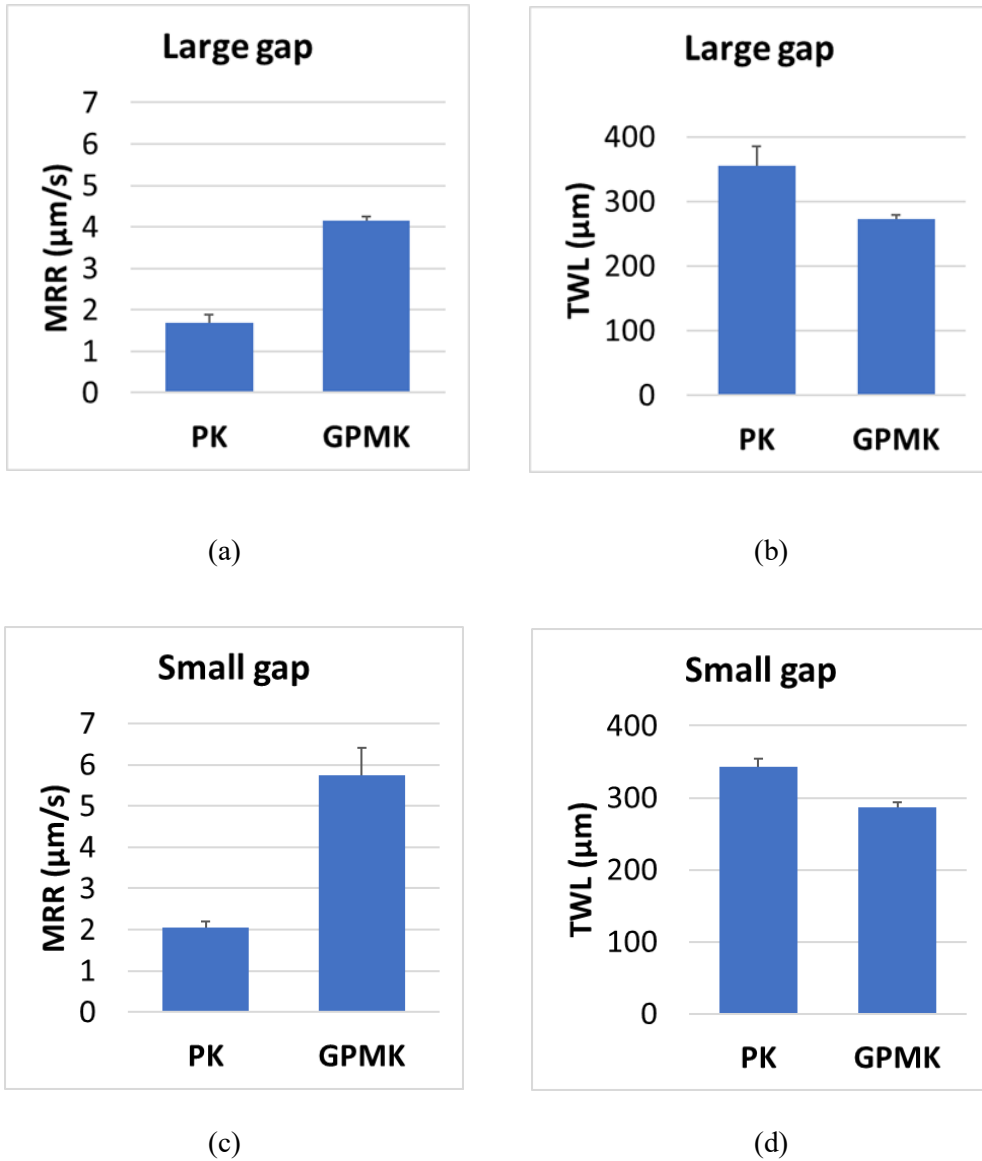


Figure 39. The results at different gap distances: (a) MRR at large gap. (b) TWL at large gap. (c) MRR at small gap. (d) TWL at small gap.

6

Micro Powder-Mixed EDM with Graphite-Powder-Mixed Kerosene

This chapter compares the machining performance of GPMK with PK in micro ED-drilling and ED-milling. Before the parameter test in each machining process, the average particle size of graphite powder and the concentration of GPMK were chosen considering the discharge gap. In micro ED-drilling, the open voltage and capacitance were selected as machining parameters, and MRR, TWL, machining gap, taper angle, and surface roughness were selected as evaluation indexes. On the other hand, in micro ED-milling, DoC, open voltage, and

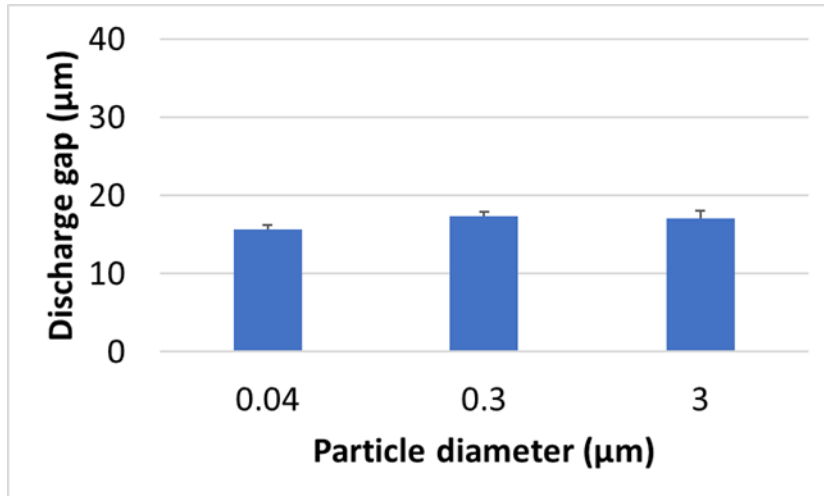
Chapter 6. Micro PMEDM with GPMK

capacitance were selected as machining parameters, and MRR, TWL, the curvature & slope of bottom surface of the machined channel, machining gap, and surface roughness were selected as evaluation indexes. After the parameter tests, final evaluations were conducted in both machining processes. In these processes, the different optimum machining conditions were selected for PK and GPMK respectively to machine same-size micro features.

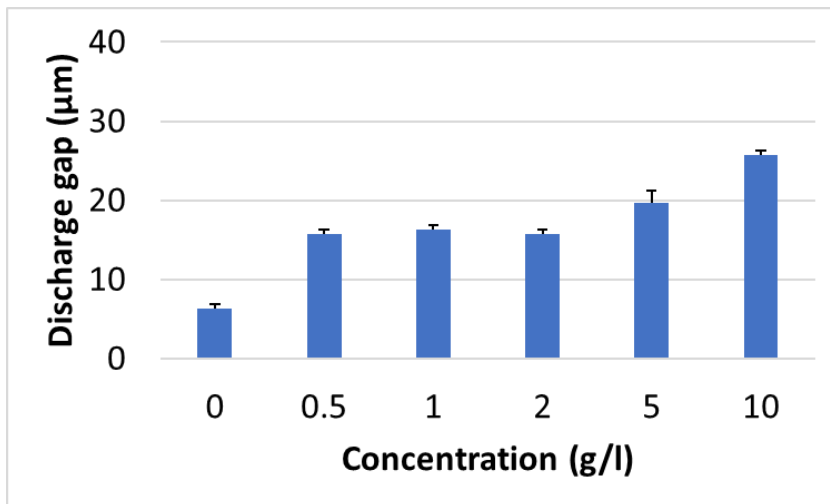
6.1 Powder particle size & concentration

The average particle size of graphite powder and the concentration of GPMK can affect the discharge gap. According to the bridging effect explained in chapter 3.1, micro discharges between the electrodes and polarized particles trigger the breakdown of the dielectric fluid. Because the polarized particle serves as stepping stones in the discharge gap, the average particle size and the number of graphite powder can influence the discharge gap.

Large discharge gap is not desirable because it can increase TWL considering the size effect on TWL as stated in section 3.2.4. Fig. 40 shows the discharge gap in terms of the average particle size and the concentration of GPMK. As the average particle diameter increased, discharge gap was slightly increased. On the other hand, discharge gap was increased after the concentration of GPMK is greater than 5 g/l. Therefore, 40 nm and 2 g/l were selected as the optimum conditions of the average particle size of graphite powder and the concentration of GPMK, respectively.



(a)



(b)

Figure 40. (a) The effect of average particle size of graphite powder on discharge gap. (b) The effect of concentration of GPMK on discharge gap.

6.2 Micro powder mixed ED-drilling

The schematic diagram and coordinates of micro ED-drilling are illustrated in Fig. 41. Among the evaluation indexes, machining gap and taper angle were calculated as follows.

$$\text{Machining gap} = \text{Inlet radius} - \text{Tool radius}$$

$$\text{Taper angle} = \tan^{-1}((\text{Inlet radius} - \text{Outlet radius})/\text{workpiece thickness})$$

Machining gap and taper angle can be affected by the second discharge during the evacuation of debris through the discharge gap. The specific machining conditions are tabulated in Table 7.

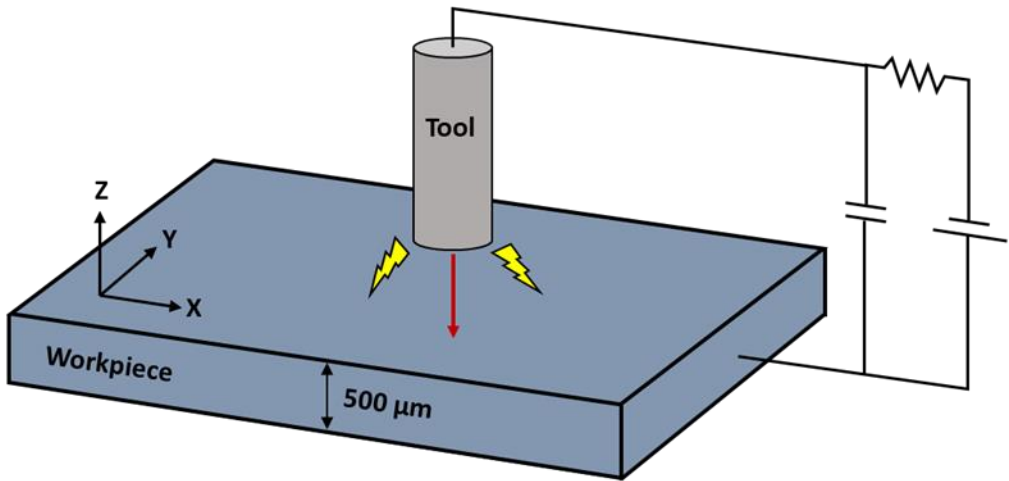


Figure 41. The schematic diagram and coordinates of micro ED-drilling.

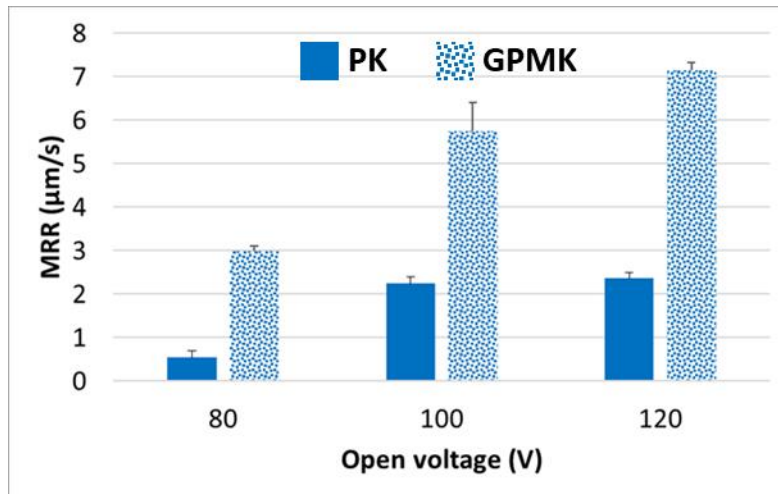
Chapter 6. Micro PMEDM with GPMK

Table 7. Machining conditions for micro ED-drilling.

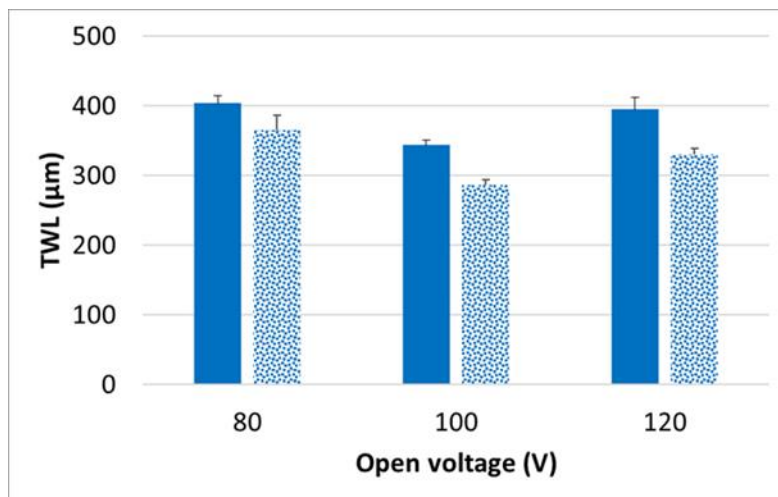
	PK	GPMK
Type	Thru hole	
Workpiece	WC-Co, Anode, 500 μm	
Tool electrode	WC-Co, ϕ 100 μm , Cathode	
Open voltage V	80, 100, 120 V	
Capacitance C	0.2, 0.5, 1, 2.5, 5 nF	
Resistance R_0	20 Ω	
Resistance R_1	1 k Ω	
Feedrate	10 $\mu\text{m/s}$	20 $\mu\text{m/s}$

6.2.1 Open voltage V

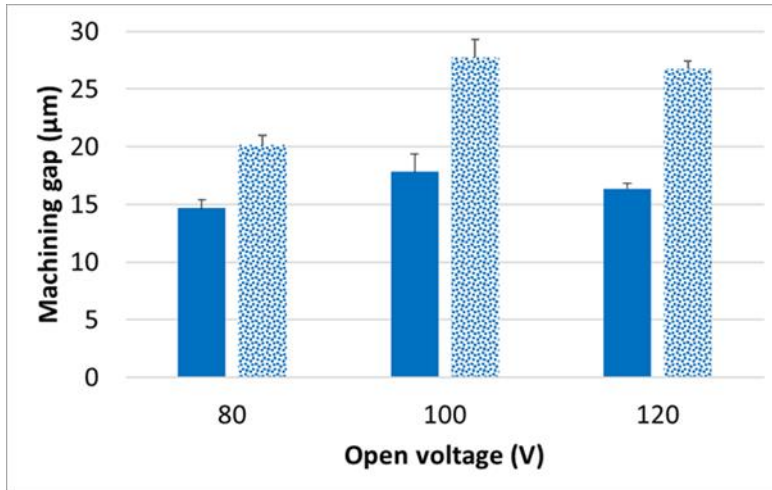
The open voltage can affect the machining results by changing the discharge energy and discharge gap. The single discharge energy is proportional to the square of the open voltage, and the discharge gap is enlarged as the open voltage is increased. The enlarged discharge gap facilitates the evacuation of machining debris between a tool electrode and a workpiece, but excessive open voltage results in unnecessary discharge energy and deteriorates the quality of the machined surface. Fig. 42 shows the machining results of three different open voltages. The capacitance was 5 nF. In both PK and GPMK, MRRs were increased as open voltage increased except 120 V in PK. Excessive tool wear could not increase MRR despite of increased discharge energy. TWLs show the lowest values at 100 V in both fluids. Even though the single discharge energy is smaller at 80 V than 100 V, the narrow discharge gap of 80 V could disturb the evacuation of debris and intensify TWL by abnormal discharges. The difference of machining gap between PK and GPMK were approximately 5 μm at 80 V and 10 μm at 100 and 120 V, which means that the tool diameter should be smaller by 10 μm at 80 V and by 20 μm at 100 V and 120 V. All values of the open voltage, GPMK had better tapers angle because the evacuation of debris was easy due to the enlarged discharge gap and the second discharge was less frequent than PK. As the optimum condition for open voltage, 100 V was selected.



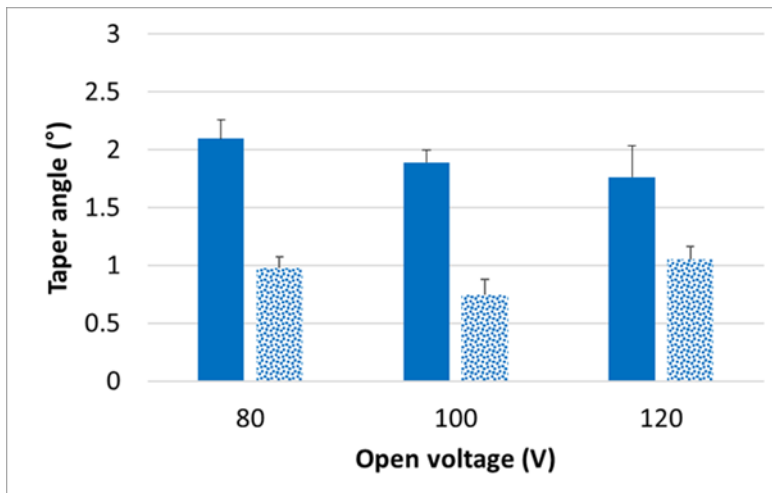
(a)



(b)



(c)

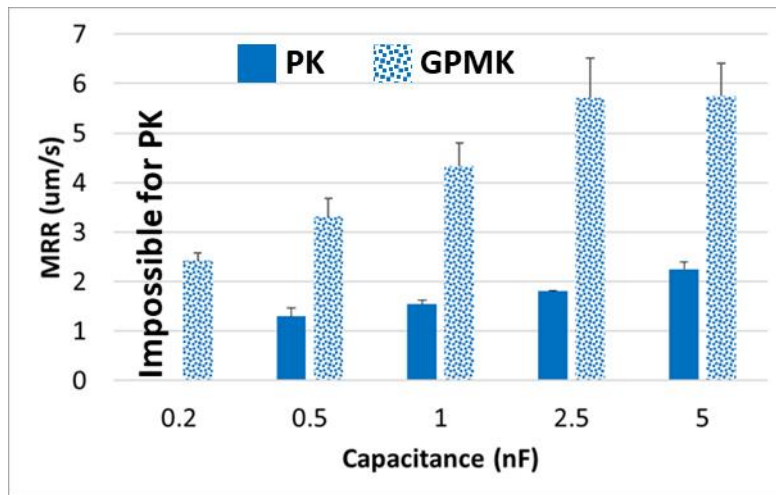


(d)

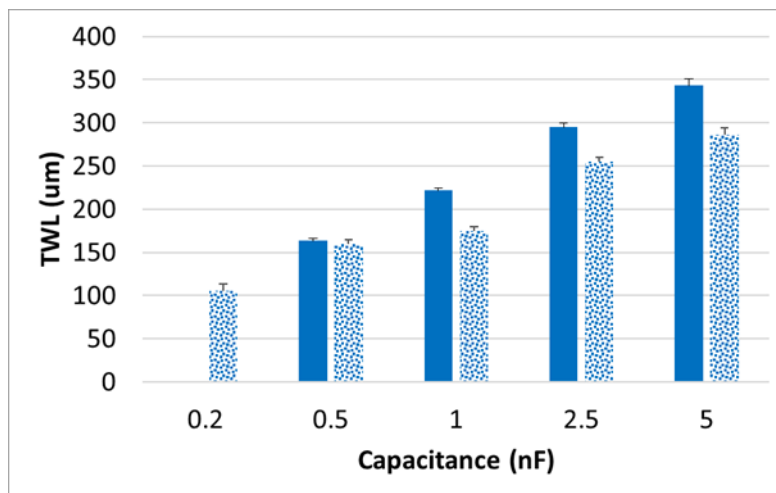
Figure 42. The machining results of open voltage: (a) MRR. (b) TWL. (c) Machining gap. (d) Taper angle.

6.2.2 Capacitance C

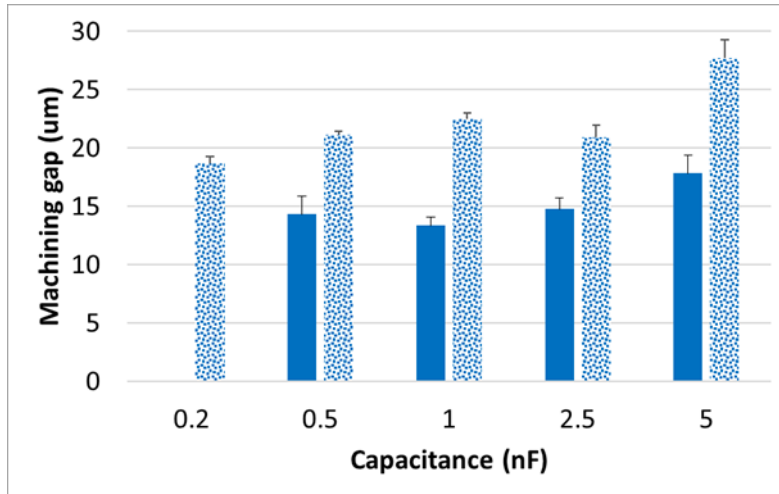
The capacitance in an RC-discharge circuit affects the machining results by changing the discharge energy and frequency. The single discharge energy and the time constant of RC charging in (4) are proportional to the capacitance, and the discharge frequency is inversely proportional to the time constant. The machining results of five different capacitances are plotted in Fig. 43. The open voltage was 100 V. In PK, the drilling of 500 μm at 0.2 nF was impossible due to the low discharge energy. A tremendous machining time was necessary because a lot of shorts and holds of the feed command occurred during machining. As the capacitance was increased, MRR and TWL were generally increased because of the increased discharge energy. Because the MRR at 0.2 nF in GPMK was higher than MRR at the maximum value of the capacitance in PK, 0.2 nF was selected as the optimum machining condition for GPMK. On the other hand, high value of capacitance was desirable for high MRR in PK, but 5 nF could result in excessive TWL and machining gap. Hence, 2.5 nF was the optimum value for PK. With optimum condition of each machining fluid, the difference of machining gap was about 3 μm . Through all values of capacitances, GPMK shows lower taper angle than PK.



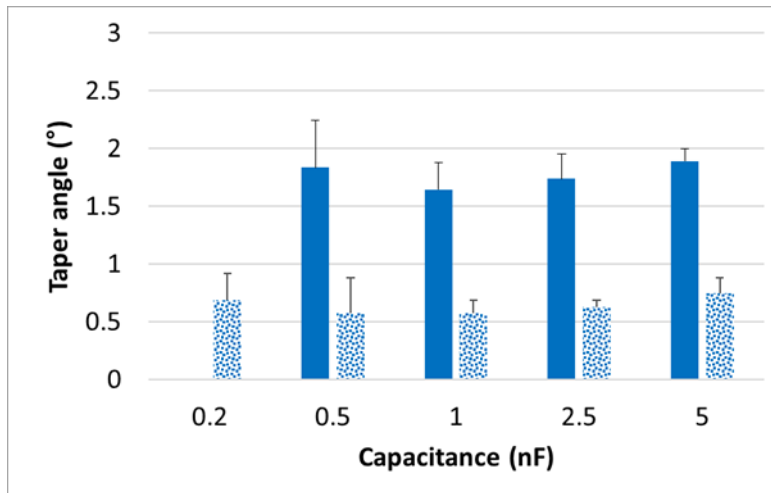
(a)



(b)



(c)



(d)

Figure 43. The machining results of capacitance: (a) MRR. (b) TWL. (c) Machining gap. (d) Taper angle.

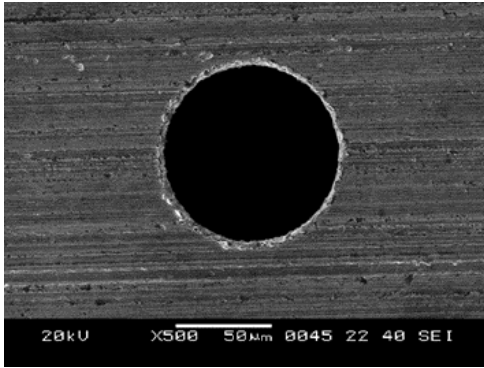
Chapter 6. Micro PMEDM with GPMK

6.2.3 Final results

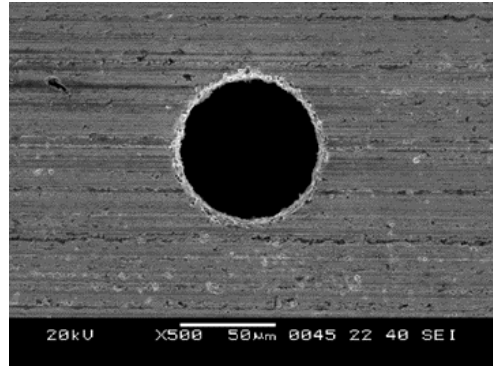
The optimum machining conditions for PK and GPMK are tabulated in Table 8 and their results are shown in Figs. 44, 45, and 46. The inlet diameter of both micro holes were around 95 μm . By GPMK, MRR was increased by 140% and TWL was decreased by 55% while the taper angle and surface roughness were decreased by 47% and 57%, respectively.

Table 8. The optimum machining condition in micro ED-drilling.

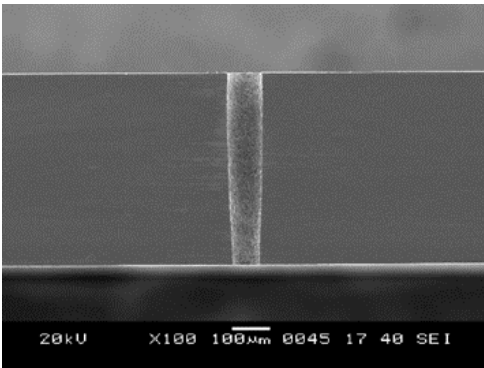
	PK	GPMK
Type	Thru hole	
Workpiece	WC-Co, Anode, 500 μm	
Tool electrode	WC-Co, ϕ 70 μm , Cathode	WC-Co, ϕ 65 μm , Cathode
Open voltage V	100 V	
Capacitance C	2.5 nF	0.2 nF
Resistance R_0	20 Ω	
Resistance R_1	1 k Ω	
Feedrate	10 $\mu\text{m/s}$	40 $\mu\text{m/s}$



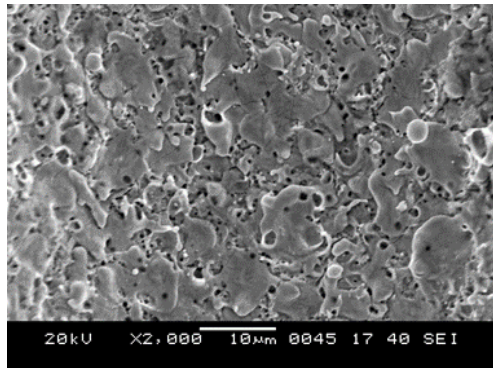
(a)



(b)



(c)



(d)

Figure 44. The optimum machining results of micro ED-drilling in PK: (a) Inlet. (b) Outlet. (c) Cross section. (d) Machined surface.

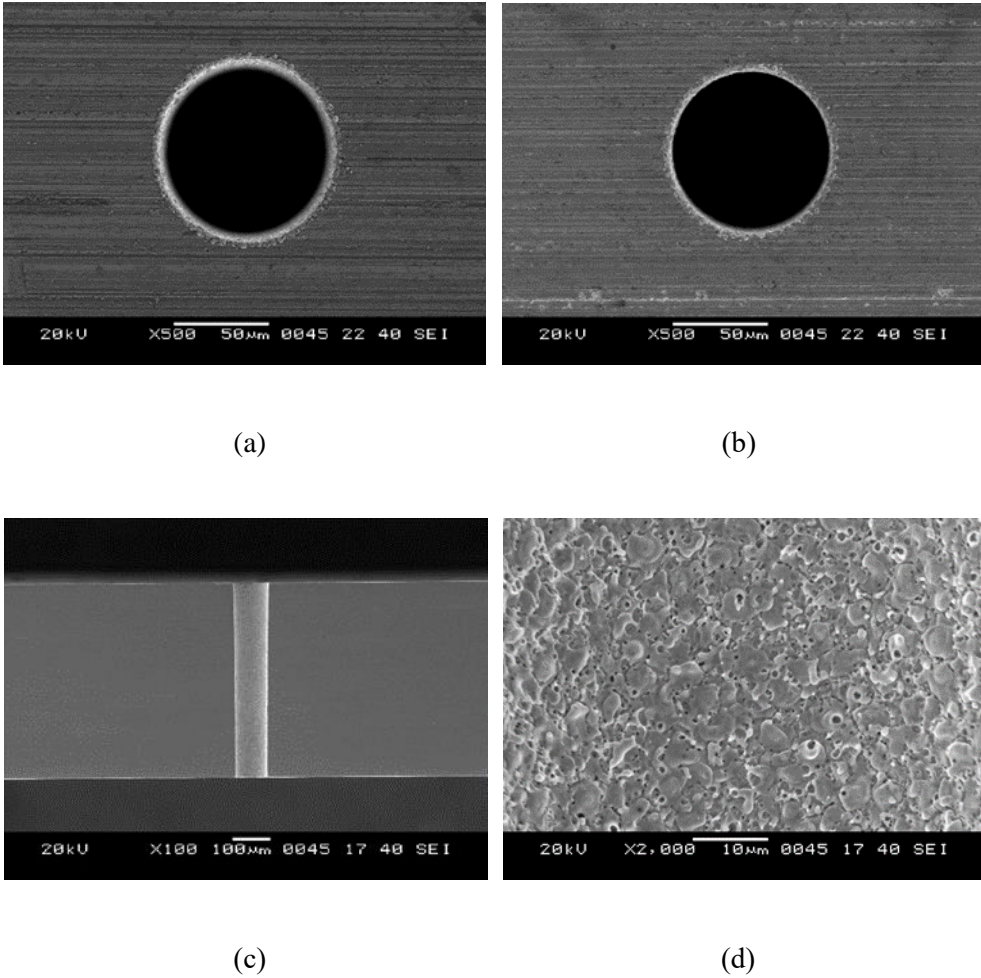
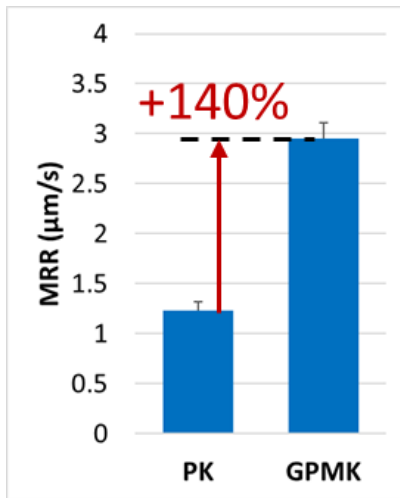
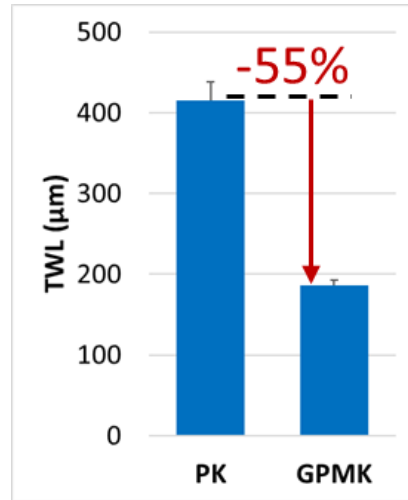


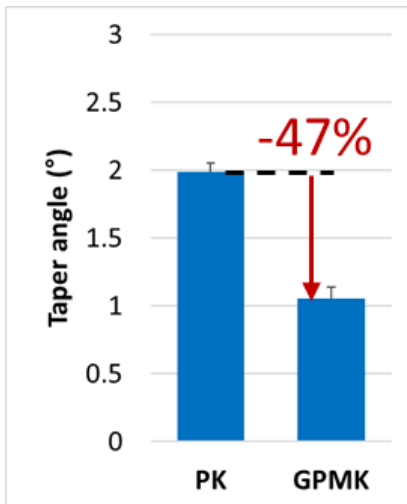
Figure 45. The optimum machining results of micro ED-drilling in GPMK: (a) Inlet. (b) Outlet. (c) Cross section. (d) Machined surface.



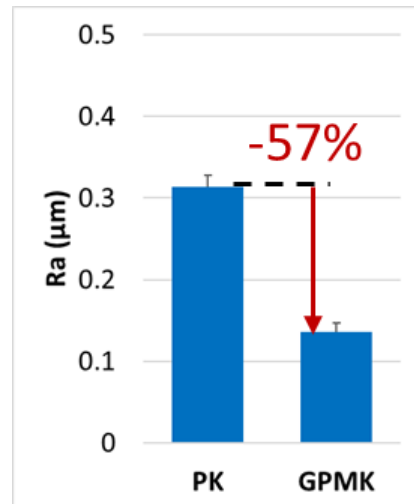
(a)



(b)



(c)



(d)

Figure 46. The performance evaluation of GPMK compared with PK in micro ED-drilling: (a) MRR. (b) TWL. (c) Taper angle. (d) Surface roughness.

6.3 Micro powder mixed ED-milling

The schematic diagram and coordinates of micro ED-milling process is illustrated in Fig. 47. It is based on layer-by-layer machining, and the thickness of each layer was called depth of cut (DoC). The DoC can influence on the curvature of bottom surface in lateral direction and the slope of bottom surface along the stroke direction. Machining gap was calculated by following equation.

$$\text{machining gap} = (\text{channel width} - \text{tool diameter})/2$$

The specific machining conditions are tabulated in Table 9.

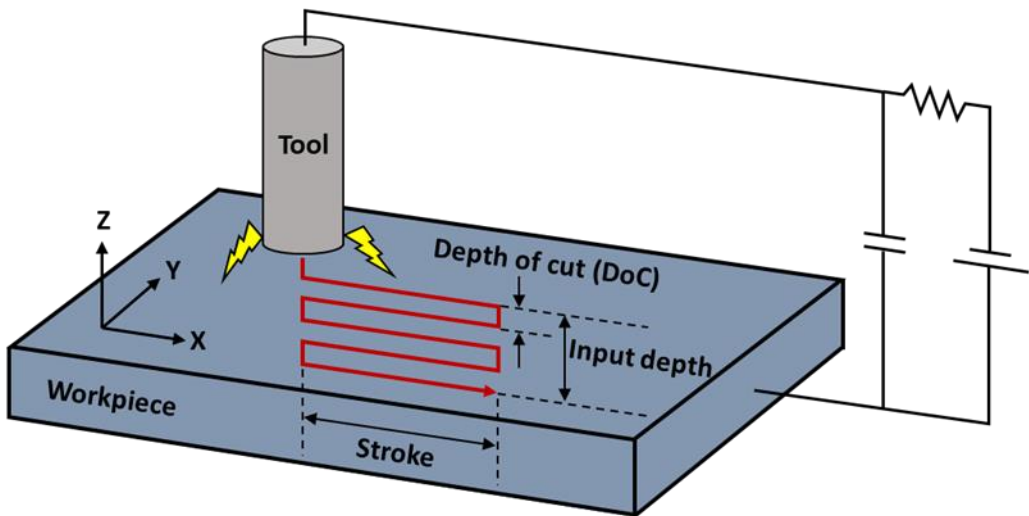


Figure 47. The schematic diagram and coordinates of micro ED-milling.

Chapter 6. Micro PMEDM with GPMK

Table 9. Machining conditions for micro ED-milling.

	PK	GPMK
Stroke	300 μm	
Input depth	150 μm	
Workpiece	WC-Co, Anode	
Tool electrode	WC-Co, ϕ 100 μm , Cathode	
Depth of cut (DoC)	1, 5, 10 ,15 μm	
Open voltage V	60, 80, 100 V	
Capacitance C	2.5, 5, 10 nF	
Resistance R_0	20 Ω	
Resistance R_1	1 k Ω	
X feedrate	40 $\mu\text{m/s}$	
Z feedrate	10 $\mu\text{m/s}$	

6.3.1 Depth of cut (DoC)

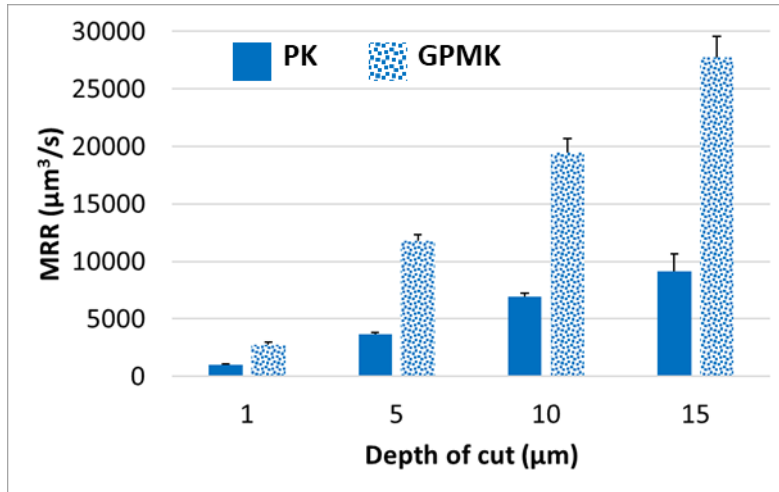
This study used a layer-by-layer milling method with the optimum DoC to achieve high MRR and geometrical accuracy of a micro channel. Due to the intensified electrical field at the edge of a tool electrode, the edge becomes blunt and its shape is directly casted to the corner of a micro channel. As the DoC becomes larger, the amount of worn-out volume at the edge of a tool electrode is also increased. Therefore, an excessive DoC could cause a rounded bottom surface and the geometrical accuracy is then considerably deteriorated. This also results in an inclined bottom surface along the stroke direction of a micro channel due to the tool wear length. On the other hand, the small DoC increases the machining time significantly, which lowers the MRR. Thus, with the optimum DoC, micro-ED milling process can achieve high MRR without compromising the high geometrical accuracy of the micro channel.

GPMK showed higher MRR and lower TWL than PK at a similar degree of flatness of the bottom surface of the micro channel. The open voltage was 100 V and the capacitance was 5 nF for both PK and GPMK. As indicated in Fig. 48, GPMK showed higher MRR and lower TWL than PK. Furthermore, with both PK and GPMK, MRR was increased as the DoC became larger. To evaluate the geometrical accuracy of the micro channel, each machined channel was ground and polished to estimate the flatness of the bottom surface. Figs. 49 and 50 respectively

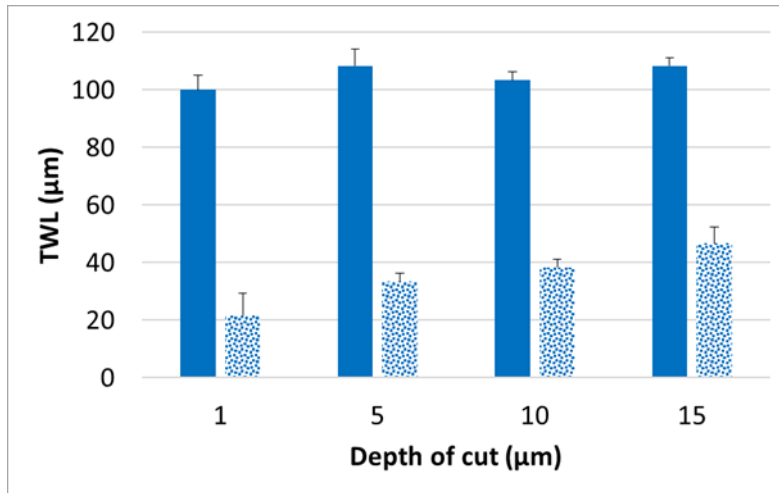
Chapter 6. Micro PMEDM with GPMK

show cross sections of the micro channels in lateral Y-Z plane and the micro tool electrodes after machining with different DoCs in PK and GPMK. Each figure has four subfigures, each of which indicates a different DoC ranging from 1 to 15 μm . As shown in both figures, a larger DoC resulted in excessive wear at the edge of the micro tool electrode and the rounded bottom surfaces of the micro channels. For a quantitative analysis, the curvature radius at the middle point of the bottom surface (Fig. 51(a)) was measured, as indicated in Fig. 51(b). Generally, the curvature radius decreased as the DoC became larger, and PK showed the slightly larger curvature radius than GPMK at each DoC. For both dielectric fluids, the curvature radii at DoCs of 1 and 5 μm were similar, but the curvature radius was decreased considerably at the DoC of 10 μm . Therefore, 5 μm was chosen as the optimum value of the DoC.

GPMK also showed almost zero inclination of the bottom surface of micro channel along the stroke direction. Fig. 52 compares the depth profiles of micro channels along the stroke direction (X-Z plane) in both dielectric fluids. At the DoC of 1 μm , almost zero inclination of the bottom surface was achieved with both PK and GPMK despite LCM was not used in these experiments. However, at the rest DoCs, obvious inclinations were observed in both fluids. Hence, LCM was used with DoC of 5 μm for the final result.



(a)



(b)

Figure 48. The machining results of PK and GPMK with several DoCs: (a) MRR.
(b) TWL.

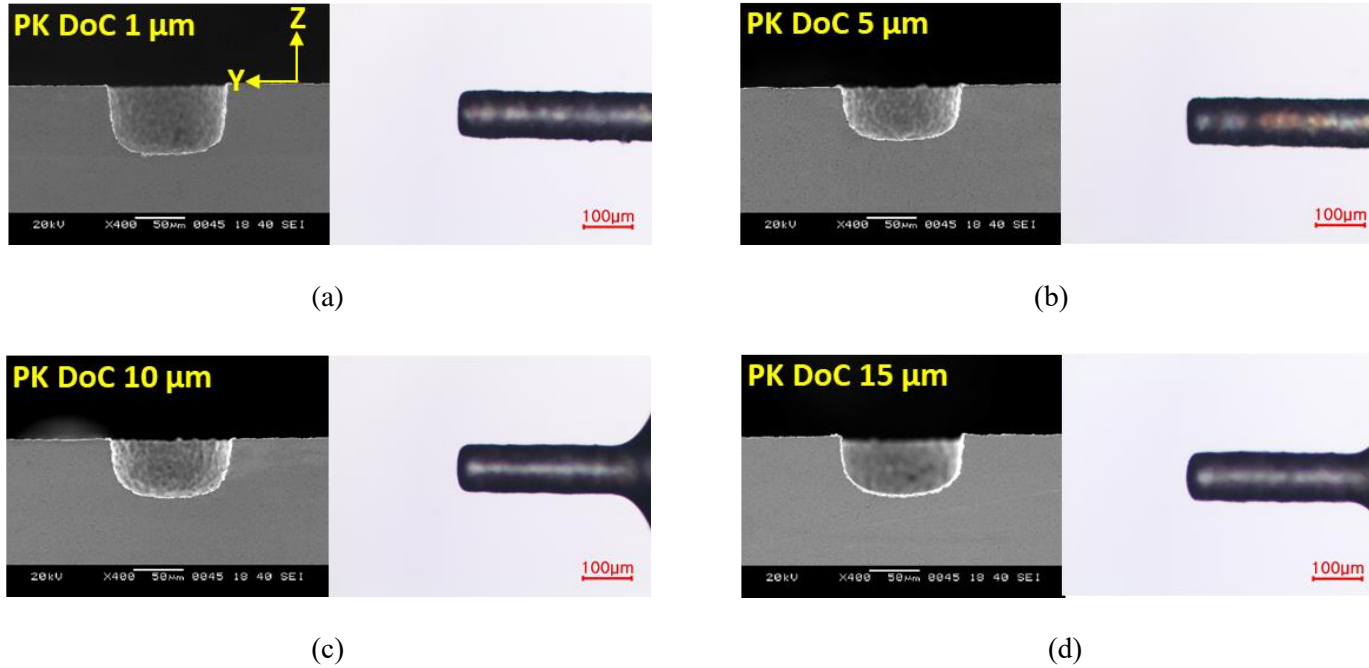
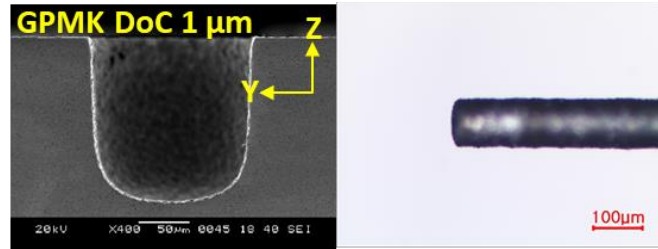
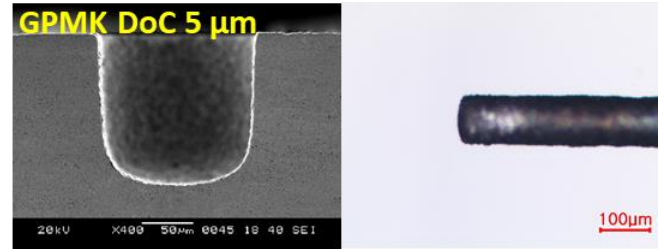


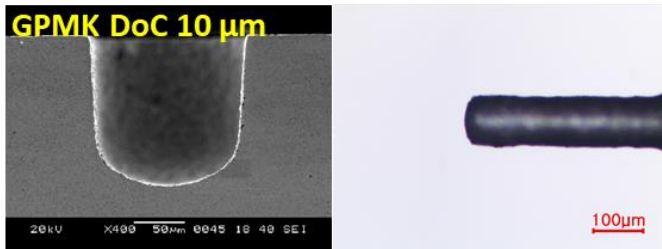
Figure 49. The cross section views in lateral Y-Z plane and the micro tool electrode after machining by PK with several DoCs: (a) 1 μm . (b) 5 μm . (c) 10 μm . (d) 15 μm .



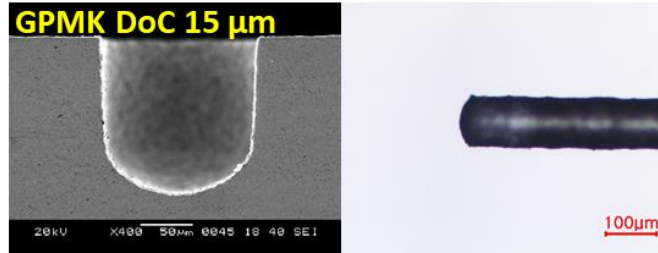
(a)



(b)

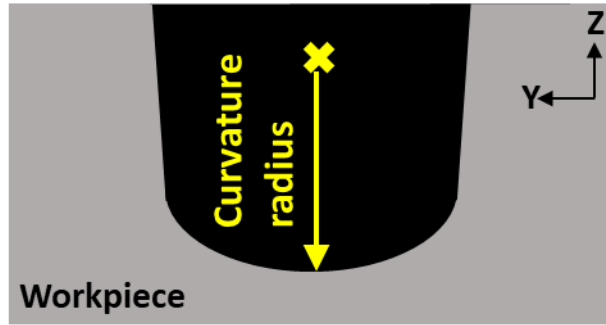


(c)

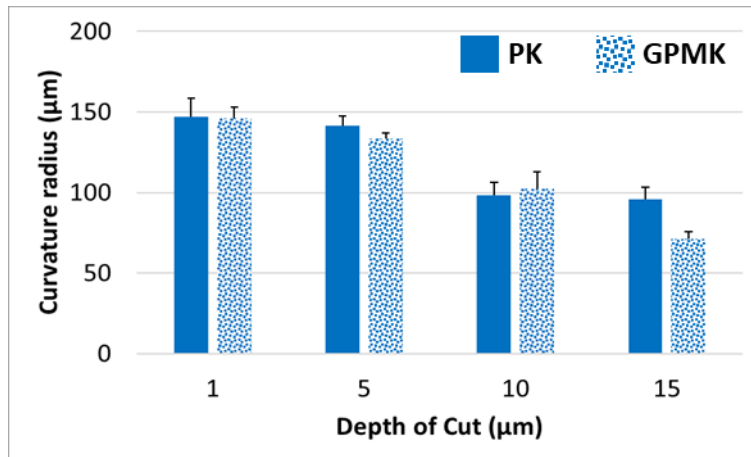


(d)

Figure 50. The cross section views in lateral Y-Z plane and the micro tool electrode after machining by GPMK with several DoCs: (a) 1 μm . (b) 5 μm . (c) 10 μm . (d) 15 μm .

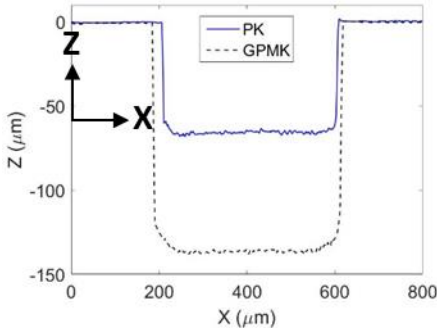


(a)

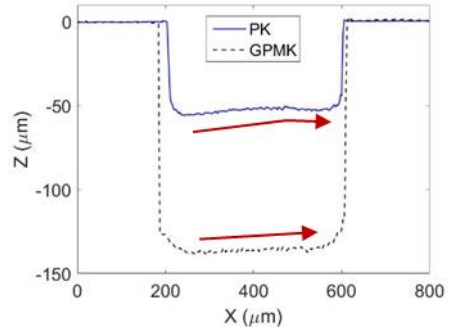


(b)

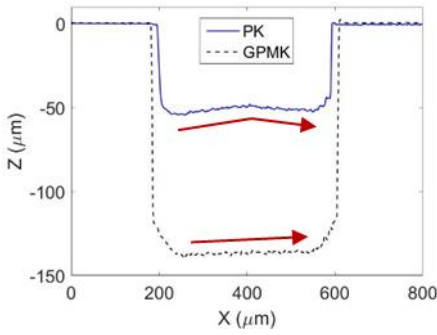
Figure 51. Curvature radius of the bottom surface of the micro channel: (a) Schematic diagram of curvature radius. (b) Curvature radii of micro channels with several DoCs.



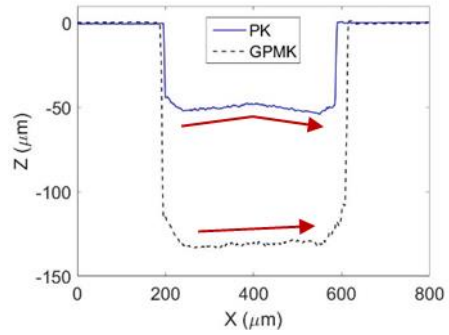
(a)



(b)



(c)

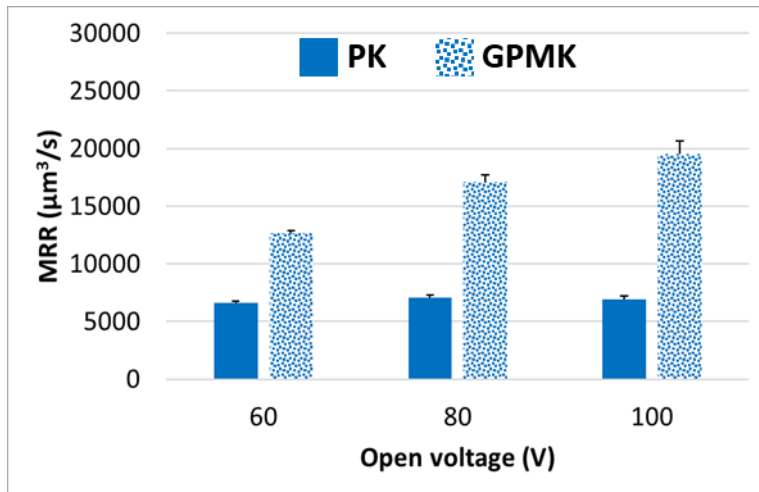


(d)

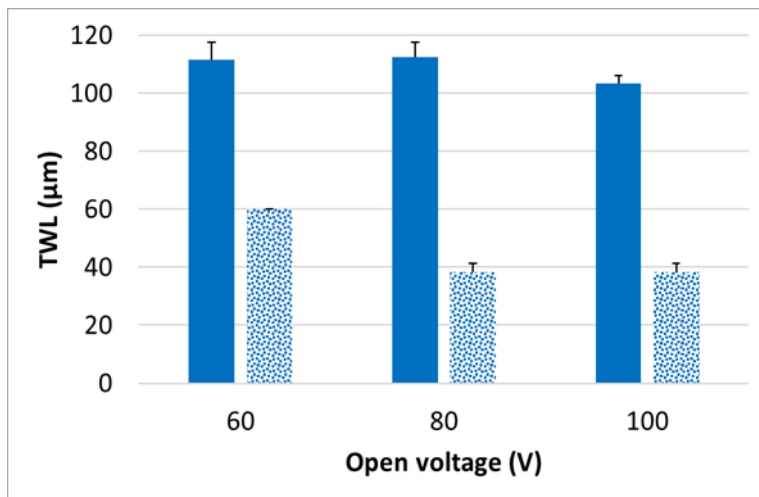
Figure 52. The slope of bottom surface of the micro channel along the stroke direction (X-Z plane) with several DoCs: (a) 1 μm . (b) 5 μm . (c) 10 μm . (d) 15 μm .

6.3.2 Open voltage V

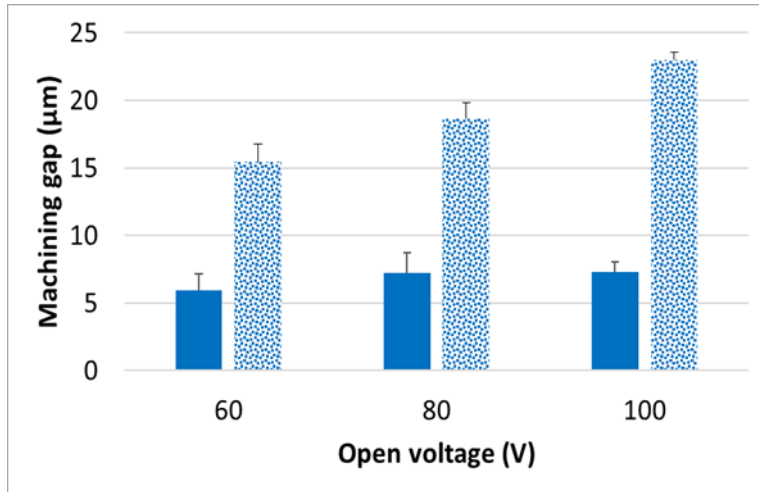
The effect of open voltage is discharge energy and discharge gap as explained in section 6.2.1. Fig. 53 shows the machining results of three different open voltages. The DoC was 10 μm and capacitance was 5 nF. As the open voltage was increased, while MRRs were similar in PK, MRRs in GPMK were increased. It could be resulted from the enlarged discharge gap of GPMK. On the other hand, TWL started to decrease at 80 V in GPMK and 100 V in PK. Owing to the effect of graphite powder on the discharge gap, the lower open voltage is sufficient for the evacuation of debris in GPMK than PK. However, graphite powder raised machining gap as open voltage was increased, whereas there was slight increase of machining gap in PK. The curvature radii were similar in the three open voltages. For low TWL and narrow machining gap as possible, 80 V and 100 V were selected for optimum machining conditions for GPMK and PK, respectively.



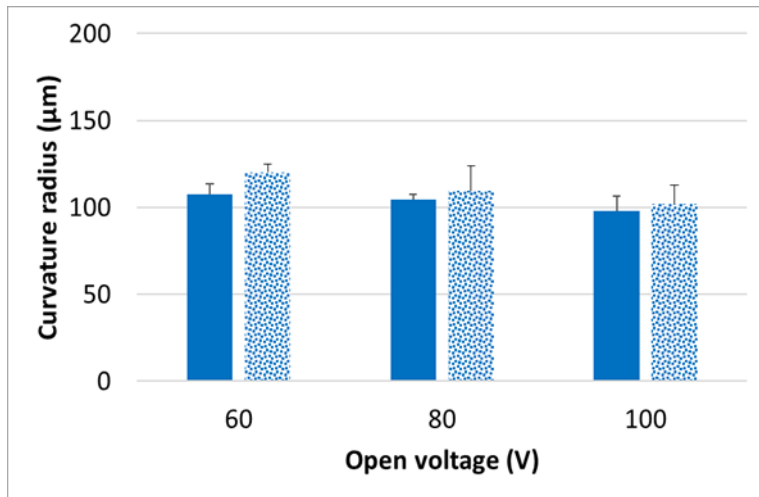
(a)



(b)



(c)

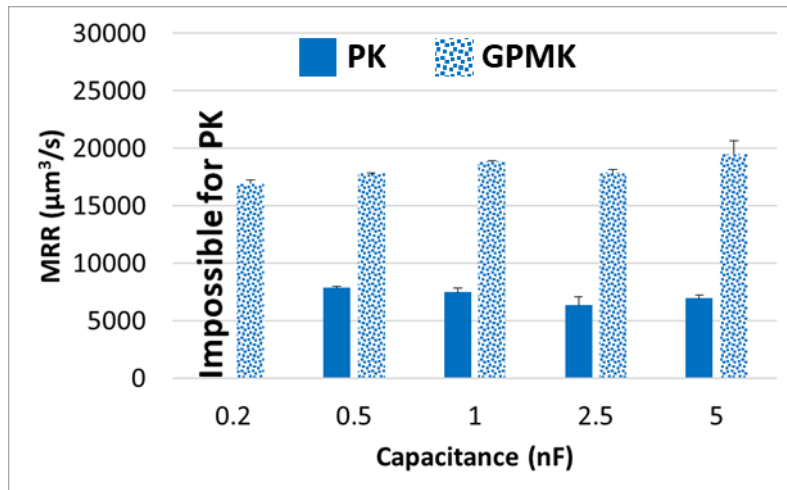


(d)

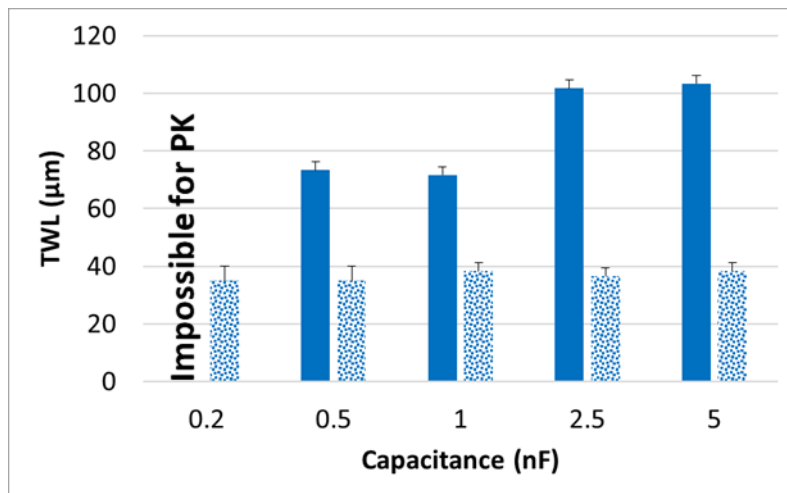
Figure 53. The machining results of open voltage: (a) MRR. (b) TWL. (c) Machining gap. (d) Curvature radius.

6.3.3 Capacitance C

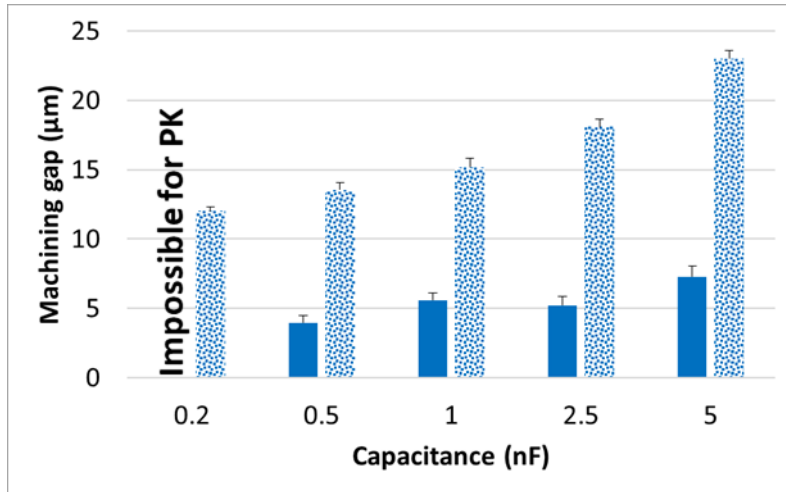
The capacitance affects discharge energy and frequency. Fig. 54 shows the machining results of the capacitance. The DoC was 10 μm and the open voltage was 100 V. Likewise the results of capacitance in micro ED-drilling, 0.2 nF was impossible to machine the micro channel in PK because it resulted in a lot of shorts and holds. As the capacitance became increased, while MRR was slightly increased in GPMK, MRR in PK were decreased. It was because of increased TWL in PK as shown in Fig. 54(b). The machining gap was increased and curvature radii were similar as the capacitance increased in both fluids. For low TWL and narrow machining gap, 0.2 nF and 0.5 nF were selected as optimum machining condition for GPMK and PK, respectively.



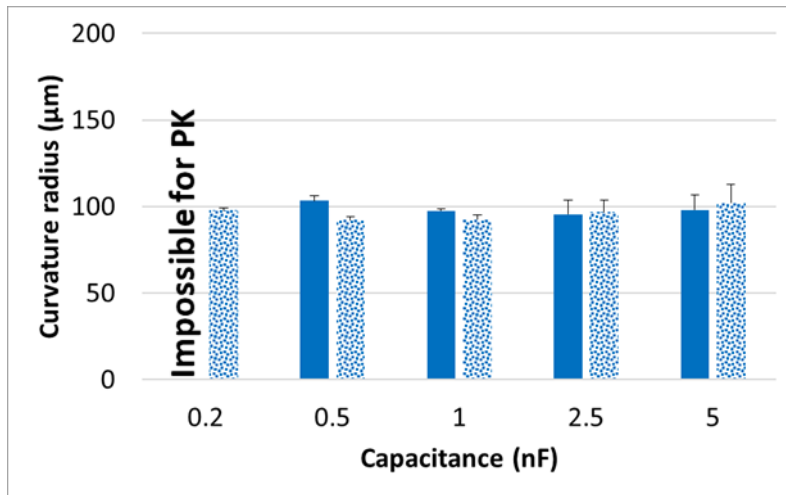
(a)



(b)



(c)



(d)

Figure 54. The machining results of capacitance: (a) MRR. (b) TWL. (c) Machining gap. (d) Curvature radius.

6.3.4 Final results

The performance evaluation of GPMK in micro ED-milling was performed. The specific machining conditions are tabulated in Table 10 and Figs. 55 and 56 show the machining results. The width, depth, and length of micro channels were approximately 110 μm , 50 μm , and 400 μm , respectively. With LCM, the bottom surfaces of both micro channels had almost zero inclination along the stroke direction. With GPMK, the curvature radius was decreased by 16% due to the higher edge wear of the tool electrode. However, MRR was increased by 61%, and TWL and surface roughness were decreased by 61% and 23%, respectively.

Chapter 6. Micro PMEDM with GPMK

Table 10. The optimum machining conditions in micro ED-milling.

	PK	GPMK
Stroke	300 μm	
Input depth	105 μm	80 μm
Workpiece	WC-Co, Anode	
Tool electrode	WC-Co, $\phi 100 \mu\text{m}$, Cathode	WC-Co, $\phi 90 \mu\text{m}$, Cathode
Depth of cut (DoC)	5 μm	
Open Voltage V	100 V	80 V
Capacitance C	0.5 nF	0.2 nF
Resistance R_0	20 Ω	
Resistance R_1	1 k Ω	
X Feedrate	40 $\mu\text{m/s}$	
Z Feedrate	5 $\mu\text{m/s}$	10 $\mu\text{m/s}$
LCM compensation length	5 μm	

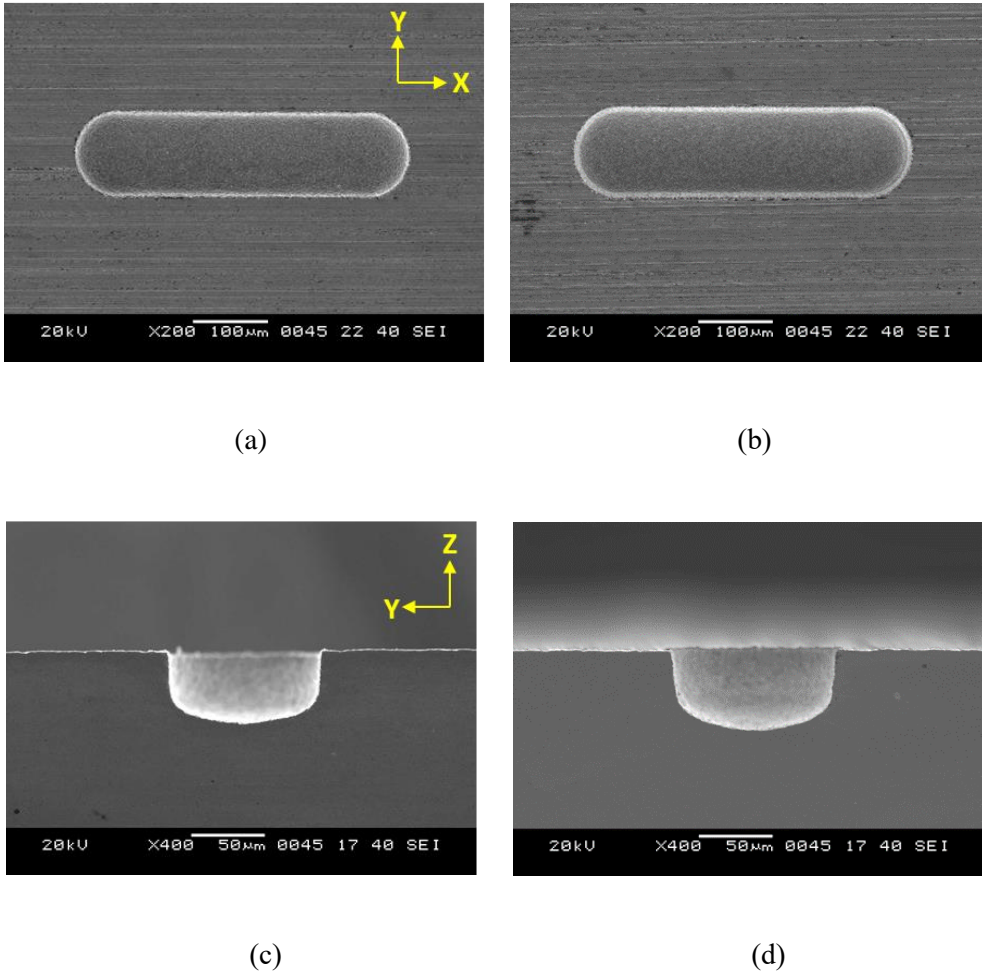
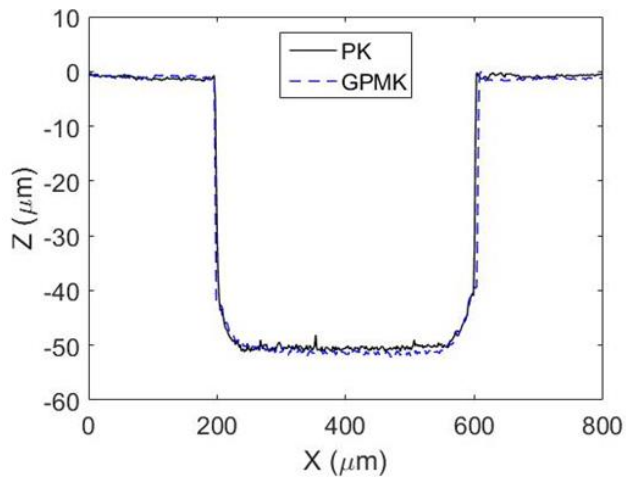
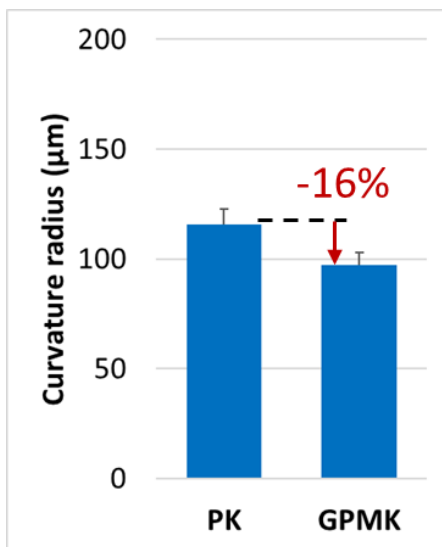


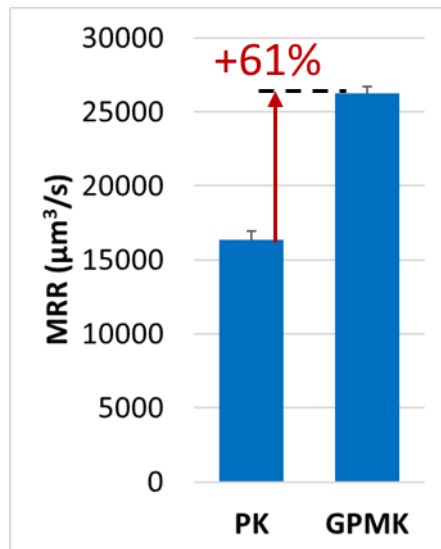
Figure 55. The optimum machining results in micro ED-milling: (a) Micro channel with PK. (b) Micro channel with GPMK. (c) Cross section view of (a). (d) Cross section view of (b).



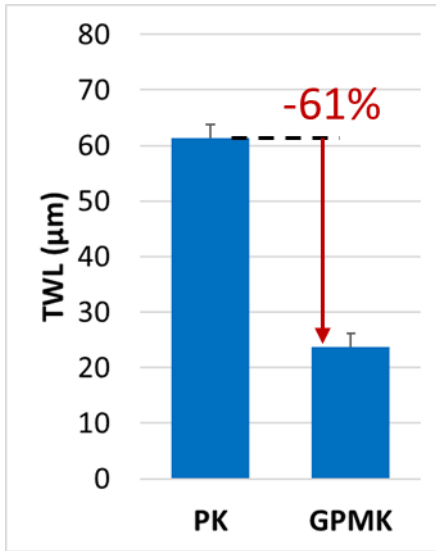
(a)



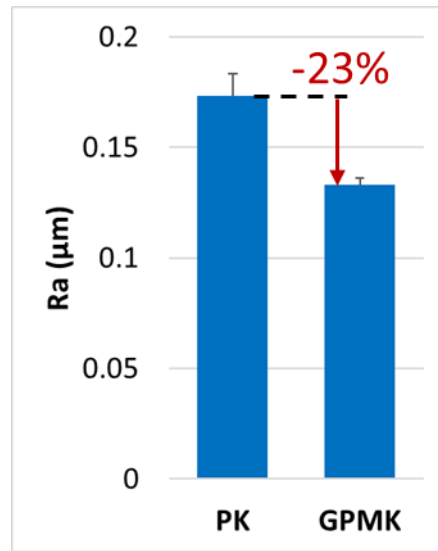
(b)



(c)



(d)



(e)

Figure 56. The performance evaluation of GPMK compared with PK in micro ED-milling: (a) Bottom slope. (b) Curvature radius. (c) MRR. (d) TWL. (e) Surface roughness.

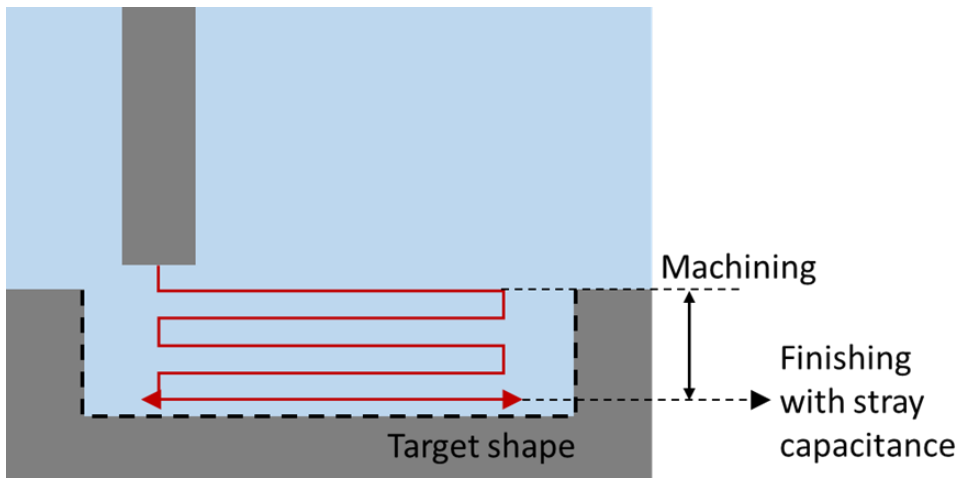


Application – a micro mold

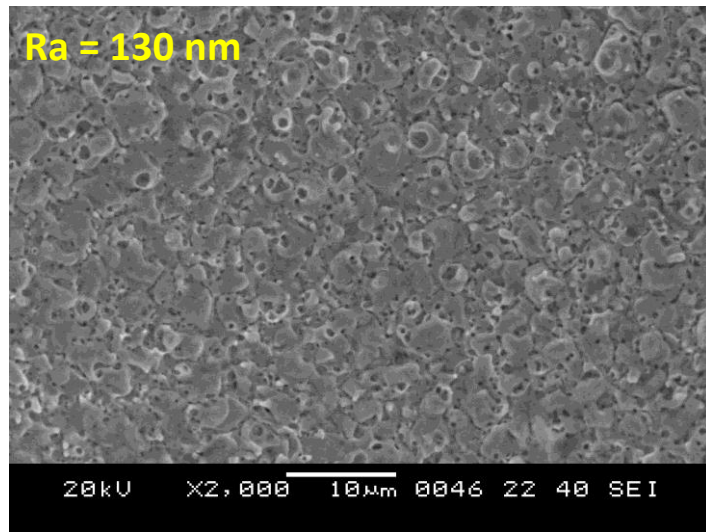
This chapter introduces a simple application of micro EDM, or a micro mold. One of the most powerful strength of EDM is fabrication of micro features on hard-to-cut material such as WC-Co. Furthermore, engineering ceramics such as zirconia (ZrO_2) can be a proper material for a micro mold. Although EDM can basically machine only conductive materials, non-conductive ceramics can be also machined using the assisting electrode (AE) method [45]. In this method, EDM machine AE on the ceramic surface, which machine ceramic indirectly by discharge energy.

7.1 ED-finishing with stray capacitance

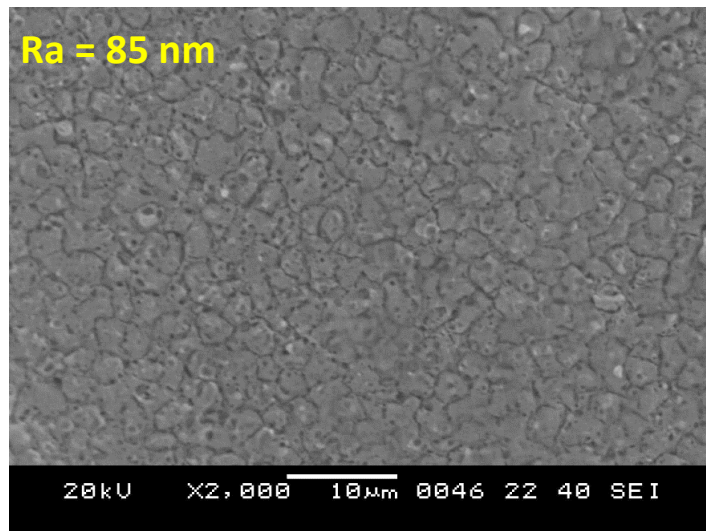
One of the most critical characteristics of a micro mold is surface roughness. Fig. 57 shows the strategy of the finishing procedure and results of micro mold fabrication of this study. Stray capacitance was used finishing step, which stems from electrical components of the RC discharge circuit and the discharge plasma channel. After the last stroke of ED-milling, the tool electrode moved along the stroke direction two more times in the last z-position with stray capacitance. As a result, the surface roughness was decreased up to 85 nm.



(a)



(b)



(c)

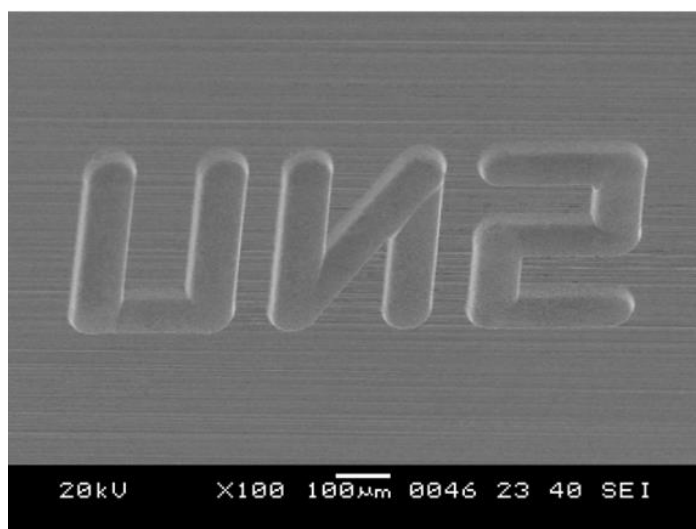
Figure 57. The finishing step of ED-milling: (a) Strategy. (b) After machining. (b) After finishing.

7.2 Micro WC-Co mold

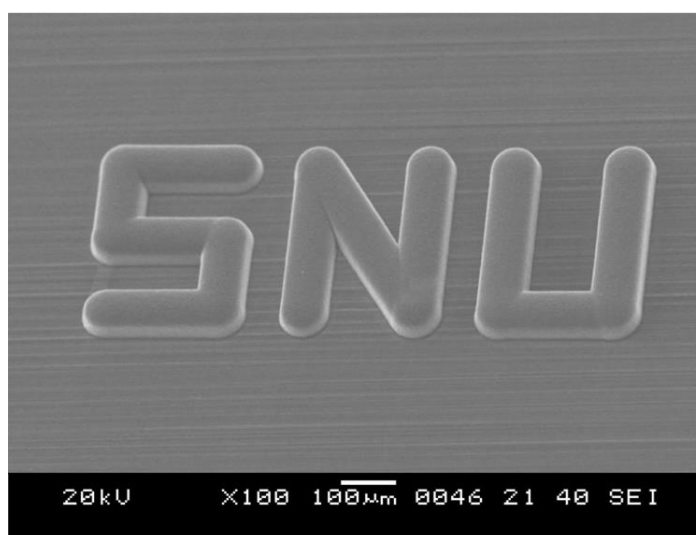
WC-Co has superior physical properties such as high mechanical strength, impact resistance, wear resistance, and erosion resistance, which are crucial characteristics for a micro mold. However, traditional cutting method is time consuming and expensive due to the tool breakage or special tool material such as a diamond. Using PMEDM, the SNU micro mold was successfully fabricated as shown in Fig. 58. The detail machining conditions are tabulated in Table 11. The width and depth of each channel were 100 μm and 50 μm , respectively.

Table 11. Machining conditions for the micro WC-Co mold.

Type	PMED-milling
Workpiece	WC-Co, Anode
Tool electrode	WC-Co, $\phi 70\ \mu\text{m}$, Cathode
Powder (particle size, concentration)	Graphite (40 nm, 2 g/l)
Depth of cut (DoC)	5 μm
Open voltage V	80 V
Capacitance C	0.2 nF
X feedrate	40 $\mu\text{m/s}$
Z feedrate	10 $\mu\text{m/s}$
LCM compensation length	5 μm



(a)



(b)

Figure 58. (a) A micro WC-Co mold. (b) Replicated PDMS.

7.3 Micro zirconia mold

As one of engineering ceramics, zirconia has superior physical properties such as high mechanical strength, impact resistance, wear resistance, erosion resistance, chemical resistance, and corrosion resistance. Even though zirconia is non-conductive, AE EDM can machine it through the following machining process as illustrated in Fig. 59.

Step 1) Using sputtering and electroplating techniques, AE is deposited on non-conductive ceramics over 10-20 μm .

Step 2) As discharge starts on the AE, indirect machining is conducted on the non-conductive ceramic surface below the AE. A dielectric fluid is hydrocarbon-based oil such as kerosene.

Step 3) Carbon ions decomposed from kerosene are deposited on the machined surface, which serve as the new AE.

Step 4) By repeated formation and removal of AE, continuous discharges machine the non-conductive ceramic material.

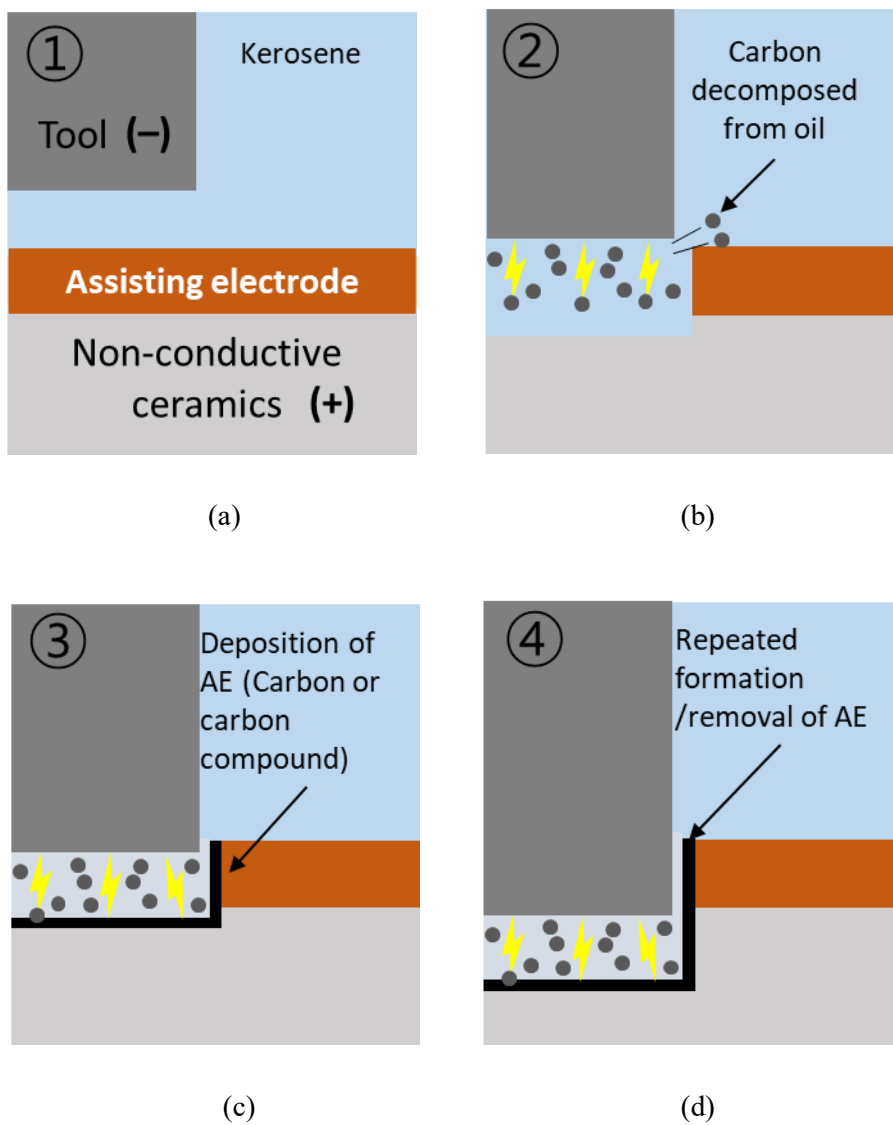
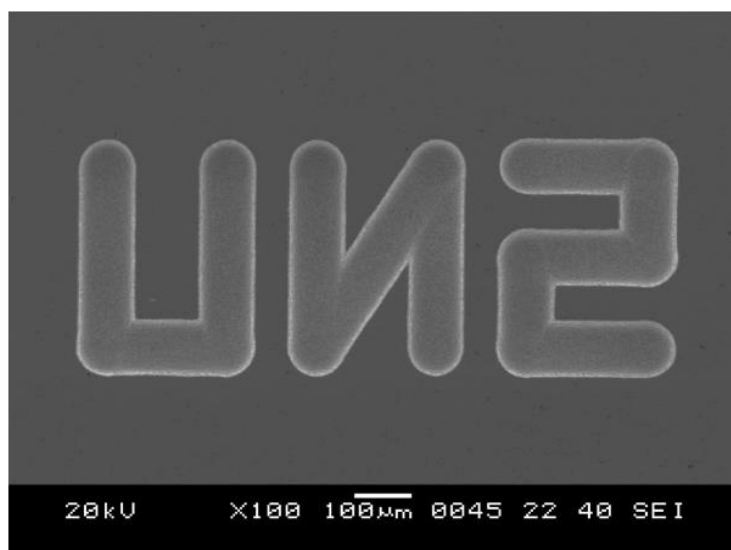


Figure 59. Machining process of AE EDM: (a) AE deposition. (b) Discharge. (c) AE generation. (d) Continuous discharge.

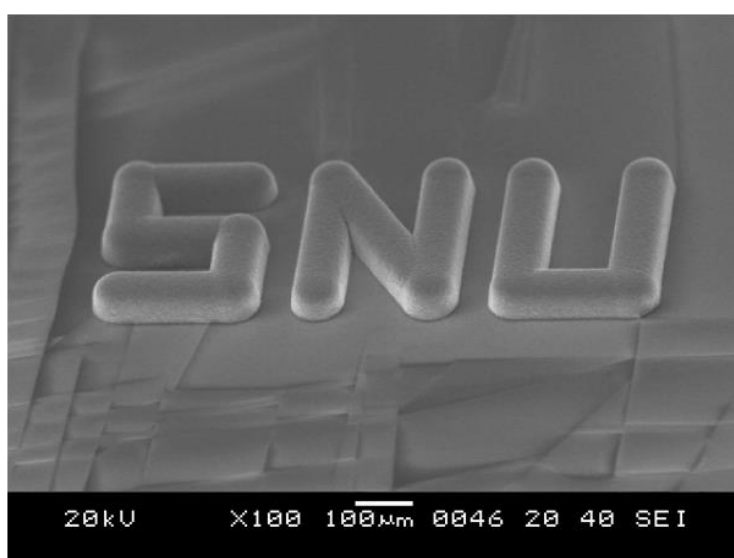
The machining conditions for the micro zirconia mold are tabulated in Table 12, and results are shown in Fig. 60. Due to the crack at the edge of micro features, the surface was polished with diamond compound. The width and depth of each channel were 100 μm and 50 μm , respectively.

Table 12. Machining conditions for the zirconia micro mold.

Type	PMED-milling
Workpiece	Zirconia, Anode
Assisting electrode (thickness)	Cu (15 μm)
Tool electrode	WC-Co, $\phi 70 \mu\text{m}$, Cathode
Powder (particle size, concentration)	Graphite (40 nm, 2 g/l)
Depth of cut (DoC)	5 μm
Open voltage V	100 V
Capacitance C	0.5 nF
X feedrate	40 $\mu\text{m/s}$
Z feedrate	10 $\mu\text{m/s}$
LCM compensation length	5 μm



(a)



(b)

Figure 60. (a) A micro zirconia mold. (b) Replicated PDMS.

8

Conclusions

This study suggests the new explanation of tool wear reduction mechanism in PMEDM and shows performance of GPMK in micro EDM. According to the modeling of RC-discharge circuit, reverse current flows by stray inductance, which intensifies tool wear due to the higher energy distribution at the tool electrode. However, with GPMK, the discharge plasma channel is extinguished quickly before reverse current flow by two reasons.

- 1) By enlarged discharge gap, the energy density of discharge plasma channel

becomes weaker than normal EDM and is extinguished.

- 2) By early discharges, at small gap between the tool electrode and workpiece, the amount of discharge energy is decreased and its plasma channel is extinguished.

In both cases, higher energy distribution is maintained at the workpiece; thus, MRR increases and TWL decreases simultaneously in PMEDM.

The performance evaluation was conducted in micro ED-drilling and ED-milling. The average particle size of graphite powder and the concentration of GPMK was adjusted to decrease the discharge gap as small as possible. With the micro tools of identical diameters, the optimum values DoC, open voltage, and capacitance were investigated by comparing the machining performances of PK and GPMK in terms of MRR, TWL, and dimensional accuracy. With optimum machining conditions, similar size micro holes and channels were machined by both fluids. As results of machining the micro hole whose inlet diameter was 95 μm and depth was 500 μm , MRR was increased 140%, and TWL, taper angle, and surface roughness were respectively decreased by 55%, 47%, and 57% with GPMK. Moreover, the micro channels whose width, depth, and length were respectively 110 μm , 50 μm , and 400 μm were also machined by both PK and GPMK. With GPMK, MRR was increased by 61%, TWL was decreased by 61%, and surface roughness

was decreased by 23%, while the curvature radius of bottom surface was decreased by 16% due to the intensified edge wear of the tool electrode.

Using micro PMEDM technique, the micro SNU pattern was successfully fabricated on WC-Co and zirconia as mold applications. Especially, AE method was employed since zirconia is one of non-conductive engineering ceramics. The width and depth of each channel were 100 μm and 50 μm , respectively. The SNU patterns of the both micro molds were successfully replicated on PDMS.

References

- [1] S. Kalpakjian, Manufacturing processes for engineering materials, 3rd ed., Menlo Park: Addison Wesley Longman, Inc., 1984.
- [2] B. H. Amstead, P. F. Ostwald and M. L. Begeman, Manufacturing process, 8th ed., New York: John Wiley & Sons, Inc., 1987.
- [3] E. P. Degarmo, J. T. Black, R. A. Kohser, and B. E. Klameccki, Materials and processes in manufacturing, 9th ed., the United States of America: John Wiley & Sons, Inc., 2003.
- [4] J. Marafona, C. Wykes, “A new method of optimising material removal rate using EDM with copper-tungsten electrodes,” International Journal of Machine Tools & Manufacture. Vol. 40, pp. 153-164, 2000.
- [5] Y. -Y. Tsai, T. Masuzawa, “An index of evaluate the wear resistance of the electrode in micro-EDM,” Journal of Materials Processing Technology, vol. 149, pp. 304-309, 2004.
- [6] K. Y. Song, D. K. Chung, M. S. Park, C. N. Chu, “Micro electrical discharge drilling of tungsten carbide using deionized water,” Journal of Micromechanics and Microengineering, vol. 19, pp. 045006, 2009.

- [7] P. Bleys, K. P. Kruth, B. Lauwers, A. Zryd, R. Delpretti, C. Tricarico, "Real-time tool wear compensation in milling EDM," *CIRP Annals-Manufacturing Technology*, vol. 51, pp.157-160, 2002
- [8] K. Y. Song, D. K. Chung, M. S. Park, C. N. Chu, "EDM turning using a strip electrode," *Journal of Material Processing Technology*, vol. 213, pp. 1495-1500, 2013.
- [9] K. Y. Song, D. K. Chung, M. S. Park, C. N. Chu, "Electrical discharge machining using a strip electrode," *Precision Engineering*, vol. 37, pp. 738-745, 2013.
- [10] H. Gotoh, T. Tani, M. Okada, A. Goto, T. Masuzawa, N. Mohri, "Wire electrical discharge milling using a wire guide with reciprocating rotation," in *proceedings of 17th CIRP conference on Electro Physical and Chemical Machining (ISEM)*, pp. 199-202, April, 2013.
- [11] M. L. Jeswani, "Effect of the addition of graphite powder to kerosene used as the dielectric fluid in electrical discharge machining," *Wear*, vol. 70, pp. 133-139, 1981.
- [12] S. H. Yeo, P. C. Tan, W. Kurnia, "Effects of powder additives suspended in dielectric on crater characteristics for micro electrical discharge machining,"

- Journal of Micromechanics and Microengineering, vol. 17, pp.N91-N98, 2007.
- [13] A. Singh, R. Singh, "Effect of powder mixed electrical discharge machining (PMEDM) on various materials with different powders: A review," International Journal for Innovative Research in Science & Technology, vol. 2, pp. 164-169, 2015
- [14] B. Singh, J. Kumar, S. Kumar, "Investigation of the tool wear rate in tungsten powder-mixed electrical discharge machining of AA6061/10%SiCp composite," Materials and Manufacturing Process, vol. 31, pp. 456-466, 2016.
- [15] M. P. Jahan, Y. S. Wong, M. Rahman, "A study on the quality micro-hole machining of tungsten carbide by micro-EDM process using transistor and RC-type pulse generator," Journal of Material Processing Technology, vol. 209, pp. 1706-1716, 2009.
- [16] M. Kunieda, B. Lauwers, K. Rajurkar, B. M. Schumacher, "Advancing EDM through fundamental insight into the process," CIRP Annals-Manufacturing Technology, vol. 54, pp.64-87, 2005.
- [17] H. G. Cheong, Y. S. Kim, C. N. Chu, "Effect of reverse current on tool wear in micro-electrical discharge milling," Precision Engineering, vol. 55, pp. 484-490, 2019.

- [18] Y. S. Kim, C. N. Chu, "The effect of graphite powder on tool wear in micro electrical discharge machining," in proceedings of 19th CIRP conference on Electro Physical and Chemical Machining (ISEM), pp. 553-558, April, 2018.
- [19] K. Y. Song, D. K. Chung, M. S. Park, and C. N. Chu, "Micro electrical discharge milling of WC-Co using a deionized water spray and a bipolar pulse," Journal of Micromechanics and Microengineering, vol. 20, pp. 045022, 2010.
- [20] E. C. Jameson, Electrical discharge machining, Michigan: Society of Manufacturing Engineers, 2001.
- [21] E. B. Guirau, The EDM handbook, Cincinnati: Hanse Gardner Publication, 1997.
- [22] K. P. Rajurkar, G. Levy, A. Malshe, M. M. Sundaram, J. McGeough, X. Hu, R. Resnick, and A. DeSilva, "Micro and nano machining by electro-physical and chemical processes," CIRP Annals-Manufacturing Technology, Vol. 55, No. 2, pp. 643-666, 2006.
- [23] Carl Sommer and Steve Sommer, Complete EDM handbook, Houston: Advance Publishing, Inc., 2005.
- [24] Y. Imai, T. Suzuki, H. Kawatsu and A. Gotowu, Applications of EDM, Tokyo: Gijtsu-Hyoron Co., Ltd., 2010.

- [25] C. Arunachalam, Modeling the electrical discharge machining process, Ph.D. Dissertation, Texas A&M University, 1995.
- [26] H. Obara, H. Satou, M. Hatano, "Fundamental study on corrosion of cemented carbide during wire EDM," *Journal of Material Processing Technology*, Vol. 149, pp. 370-375, 2004.
- [27] K. Taniguchi, T. Matsura, and K. Kida, *Discharge phenomena and their applications*, Japan: Kyoritsu Shuppan Co., Ltd., 2007.
- [28] H. Kobayashi, *Technologies of electrical discharge*, Japan: Nikkan Kogyo Shimbun Ltd., 2008.
- [29] D. K. Chung, B. H. Kim, C. N. Chu, "Micro electrical discharge milling using deionized water as a dielectric fluid," *Journal of Micromechanics and Microengineering*, vol. 17, pp. 867-874, 2007.
- [30] D. K. Chung, H. S. Shin, B. H. Kim, C. N. Chu, "High frequency micro wire EDM for electrolytic corrosion prevention," *International Journal of Precision Engineering and Manufacturing*, vol. 12, pp.1125-1128, 2011.
- [31] D. K. Chung, H. S. Shin, M. S. Park, C. N. Chu, "Machining characteristics of micro EDM in water using high frequency bipolar pulse," *International Journal of Precision Engineering and Manufacturing*, vol. 12, pp.195-201, 2011.

- [32] D. K. Chung, H. S. Shin, C. N. Chu, "Modeling and experimental investigation for electrolytic corrosion prevention in high frequency micro EDM using deionized water," *Microsystem Techonolgy*, vol. 18, pp. 703-712, 2012.
- [33] K. Y. Song, D. K. Chung, M. S. Park, C. N. Chu, "Water spray electrical discharge drilling of WC-Co to prevent electrolytic corrosion," *International Journal of Precision Engineering and Manufacturing*, vol. 13, pp.1117-1123, 2012.
- [34] J. W. Jung, S. H. Ko, Y. H. Jeong, B. K. Min, and S. J. Lee, "Real-time gap control for micro-EDM: Application in a microfactory," *International Journal of Precision Engineering and Manufacturing*, Vol. 9, pp. 3-6, 2008.
- [35] H. L. Yu, J. J. Luan, J. Z. Li, Y. S. Zhang, Z. Y. Yu, and D. M. Guo, "A new electrode wear compensation method for improving performance in 3D micro EDM milling," *Journal of Micromechanics and Microengineering*, Vol. 20, pp. 055011, 2010.
- [36] M. T. Yan, K. Y. Huang, and C. Y. Lo, "A study on electrode wear sensing and compensation in micro-EDM using vision system," *International Journal of Advanced Manufacturing and Technology*, Vol. 42, pp. 1065-1073, 2009.
- [37] P. Bleys, J. P. Kruth, and B. Lauwers, "Sensing and compensation of tool wear

- in milling EDM,” *Journal of Materials Processing Technology*, Vol. 140, pp. 139-146, 2004.
- [38] Z. Y. Yu, T. Masuzawa, M. Fujino, “Micro-EDM for three-dimensional cavities – Development of uniform wear method-,” *CIRP Annals*, vol. 47, pp. 169-172, 1998.
- [39] M. Hara, H. Nakagawa, J. Suehiro, T. Shinohara, “Electrical breakdown triggered by a free conducting spherical particle in saturated liquid He I and He II under uniform dc field,” *IEEE Transactions on Dielectrics and Electrical Insulation*, vol. 10, pp. 1022-1031, 2003.
- [40] W. S. Zhao, Q. G. Meng, Z. L. Wang, “The application of research on powder mixed EDM in rough machining,”
- [41] Y. S. Wong, L. C. Lim, Iqbal Rahuman, W. M. Tee, “Near-mirror-finish phenomenon in EDM using powder-mixed dielectric,” *Journal of Materials Processing Technology*, vol. 79, pp. 30-40, 1998.
- [42] W. Natsu, M. Shimoyamada, M. Kunieda, “Study on expansion process of EDM arc plasma,” *JSME International Journal Series C*, vol. 49, pp. 600-605, 2006.
- [43] M. P. Jahan, M. Rahman, “Study on the nano-powder-mixed sinking and

milling micro-EDM of WC-Co,” *International Journal of Advanced Manufacturing Technology*, vol. 53, pp. 167-180, 2011.

[44] T. Masuzawa, M. Fujino, K. Kobayashi, T. Suzuki, N. Kinoshita, “Wire electro-discharge grinding for micro-machining,” *CIRP Annals-Manufacturing Technology*, vol. 34, pp.431-434, 1985.

[45] N. Mohri, Y. Fukuzawa, T. Tani, N. Saito, K. Furutani, “Assisting electrode method for machining insulating ceramics,” *CIRP Annals*, vol. 45, pp. 201-204, 1996.

[46] M. Zahiruddin and M. Kunieda, “Energy distribution ratio into micro EDM electrodes,” *Journal of Advanced Mechanical Design, Systems, and Manufacturing*, Vol. 4, No. 6, pp. 1095-1106. 2010.

국문 초록

본 연구는 미세 방전 가공에서 흑연 파우더 혼합 등유에 의한 공구 마모 저감 원리를 규명한다. RC 방전 회로는 에너지 크기가 작고 짧은 지속 시간의 방전 펄스를 생성하기 때문에 미세 방전 가공에서 트랜지스터 회로보다 널리 쓰인다. 미세 방전 현상에서는 전자와 양극의 충돌로 인하여 양극의 에너지 분포가 높기때문에 재료 가공율을 높이고 공구 마모를 줄이기 위하여 공구를 음극으로 대전시킨다. 하지만 방전이 일어나는 동안 RC 방전 회로에 내재되어 있는 인덕턴스 때문에 방전 플라즈마 채널이 소멸되기 전에 전류의 방향이 역전된다. 이러한 역전류는 공구 마모를 증가시키고 가공 효율을 악화시킨다. 본 연구에서 흑연 파우더 혼합 등유는 다음의 두 가지 방법으로 역전류가 흐르기 전에 방전 플라즈마 채널이 소멸될 수 있는 환경을 조성함으로써 공구 마모를 저감시킨다. 첫 번째로, 흑연 파우더 혼합 등유에 의해 넓어진 방전 간극에 의하여 방전 에너지 밀도는 약해지고 방전 플라즈마 채널은 절연액에 의하여 쉽게 소멸된다. 두 번째로, 공구가 공작물에 가깝게 접근하더라도 축전기가 완충되기 전에 작은 충전 에너지가 조기 방전되고, 이러한 조기 방전에 의한 플라스

마 채널은 그 에너지 크기가 작기 때문에 역전류가 흐르기 전에 소멸된다. 흑연 파우더 혼합 등유에 의한 미세 방전 밀링과 드릴링의 가공 성능과 품질이 순수한 등유에 비교하여 평가되었다. 각각 최적의 가공 조건에서 비교하면, 미세 방전 드릴링에서 흑연 파우더 혼합 등유에 의하여 재료 가공율은 140% 증가하였고, 공구 마모는 55%, 표면 조도는 57% 감소하였다. 미세 방전 밀링에서는 흑연 파우더 혼합 등유에 의하여 재료 가공율은 61% 증가하였고, 공구 마모는 61%, 표면 조도는 23% 감소하였다.

.....

주요어 : 미세 방전 가공; 흑연 파우더 혼합 등유, 공구 마모

학 번 : 2015-30997